International Journal of Heat and Mass Transfer 136 (2019) 324–354

Contents lists available at ScienceDirect

International Journal of Heat and Mass Transfer

journal homepage: www.elsevier.com/locate/ijhmt

Review

Review of single-phase and two-phase nanofluid heat transfer in macro-channels and micro-channels

Gangtao Liang [a], Issam Mudawar [b,*]

[a] Key Laboratory of Ocean Energy Utilization and Energy Conservation of Ministry of Education, School of Energy and Power Engineering, Dalian University of Technology, Dalian 116024, China

[b] Purdue University Boiling and Two-Phase Flow Laboratory (PU-BTPFL), School of Mechanical Engineering, 585 Purdue Mall, West Lafayette, IN 47907, USA

ARTICLE INFO

Article history:
Received 2 January 2019
Received in revised form 14 February 2019
Accepted 25 February 2019
Available online 7 March 2019

Keywords:
Nanofluid
Flow boiling
Heat transfer coefficient
Heat transfer enhancement
Critical heat flux (CHF)

ABSTRACT

This paper provides a comprehensive review of published literature concerning heat transfer benefits of nanofluids for both macro-channels and micro-channels. Included are both experimental and numerical findings concerning several important performance parameters, including single-phase and two-phase heat transfer coefficients, pressure drop, and critical heat flux (CHF), each being evaluated based on postulated mechanisms responsible for any performance enhancement or deterioration. The study also addresses issues important to heat transfer performance, including entropy minimization, hybrid enhancement methodologies, and nanofluid stability, as well as the roles of Brownian diffusion and thermophoresis. Published results point to appreciable enhancement in single-phase heat transfer coefficient realized in entrance region, but the enhancement subsides downstream. And, while some point to the ability of nanofluids to increase CHF, they also emphasize that this increase is limited to short duration boiling tests. Overall, studies point to many important practical problems associated with implementation of nanofluids in cooling situations, including clustering, sedimentation, and precipitation of nanoparticles, clogging of flow passages, erosion to heating surface, transient heat transfer behavior, high cost and production difficulties, lack of quality assurance, and loss of nanofluid stability above a threshold temperature.

Contents

* Corresponding author.
E-mail address: mudawar@ecn.purdue.edu (I. Mudawar).
URL: https://engineering.purdue.edu/BTPFL (I. Mudawar).

https://doi.org/10.1016/j.ijheatmasstransfer.2019.02.086

Nomenclature

c_1, c_2	empirical constants
D	channel hydraulic diameter
d_p	nanoparticle diameter
f	friction factor
G	mass velocity
h	heat transfer coefficient
k	thermal conductivity
m_1, m_2	empirical exponents
$\dot{m}$	mass flow rate
Nu	Nusselt number
P	pressure
Pe	Peclet number
Pr	Prandtl number
q''	heat flux
q''_{CHF}	critical heat flux
Re	Reynolds number
T	temperature
ΔT_{sat}	surface superheat
u	velocity
x	axial distance

Greek symbols

α	thermal diffusivity
δ_v^+	dimensionless thickness of laminar sub-layer
μ	dynamic viscosity
ρ	density
ϕ	nanoparticle volume concentration

Subscripts

f	liquid
out	channel outlet
p	particle
sat	saturation
sub	subcooling
v	laminar sub-layer
w	wall
$water$	pure water

1. Introduction

1.1. High heat flux cooling background and applications

During the past three decades, aggressive micro- and nano-miniaturization in the development of computer electronic components has created an urgent need for innovative cooling schemes aimed at maintaining device temperatures safely below limits that are dictated by both material constraints and device reliability. By the early 1980s, this trend led to rapid escalation in heat dissipation rate, causing a shift from reliance on fan-cooled heat sink attachments to cooling schemes employing dielectric liquid coolants, using a variety of single-phase cooling schemes that relied entirely on the coolant's sensible heat rise to remove the heat. However, by the mid-1980s, heat dissipation from devices used in supercomputers began to exceed 100 W/cm^2, well beyond the capabilities of single-phase liquid cooling schemes [1]. In response, cooling system developers shifted their attention to two-phase cooling schemes in an effort to capitalize on the coolant's both sensible and latent heat, which allowed rejection of far greater amounts of heat than single-phase schemes, while maintaining lower device temperatures. In recent years, it has been estimated that heat dissipation from specialized electronic devices already exceeded 1000 W/cm^2 [2].

But heat dissipation concerns are not limited to computer devices. Since the early 1990s, rapid developments in many other applications posed similar heat removal challenges. They include, in addition to computers and data centers, x-ray medical devices, hybrid vehicle power electronics, heat exchangers for hydrogen storage, fusion reactor blankets, particle accelerator targets, magnetohydrodynamic (MHD) electrode walls, rocket nozzles, satellite and spacecraft avionics, laser and microwave directed energy weapons, advanced radar, turbine blades, and air-fuel heat exchangers for high-Mach aircraft [3]. Key to safe and reliable operation in all these applications is ability to maintain device temperature safely below critical heat flux (CHF). Exceeding this limit is accompanied by rapid transition from highly efficient nucleate boiling to very deficient film boiling. This transition can trigger sharp increase in surface temperature that may lead to permanent device damage.

1.2. Two-phase cooling solutions

In response to the continuing trend of increased heat dissipation, a broad variety of thermal management techniques have been investigated at the Purdue University Boiling and Two-Phase Flow Laboratory (PU-BTPFL) [3,4] for over three decades. They include passive (pump-free) cooling schemes, including capillary-driven devices (heat pipes, capillary pumped loops, and loop heat pipes) [5] and pool boiling thermosyphons [6]. For more demanding situations, pumped flow solutions were sought to capitalize on heat transfer merits of increased fluid motion, using such schemes as falling film [7], channel flow boiling [8–10], micro-channel flow boiling [11–14], jet-impingement [15], and spray [16,17], as well as hybrid cooling schemes combining merits of micro-channels and jet impingement [18]. With rapid developments in the above-mentioned high-heat-flux applications, it is conceivable that heat dissipation will become far more severe, which would necessitate boosting cooling performance further using a variety of enhancement techniques. The present study concerns enhancement of macro-channel and micro-channel flow boiling heat transfer.

Channel flow cooling regimes include single-phase liquid and nucleate boiling. These regimes are readily identifiable with the aid of boiling curve, Fig. 1, which depicts variation of heat flux from device surface to coolant with wall superheat (wall temperature minus liquid saturation temperature). The two regimes are demarcated by onset of boiling (ONB) (or incipient boiling), while CHF represents the upper limit for nucleate boiling. For all heat-flux-controlled applications, optimum cooling is achieved by maintaining conditions above ONB, but safely below CHF.

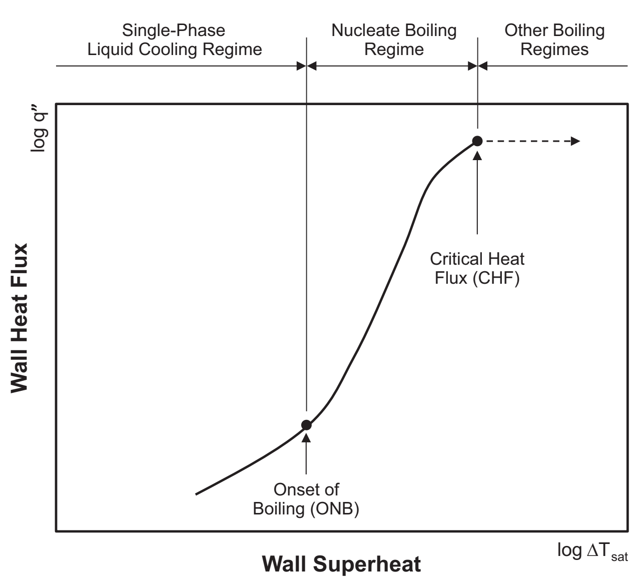

Fig. 1. Boiling curve capturing single-phase liquid cooling and nucleate boiling regimes.

1.3. Heat transfer enhancement techniques

Techniques that have been proposed to improve heat transfer can be classified into two major groups [19]: active and passive. As discussed above, active techniques, which include flow boiling, require use of external power, and include mechanical mixing, vibration, surface and/or liquid rotation, suction and/or injection, and application of electrostatic or magnetic field. In contrast, passive techniques require no direct application of external power, and can be realized by modifying fluid properties, surface roughness, or use of surface attachments to increase surface area and intensify turbulence. Since flow boiling is pump-driven, and therefore an active cooling technique, is the primary objective of the present study to enhance heat transfer performance by modifying fluid properties, a predominantly passive cooling scheme, using nanofluids.

One application where heat transfer enhancement is highly desirable is thermal management in space systems. Absence of gravity is known to greatly compromise cooling performance by triggering CHF at relatively low heat fluxes [20–24]. Hence, a variety of enhancement methods are being sought for this application. One advantage of using nanofluids in microgravity is absence of nanoparticle settling in the base fluid, which, as discussed later, is a serious concern for systems operating in Earth gravity.

1.4. Nanofluid definition and preparation methods

Cooling performance for conventional heat transfer coolants, such as water, refrigerants, oils, and ethylene glycol, is dictated largely by the liquid's thermophysical properties. By dispersing solid particles in the liquid, these properties, especially thermal conductivity, can be improved greatly. Nanofluid is a kind of heat transfer fluid containing nanoparticles (typically 1–100 nm in size) that are suspended uniformly and stably in liquid [25]. Nanoparticles materials include chemically stable metals (*e.g.*, gold, silver, copper), metal oxides (*e.g.*, alumina, zirconia, silica, titania), and various forms of carbon (*e.g.*, diamond, graphite, carbon nanotubes, fullerene) [26]. The first study of nanofluids dates back to 1993, when Masuda et al. [27] measured appreciable changes in thermal conductivity and viscosity of liquids with addition of 13-nm Al_2O_3, 12-nm SiO_2, and 27-nm TiO_2 nanoparticles. But the concept of heat transfer enhancement with nanofluids was proposed a couple of years later by Choi and Eastman [28]. Since then, numerous studies have been published, addressing implementation of nanofluids in a variety of cooling situations.

Preparation of nanofluids is achieved using either two-step or one-step methods [25]. In a typical two-step method, nanoparticles, nanotubes, or nanofibers are first produced in the form of dry powder by physical or chemical treatment (*e.g.*, inert gas condensation and chemical vapor deposition), followed by dispersion of the powder into base liquid. A major problem with the two-step method is aggregation of nanoparticles in the base liquid. Furthermore, while the two-step method works fairly well for oxide nanoparticles, it is not equally effective for metallic nanoparticles. In the one-step method, which is more complicated and requires adherence to stringent preparation requirements, synthesis and dispersion of nanoparticles in base liquid are achieved simultaneously, providing improved dispersibility and stability. Fig. 2 shows Transmission Electron Microscope (TEM) images of carbonic nanofluid prepared using the one-step method, and alumina nanofluid

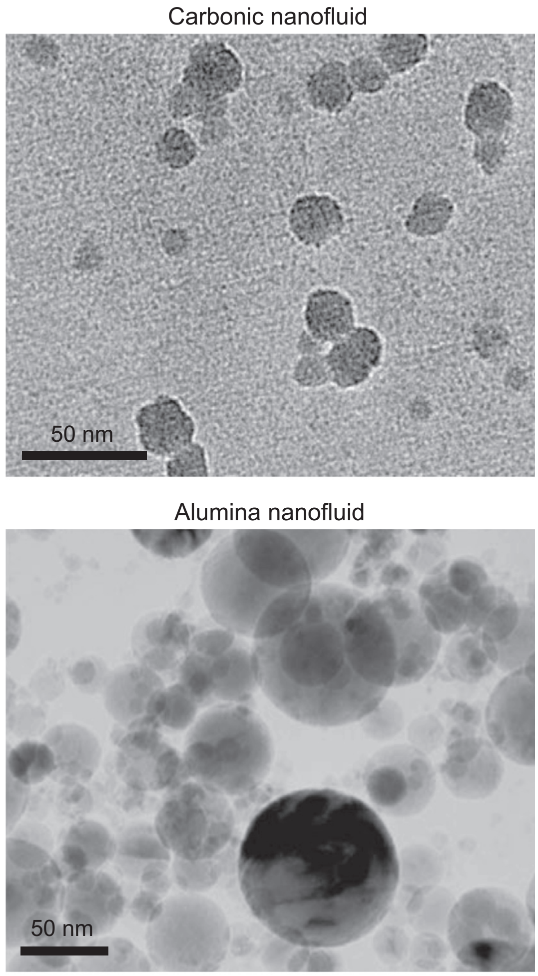

Fig. 2. TEM images of water-based carbonic nanofluid prepared using the one-step method, and alumina nanofluid using the two-step method. Adapted from Kim et al. [29].

using the two-step method. Detailed methods for computing thermal properties of nanofluids can be found in a previous review article on nanofluid pool boiling by the present authors [58].

1.5. Prior nanofluid heat transfer reviews

Several review articles focused on nanofluid heat transfer have been published in the past, which addressed either (1) enhancement of single-phase convective heat transfer and flow boiling along with other modes of heat transfer (*e.g.,* pool boiling), or were dedicated exclusively to (2) single-phase convection or (3) flow boiling. Examples of the first category of reviews include those by Wang and Mujumdar [30], Wen et al. [31], Godson et al. [32], Murshed et al. [33], Barber et al. [34], Wu and Zhao [35], Cheng and Liu [36], Celen et al. [37], Bahiraei and Hangi [38], Fang et al. [39], and Salman et al. [40]. Examples of reviews dedicated entirely to single-phase convective heat transfer include those by Daungthongsuk and Wongwises [41], Mahian et al. [42], Hussein et al. [43,44], Kakaç and Pramuanjaroenkij [45], Yu et al. [46], Sundar and Singh [47], Mohammed et al. [48], and Vanaki et al. [49]. On the other hand, Fang et al. [50] focused their entire review on flow boiling.

The present review will be focused exclusively on use of nanofluids to enhance single-phase liquid convection and nucleate flow boiling in both macro-channels and micro-channels.

1.6. Macro-channel versus micro-channel flow

Micro-channel cooling is arguably one of the most effective thermal management schemes in use today. Here, cooling is achieved mostly with the aid of a thermally conductive heat sink containing a large number of parallel, small diameter channels. These heat sinks feature simplicity in design and construction, and are very compact and lightweight.

Micro-channel heat sinks can be used in both single-phase and two-phase situations. Single-phase heat sinks rely on small hydraulic diameter to achieve high heat transfer coefficients. On the other hand, aside from benefits of small hydraulic diameter, two-phase heat sinks allow the coolant to undergo phase change along the channels and capitalize on latent heat content rather than sensible heat alone. This enables attainment of heat transfer coefficients far greater than those possible with single-phase heat sinks, and reduces both coolant flow rate (required to dissipate same amount of heat) and coolant inventory. Two-phase heat sinks also provide better temperature uniformity by maintaining heat sink temperature close to the coolant's saturation temperature.

An important distinction between macro-channels and micro-channels is hydraulic diameter. While transitional diameter between the two varies with coolant and operating conditions, diameters in micro-channel heat sinks are typically below about 1 mm [3,11,51]. Another method to identify micro-channels is by using Confinement number.

Despite their many advantages, compared to macro-channels, micro-channels produce far greater pressure drop and corresponding higher degrees of compressibility (changes in specific volumes of vapor and liquid phases with pressure), flashing (changes in enthalpies of vapor and liquid phases with pressure), and increased likelihood of two-phase choking. It is for all these reasons that the present review will address the fluid flow and heat transfer characteristics of macro-channels and micro-channels separately.

1.7. Objectives of present review

This study is a follow-up to a series of recent reviews by the present authors addressing a variety of important heat transfer phenomena and cooling schemes, including mechanics of liquid drop impact on a liquid film [52] and on a heated wall [53], spray cooling in the single-phase and nucleate boiling regimes [54] and in high temperature boiling regimes and quenching situations [55], pool boiling CHF [56,57], and pool boiling enhancement techniques using additives and nanofluids [58] and surface modifications [59]. Unlike prior nanofluid heat transfer reviews, the present paper will provide a comprehensive review and assessment of all aspects of nanofluid heat transfer enhancement for both macro-channels and micro-channels.

The present review will be presented in two parts, single-phase convection and flow boiling, with each part segregating findings for macro-channels from those for micro-channels. Each part will address enhancement mechanisms as well as predictive analytical and numerical models; the flow boiling part will also include discussion of nanofluid impact on CHF. Also included will be such related topics as entropy analysis, hybrid enhancement techniques, destabilization criteria, practical concerns, and recommendations for future work. It should be noted that, unless stated otherwise, the base fluid used in the studies reviewed is pure water.

2. Single-phase convective heat transfer

2.1. Heat transfer in macro-channels

2.1.1. Laminar flow

2.1.1.1. Entrance effects. Single-phase flow in macro-channels can be grouped into three separate regions: entrance, developing, and fully developed. Wen and Ding [60] found that enhancement of single-phase convective heat transfer coefficient in tubes using Al_2O_3 nanofluids is significant in the entrance region but decreases downstream. This behavior was confirmed by Ho et al. [61], Lai et al. [62], and Hojjat et al. [63]; the latter achieved pseudoplastic rheological shear thinning with non-Newtonian fluids (aqueous solution of carboxymethyl cellulose based Al_2O_3, CuO and TiO_2 nanofluids). This enhancement implied that heat transfer coefficient for nanofluids is also channel-length dependent [64]. Wen and Ding reported that enhanced thermal conductivity is not the sole reason for the heat transfer enhancement. They proposed that enhancement is also the outcome of particle migration, which is responsible for non-uniform distributions of thermal conductivity and viscosity, leading to reduction in thermal boundary layer thickness. Follow-up modeling by Wen and Ding [65] provided further evidence of particle migration, especially for large particles and high concentrations. Entrance enhancement effects were also confirmed numerically by He et al. [66] for TiO_2 nanofluids.

Using carbon nanotube (CNT) nanofluids, Ding et al. [67] showed that heat transfer enhancement is a function of axial distance from the inlet, increasing at first before reaching maximum value, and then decreasing downstream. They measured enhancement values as high as 350%, which was achieved at a Reynolds number of $Re = 800$ and 0.5 wt% concentration, where

$$Re = \frac{\rho_f u_f D}{\mu_f} \quad (1)$$

ρ_f, μ_f, u_f are, respectively, the nanofluid's density, dynamic viscosity, and mean velocity, and D the channel's hydraulic diameter. They also showed that axial distance corresponding to maximum enhancement increases with increases in both CNT concentration and Re. And, aside from enhanced thermal conductivity, they suggested additional enhancing mechanisms resulting from particle rearrangement, including increased shear induced thermal conduction, decreased thermal boundary thickness, and very high length-to-diameter aspect ratio of CNTs. Ding et al. [68] later proposed that competing effects of particle migration on thermal boundary layer thickness and effective thermal conductivity can lead to enhancement or deterioration of heat transfer for different nanofluids.

Unlike the aforementioned investigators, Garg et al. [69], who used CNT nanofluids, found that percentage enhancement in heat transfer coefficient increases monotonically in the flow direction as axially increasing bulk temperature increases thermal conductivity of the nanofluid considerably. They also noted that enhancement at a particular axial distance decreases slightly with increasing Re, which they attributed to decreased thermal conductivity enhancement resulting from lower bulk fluid temperature. Another important finding from their study is strong dependence of heat transfer performance on the nanofluid's preparation method, reporting an optimum ultrasonication duration for maximum heat transfer enhancement, exceeding which the enhancement decreases.

Liu and Yu [70] studied convective heat transfer of Al_2O_3 nanofluids in a 1.09-mm diameter channel, with Reynolds numbers ranging from 600 to 4500, which covered laminar, transition, and early turbulent flow conditions. They measured remarkable entrance region heat transfer enhancement in laminar flow, which they attributed to flattening of velocity profile caused by flow-induced particle migration. However, they achieved little enhancement in Nusselt number,

$$Nu = \frac{hD}{k_f} \quad (2)$$

since the increase in heat transfer coefficient, h, was balanced by an increase in thermal conductivity, k_f. As shown in Fig. 3, they

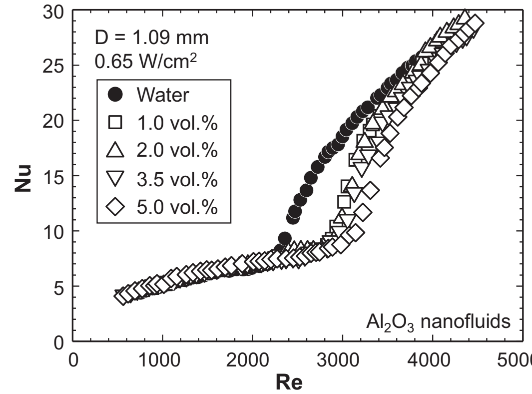

Fig. 3. Nusselt number versus Reynolds number for pure water and water-based Al_2O_3 nanofluids in a 1.09-mm diameter channel at 0.65-W/cm^2 wall heat flux. Adapted from Liu and Yu [70].

observed delay in onset of transition to turbulent flow to higher Re. Notice that, in the transition range, values for both Nu and h (also friction factor) for the nanofluids are below those for the base fluid, but those differences diminish greatly in the turbulent range. They concluded that, to achieve measurable heat transfer enhancement, use of nanofluids must be limited to either the low Re laminar range or high Re turbulent range. Unlike most prior investigators, Karimzadehkhouei et al. [71] found no appreciable heat transfer enhancement with TiO_2 and Al_2O_3 nanofluids for $Re < 1000$. However, they did observe appreciable enhancement for turbulent flow, which they attributed to increased nanoparticle mixing at high Re.

2.1.1.2. Fully developed laminar flow. Using 0.01–0.3 vol% Al_2O_3 nanofluids, Hwang et al. [72] showed that friction factor in the fully developed laminar region agrees well with analytical predictions based on the Darcy correlation. And, the convective heat transfer coefficient increased with increasing nanoparticle concentration, by up to 8% at 0.3 vol%, compared to the base fluid (water). Interestingly, this enhancement is greater than the enhancement in effective thermal conductivity, and, as shown in Fig. 4, cannot be predicted according to the Shah correlation [73] for fully developed laminar flow. They attributed the added enhancement to flattening in velocity profile caused by nanoparticle migration. Similar findings were reported by Heris et al. [74,75], who found that incorporating nanofluid properties in the single-phase heat transfer correlation could not predict measured heat transfer enhancement. They attributed the enhancement to combination of increased

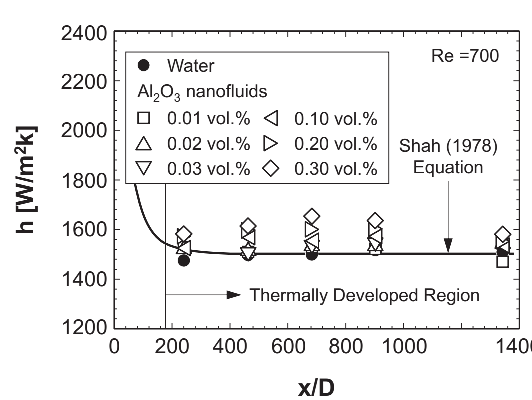

Fig. 4. Axial variations of local heat transfer coefficient for different Al_2O_3 nanofluids in the fully developed laminar regime with $Re = 700$ and channel diameter of 1.812 mm. Adapted from Hwang et al. [72].

thermal conductivity as well as chaotic movement, fluctuations, and interactions of nanoparticles. In follow-up work, they reported that enhancement in heat transfer coefficient increases with increasing Al_2O_3 or CuO nanoparticle concentrations over a range of 0.2–2.5 vol% [75,76]. Another observation was increased enhancement with decreasing nanoparticle size for a given concentration [77,78], with CuO nanofluids providing better heat transfer performance than Al_2O_3 nanofluids for the same concentration [79]. Rostamani et al. [80] also showed that CuO nanofluids provide better heat transfer than Al_2O_3 and TiO_2 nanofluids, including in the turbulent flow regime. On the other hand, Mansour et al. [81] reported that the heat transfer coefficient for Al_2O_3 nanofluid flow in inclined tubes decreases slightly with increasing particle concentration in the range of 0–4 vol%, which they attributed to increased viscosity at low *Re*. Bhanvase et al. [82] showed that the mixture of water and ethylene glycol based TiO_2 nanofluid enhances the heat transfer coefficient by 105% at 0.50 vol% compared to the base fluid mixture. Rea et al. [83] showed that traditional laminar flow model predictions for heat transfer coefficient and pressure drop are quite effective at predicting measured values for nanofluid flow in a vertical tube when thermal properties are based on homogeneous mixture premises.

Anoop et al. [84] showed experimentally that 45-nm Al_2O_3 particles yield higher heat transfer coefficients than 150-nm particles in the laminar developing region, where heat transfer enhancement is higher than that in the fully developed region. Similar trends concerning particle size effects were achieved numerically by Moraveji et al. for the developing region [85] and fully developed laminar region [86], through measurement by Ebrahimnia-Bajestan et al. [87] for Al_2O_3, CuO, CNT and titanate nanotube (TNT) nanofluids, and by Akbari et al. [88] for Al_2O_3 non-Newtonian nanofluids. It should be noted, however, that Kulkarni et al. [89] also noted a decrease in heat transfer coefficient of ethylene glycol and water mixture based SiO_2 nanofluids with decreasing nanoparticle size for turbulent flow. A similar turbulent flow trend was reported by Bahiraei and Hangi [90] for Mn-Zn ferrite magnetic nanofluid. On the other hand, He et al. [91] showed that the heat transfer coefficient for TiO_2 nanofluids is insensitive to average particle size in the range of 95–210 nm for both laminar and turbulent flow regimes. Overall, these studies point to lack of consensus concerning effects of nanoparticle size for different flow regimes.

Heris et al. [92,93] reported that, compared to liquid flow in a circular duct, flow in a square cross-section offers the advantage of lower pressure drop, but at the expense of inferior heat transfer performance. However, the heat transfer coefficient for the square duct could be enhanced with nanofluid use, increasing with increasing nanoparticle concentration, especially at high flow rates. Santra et al. [94] achieved similar heat transfer enhancement by suspending Cu nanoparticles in Newtonian and non-Newtonian base fluids. And, despite 32% enhancement in heat transfer coefficient with 2.0 vol% Al_2O_3 nanofluid, Heyhat et al. [95] showed that maximum pressure drop for the same concentration and $Re = 360$ is 5.7 times higher than for pure water. Ho et al. [96] reported superior heat transfer enhancement with hybrid suspensions in water, which included Al_2O_3 particles (providing improved thermal conductivity), and microencapsulated phase-change-material (PCM) *n*-eicosane particles (providing improved specific heat); the enhancement for both suspensions was independent of flow rate. Follow-up study by Ho et al. [97] culminated in an expression for heat transfer effectiveness. Asirvatham et al. [98] suggested that heat transfer enhancement with nanofluids is mostly the result of accelerated energy exchange resulting from both improved thermophysical properties and chaotic movement of particles. Maïga et al. [99,100] cautioned that, despite the heat transfer benefits in both the laminar and turbulent regimes, nanofluids produce adverse effects in the form of increased wall shear.

Yu et al. [101] reported that established correlations for pure fluids provide satisfactory predictions for both the friction factor and *Nu* for nanofluids containing spherical nanoparticles, but are far less accurate for nanofluids containing rod-like nanoparticles with length-to-diameter ratio greater than unity. Yang et al. [102] showed lower enhancement in heat transfer coefficient for graphite nanofluids than predicted by either conventional heat transfer correlations for homogeneous fluids, or by correlations developed for nanoparticle suspensions with aspect ratio close to unity. On the other hand, Ebrahimnia-Bajestan et al. [87] showed that increasing aspect ratio has a positive effect on the heat transfer coefficient. And Chen et al. [103] found that enhancements of both thermal conductivity and convective heat transfer coefficient using titanate nanotube nanofluids are considerably higher than those of the same base fluid containing spherical titania nanoparticles. Ebrahimi et al. [104] found numerically that cylindrical CNTs offer lower thermal resistance in small channels compared to nanofluids containing spherical nanoparticles. Overall, these references point to the important influence of nanoparticle shape on heat transfer performance. Given the large variations of nanoparticle shape and/or length-to-diameter ratio (*e.g.,* CNT nanoparticles with aspect ratio exceeding 100, spherical particles with aspect ratio of unity, and disc-like nanoparticles with aspect ratio as small as 0.02), these variations must be carefully reported in conjunction with the nanofluid used.

Aminfar et al. [105] performed 3D numerical simulations of magnetic Fe_3O_4 nanofluid (also termed ferrofluid) flow in a vertical tube using a two-phase mixture model and control volume technique. They showed that *Nu* could be adjusted by varying intensity and gradient of an externally applied magnetic field, with negative gradient increasing and positive gradient decreasing *Nu*. Azizian et al. [106] reported that local heat transfer coefficient of Fe_3O_4 nanofluids can be increased by up to 300% by application of magnetic field, explaining this enhancement as the result of particle migration induced by magnetic field gradient, and this had no effect on pressure drop. Lajvardi et al. [107] and Asfer et al. [108] showed experimentally that Fe_3O_4 ferrofluid does not improve heat transfer in the absence of magnetic field, implying that any effects of ferrofluid thermophysical properties on heat transfer are negligible, a finding that contradicts that of Goharkhah et al. [109]. Asfer et al. also pointed out that convective heat transfer coefficient for ferrofluid flow subjected to magnetic field may increase or decrease depending on ratio of magnetic force to inertia acting on the ferrofluid, interaction of ferrofluid flow with aggregate of nanoparticles formed on the tube wall closest to the magnets, and enhancement in local thermal conductivity resulting from chain like clusters of nanoparticles. Goharkhah et al. [110,111] proposed applying alternating magnetic field to Fe_3O_4 nanofluid flow, which yielded higher heat transfer enhancement compared to constant field; they attributed the added enhancement to disruption of thermal boundary layer and increased mixing within the flow. In contrast, they suggested that enhancement from constant magnetic field is confined to the surface, caused by increased local thermal conductivity resulting from migration of nanoparticles towards the surface.

Overall, using conventional pure fluid correlations (*e.g.*, Darcy correlation) to estimate the friction factor for laminar nanofluid flow can yield accurate predictions. However, conventional correlations fail to predict the single-phase convective heat transfer coefficient, which points to a need for new correlations that would account for nanoparticle migration, increased thermal conductivity, chaotic movement, fluctuations, and interactions of nanoparticles. Additionally, correlations must address effects of nanoparticle size and shape.

2.1.2. Turbulent flow

2.1.2.1. Predictive methods. Xuan and co-workers [112,113] showed that the Dittus-Boelter correlation [114] is inaccurate for prediction of single-phase convective heat transfer coefficient for turbulent nanofluid flow. Instead, they proposed the correlation

$$Nu = c_1\left(1.0 + c_2\phi^{m_1}Pe_p^{m_2}\right)Re^{m_3}Pr^{0.4} \tag{3}$$

where coefficients c_1 and c_2, and exponents m_1, m_2 and m_3 were determined empirically, ϕ is nanoparticle volume concentration, and Pe_p particle Peclet number, which is defined as

$$Pe_p = \frac{u_f d_p}{\alpha} \tag{4}$$

α and d_p being the nanofluid's thermal diffusivity and nanoparticle diameter, respectively. Pak and Cho [115] found, for turbulent flow of Al_2O_3 and TiO_2 nanofluids with $Re = 10^4$–10^5, that convective heat transfer coefficient for 3 vol% is 12% smaller than that for pure water, and proposed the alternative correlation

$$Nu = 0.021Re^{0.8}Pr^{0.5} \tag{5}$$

which is applicable to $Pr = 6.54$–12.33. However, Duangthongsuk and Wongwises [116] found that the above correlation underestimates their TiO_2 nanofluid data for nanoparticle concentrations exceeding 0.2 vol%. They therefore developed alternative formulations for Nu and friction factor, f,

$$Nu = 0.074Re^{0.707}Pr^{0.385}\phi^{0.074} \tag{6a}$$

$$\text{and} \quad f = 0.961Re^{-0.375}\phi^{0.052} \tag{6b}$$

respectively, which both account for concentration effects. Maïga et al. [117] showed numerically that the enhancement in heat transfer coefficient increases with increasing nanoparticle concentration, and proposed the following heat transfer relation,

$$Nu = 0.085Re^{0.71}Pr^{0.35} \tag{7}$$

Sajadi and Kazemi [118] found no significant influence of nanoparticle concentration on heat transfer of TiO_2 nanofluids below 0.25 vol%, however, pressure drop did increase with increasing concentration. Teng et al. [119] found that conventional relations fail to predict their pressure drop data; they also showed that the fractional increase in pressure drop is smaller for turbulent flow than for laminar. Kim et al. [29] compared performances of alumina and carbonic nanofluids, employing detailed rheological and thermophysical property measurements. They showed that a 3 vol% alumina nanofluid enhances heat transfer coefficient in both the laminar and turbulent regimes, especially in the entrance region, while a 3.5 vol% carbonic nanofluid fails to show any enhancement in the turbulent regime. Additionally, heat transfer enhancement was always much higher than the increase in thermal conductivity, which implied that the improvement of thermal conductivity is not the sole reason for the heat transfer enhancement. Similar conclusions were drawn by Godson et al. [120], who achieved 69% enhancement with 0.9 vol% silver nanofluid [121], and by Torii and Yang [122] with diamond nanofluid.

Using 0.025–0.1 wt% graphene nanoplatelet nanofluid, Sadeghinezhad and co-workers [123–125] achieved 200% enhancement in heat transfer coefficient for fully developed turbulent flow, but a far milder increase in pressure drop of only 14.7%. The heat transfer coefficient was also observed to increase with increasing specific surface area (m^2/g) of the nanofluid. Using 0.02 vol% graphene nanofluid, Akhavan-Zanjani et al. [126,127] achieved 6.04% and 14.2% enhancements in heat transfer coefficient at $Re = 10850$ and 1850, respectively, corresponding to a 10.3% enhancement in the thermal conductivity. However, lower concentrations in the range of 0.005–0.02 vol% decreased Nu, albeit without influencing pressure drop [126]. Esfe et al. [128] performed turbulent flow measurements for COOH-functionalized double-walled CNTs suspended in water. For concentrations in the range of 0.01–0.4 vol %, they achieved 32% enhancement in heat transfer coefficient, corresponding to a 20% increase in pressure drop. Esfe et al. [129] showed that MgO nanofluids fail to provide significant heat transfer enhancement, and Nu can be predicted according to the classical Gnielinski correlation [130],

$$Nu = \frac{(f/8)(Re-1000)Pr}{1+12.7(f/8)^{1/2}(Pr^{2/3}-1)} \tag{8}$$

Williams et al. [131] showed that fully developed turbulent flow data for 0.9–3.6 vol% Al_2O_3 and 0.2–0.9 vol% ZrO_2 nanofluids agree well with Dittus-Boelter's heat transfer correlation, and conventional friction correlations of Blasius and MacAdams, which are given, respectively, by

$$\text{Dittus-Boelter}: \quad Nu = 0.023Re^{0.8}Pr^{0.3} \tag{9a}$$

$$\text{Blasius}: \quad f = 0.316Re^{-0.25}, \quad \text{for } Re < 30{,}000 \tag{9b}$$

$$\text{MacAdams}: \quad f = 0.184Re^{-0.2}, \; \text{for } Re > 30{,}000 \tag{9c}$$

when using measured temperature-dependent and particle concentration-dependent thermal conductivity and viscosity of the nanofluid. Kayhani et al. [132] achieved good predictions for TiO_2 nanofluids with the Gnielinski and Blasius correlations for heat transfer and friction factor, respectively. Similar findings were reported by Rostamani et al. [80], who numerically investigated heat transfer enhancement using Al_2O_3, CuO, and TiO_2 nanofluids. Ferrouillat et al. [133] also showed that conventional heat transfer and pressure drop correlations are quite effective at predicting nanofluid data, provided dimensional numbers in these correlations are based on the nanofluid's measured thermal and physical properties.

However, Sharma et al. [134,135] and Godson et al. [120] showed that Gnielinski's correlation underestimates heat transfer performance for Al_2O_3 and Ag nanofluids by 12% and 40%, respectively. Yu et al. [136] also showed that a 50–60% enhancement in heat transfer coefficient they measured using 3.7 vol% SiC nanofluid is underpredicted by 14–32%. Gnielinski's correlation also underestimated 0.6 vol% Ni nanofluid enhancement data of Sundar et al. [137] by 26%. Hojjat et al. [138] reported poor agreement between predictions based on correlations for viscous non-Newtonian fluids and their own data for non-Newtonian nanofluids. Zamzamian et al. [139] found that experimental data and theoretical predictions coincid only at low temperatures, and depart appreciably at high temperatures.

Overall, these studies suggest that applicability of heat transfer and pressure drop correlations devised for pure liquids to nanofluids remains questionable, and point to the need for further study using different types of nanofluids.

2.1.2.2. Buongiorno model. Buongiorno [140] conducted a pioneering study in which Brownian diffusion and thermophoresis were identified as primary slip mechanisms for nanofluids, a hypothesis that was also confirmed by Singh et al. [141]. Buongiorno also proposed that nanofluid properties may vary significantly within the boundary layer because of changes to the temperature gradient, resulting in a thermophoresis effect causing nanoparticles to move away from the wall and therefore greatly decreased viscosity within the boundary layer, thereby contributing to the heat transfer enhancement observed with nanofluids. This explanation is a fundamental departure from earlier studies adopting the homogeneous flow assumption, in which only increased thermal conductivity is claimed as responsible for the heat transfer enhancement. It also departs from the dispersion assumption, where both thermal conductivity and nanoparticle dispersion are deemed primary contributors to the heat transfer enhancement. Identifying Brownian diffusion and thermophoresis as the dominant enhancement mechanisms, Buongiorno developed the following modified Gnielinski expression to predict Nu,

$$Nu = \frac{(f/8)(Re - 1000)Pr}{1 + \delta_v^+ (f/8)^{1/2} \left(Pr_v^{2/3} - 1 \right)} \tag{10}$$

where δ_v^+ and Pr_v are dimensionless thickness and Prandtl number of the laminar sub-layer, respectively.

While experimental results by Yu et al. [136] do not support the mechanisms of Brownian diffusion and thermophoresis, Yang et al. [142,143], Malvandi and co-workers [144–152], Hedayati and Domairry [153–155], Garoosi et al. [156], Nield and Kuznetsov [157], Maghrebi et al. [158], Xu et al. [159], Schio et al. [160], Alvariño et al. [161], and Heyhat and Kowsaryall [162] all explained heat transfer trends of nanofluids based on the Buongiorno model. Yang et al. [142] considered the effects of nanoparticle concentration distribution on the continuity, momentum and energy equations in their modified model, and pointed out that lower volume fraction of particles near the wall is responsible for reduced viscosity in the wall region, which leads to high velocity and high temperature gradient near the wall [143]. Malvandi et al. [144,151] also accounted for effects of slip boundary condition resulting from nanoparticle migration near the wall, which contributes to the heat transfer enhancement. Velocity slip was also addressed in simulations by Khan et al. [163] involving a channel with non-parallel walls. Follow-up studies by Malvandi and Ganji [145,146,150] showed that nanoparticles migrate from the heated walls towards the core region of the channel, driven by the temperature gradient [149], forming a non-uniform particle distribution. Nanoparticle volume concentration was reported to gain uniformity with decreasing nanoparticle size [164]. And presence of magnetic field served to increase the near-wall velocity gradient, thereby increasing slip velocity, heat transfer rate, and pressure drop. Malvandi and Ganji [147] also found that asymmetrical wall heating prevents enrichment of near-wall velocity, resulting in reduced heat transfer enhancement compared to symmetrical heating. Malvandi et al. [152] showed that ignoring temperature dependency of thermophysical properties does not significantly influence flow field or heat transfer behavior of nanofluids. Hedayati and Domairry [153–155] adopted the Buongiorno model in numerical modeling of convective heat transfer in vertical and horizontal channels by employing wall slip boundary condition. They suggested that Brownian motion reduces nanoparticle concentration gradient by distributing particles in a homogeneous pattern. In contrast, thermophoresis diffused nanoparticles in a direction opposite to that of the temperature gradient and tends to accumulate them regionally. They concluded that rheological and thermal characteristics of the nanofluid, which depend strongly on nanoparticle arrangement in the flow, are governed by these two opposing effects.

Because its direction is opposite to that of the temperature gradient, thermophoresis tends to move nanoparticles from the wall region to the core, resulting in decreased viscosity (which is positive for heat transfer) and decreased thermal conductivity (which is negative for heat transfer) within the boundary layer. In essence, thermophoresis creates a gradient of nanoparticle concentration inside the channel. However, Brownian motion tends to distribute nanoparticles uniformly. Once thermophoresis precipitates the nanoparticle concentration gradient, its effects are counterbalanced by the Brownian force. However, it is difficult to state which effect is dominant, especially that the relative significance of each varies from case to case. For example, decreasing particle size enhances Brownian motion but suppresses thermophoresis [155].

2.1.2.3. Effects of nanoparticle concentration. Using SiO_2 nanofluids, Azmi et al. [165] showed that nanofluid heat transfer coefficient and pressure drop both increase with increasing nanoparticle concentration up to 3.0 vol%, above which they both decrease. However, Kulkarni et al. [89] found that the heat transfer coefficient and pressure drop of ethylene glycol/water mixture (60:40 by weight) based SiO_2 nanofluids increase with increasing nanoparticle concentration even at 10 vol%. Sundar et al. [137] reported that heat transfer coefficients for 0.02–0.6 vol% Ni nanofluids and Fe_3O_4 nanofluids [166] increase with increasing nanoparticle concentration, due mostly to Brownian motion and micro-convection of particles in the base fluid. Ko et al. [167] found that, under laminar flow conditions, friction factor for CNT nanofluid stabilized by surfactant addition is much larger than for CNT nanofluid prepared by acid treatment, while, under turbulent conditions, both result in fairly similar pressure drops. Zarringhalam et al. [168] showed that influences of nanoparticle concentration on both heat transfer coefficient and pressure drop in the turbulent regime are more appreciable at lower than higher Re.

Duangthongsuk and Wongwises [116] achieved up to 26% enhancement in heat transfer coefficient for TiO_2 nanofluids with nanoparticle concentrations below 1.0 vol%, as shown in Fig. 5. But, the trend reversed above 1.0 vol%, and heat transfer coefficient at 2.0 vol% was 26% lower than for pure water. On the other hand, Kayhani et al. [132] reported that heat transfer coefficient for TiO_2 nanofluids increases with increasing concentration over the entire range of 0.1–2.0 vol%, independent of Re. Arani and Amani [169] showed that Nu for TiO_2 nanofluids increases with increasing concentration in the range of 0.002–0.02 vol%. Follow-up study by Arani and Amani [170] found that Nu does not increase when decreasing TiO_2 nanoparticle size. Using an annular duct with constant wall temperature, Nasiri et al. [171] showed that heat transfer enhancements for both TiO_2 and Al_2O_3 nanofluids increase with increasing particle concentration in the range of 0.1–1.5 vol%. They also reported that any differences in heat transfer enhancement between the two nanofluids are minor.

Fotukian and Esfahany [172] found that Al_2O_3 nanofluids in concentrations below 0.2 vol% have little impact on heat transfer. Follow-up work by Fotukian and Esfahany [173] examined the performance of CuO nanofluids in concentrations below 0.24 vol%. A 25% increase in heat transfer coefficient (and corresponding 20% increase in pressure drop) was predicted well by Buongiorno's correlation [140], Eq. (10), overestimated by the Maïga et al. correlation [117], Eq. (7), and underestimated by the correlation of Pak

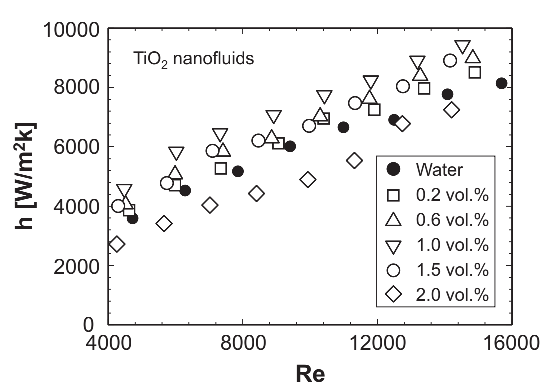

Fig. 5. Effects of nanoparticle concentration on single-phase heat transfer coefficient for TiO_2 nanofluids in 8.13-mm diameter channel. Adapted from Duangthongsuk and Wongwises [116].

and Cho [115], Eq. (5), and Xuan and Li [112], Eq. (3). Vakili et al. [174] found that heat transfer enhancement for ethylene glycol/distilled water based TiO_2 nanofluid is higher than for pure water as base fluid; Mojarrad et al. [175] arrived at a similar conclusion for Al_2O_3 nanofluid.

Overall, most of the studies addressed in this section provide findings corresponding to specific ranges of nanoparticle concentrations, which vary greatly from one study to another. There does appear to be general consensus that heat transfer improves with increasing concentration, but some studies also point to existence of an optimum concentration corresponding to maximum heat transfer enhancement, above which appreciable clustering of nanoparticles in the base fluid begins to adversely influence heat transfer performance.

2.2. Heat transfer in micro-channels ($D < 1$ mm)

2.2.1. Entrance effects

Unlike the observation made earlier concerning declining heat transfer enhancement downstream from the entrance region in macro-channels, Lelea and Nisulescu [176], who also observed high heat transfer enhancement in the entrance region of micro-channels, showed that the enhancement keeps increasing downstream because of more pronounced viscous dissipation near the channel walls. Chabi et al. [177] investigated laminar heat transfer in the entrance region of a micro-channel heat sink using 0.1 and 0.2 vol% CuO nanofluids. They detected maximum local heat transfer coefficient at the channel entrance, which they attributed to entrance effects and small boundary layer thickness. They also measured maximum enhancement in average heat transfer coefficient for $Re = 1150$ of 18% and 40% for 0.1 and 0.2 vol%, respectively, but increasing Re compromised the enhancement because of rapid formation of sediment and nanofluid instability. Azizi et al. [178] found Nu for 0.05–0.3 wt% Cu nanofluids to increase at first with increasing Re, but decrease after reaching a maximum, Fig. 6, a trend they attributed to agglomeration or sedimentation of nanoparticles at higher flow rates, as well as shorter residence time for coolant in a micro-channel heat sink reducing contact time for heat exchange with the walls. Follow-up study by Azizi et al. [179] using Cu nanofluid also showed considerable enhancement of Nu in the entrance region of a micro-channel heat sink.

2.2.2. Heat transfer enhancement and pressure drop penalty

Jang and Choi [180] and Farsad et al. [181] showed numerically that water-based nanofluids enable micro-channel heat sinks to dissipate heat fluxes as high as 1350–2000 W/cm^2. Chein and Huang [182] found analytically that nanofluid flow in a micro-channel heat sink does not increase pressure drop, while Ho et al. [183] reported only a slight increase in the friction factor. Ho and Chen [184] found, for fixed flow rate in a micro-channel heat sink, that the merit of using Al_2O_3 when taking pumping power penalty into account improves with increasing nanoparticle concentration up to a maximum of 6.0 wt%. Wang et al. [185] showed experimentally, for CNT nanofluid flow in a 0.952-mm stainless steel tube, heat transfer enhancements at $Re = 120$ up to 70% and 190% for concentrations of 0.05 and 0.24 vol%, respectively. Since thermal conductivity in these experiments was enhanced by less than 10%, they concluded that thermal conductivity is not the sole reason for the measured enhancement. Lee et al. [186] pointed out that thermal conductivity for CNT nanofluids is dictated not only by nanoparticle concentration, but tube shape as well; only long and uniform nanotubes provided the desired appreciable increase in thermal conductivity. They also pointed out important practical concerns when flowing nanofluids in small diameter tubes, including both clogging and wall abrasion as nanoparticles tended to entangle and adhere to each other to form large clusters.

Chein and Chuang [187] showed that water-based CuO nanofluid flow in a micro-channel heat sink enhances heat dissipation compared to pure water at low flow rates, but no enhancement is achieved at high flow rates. Li and Kleinstreuer [188] showed that CuO nanofluid flow in a trapezoidal micro-channel does provide the intended heat transfer enhancement. Mohammed et al. [189] found numerically that nanofluids increase the single-phase heat transfer coefficient with little pressure drop penalty rise at low concentrations, but fail to enhance heat transfer at high concentration (5 vol%). In follow-up study, Mohammed et al. [190,191] provided a comprehensive assessment of material effects, including base fluid (water, ethylene glycol, oil, and glycerin), substrate (copper, aluminum, steel, and titanium), and nanoparticle (Ag, Al_2O_3, CuO, SiO_2, and TiO_2) on heat transfer in micro-channel heat sinks with rectangular and trapezoidal channels. Overall, glycerin-based nanofluid provided lowest thermal resistance, and SiO_2 particles yielded highest heat transfer coefficient. And, average heat transfer coefficient was greater for low Prandtl number fluids with high thermal diffusivity particles than those with low thermal diffusivity. Rimbault et al. [192] showed experimentally that CuO nanofluid imposes severe pressure drop penalty, especially at high nanoparticle concentrations. For example, compared to pure water (base fluid), 4.5 vol% concentration increased pressure drop by 70% and 58% for isothermal and heating conditions, respectively. They also pointed out that, despite the measured enhancement in heat transfer at low concentrations, the nanofluid's overall performance, defined as ratio of transferred heat to pumping power, for a given Re, is lower than for pure water; and performance decreases even further with increasing concentration.

Sohel et al. [193] showed analytically that 0.5–4.0 vol% CuO nanofluid flow in a copper micro-channel heat sink having circular channels provides far better heat transfer performance and lower friction factor than Al_2O_3 and TiO_2 nanofluids. Follow-up experimental work by Sohel et al. [194] focused on heat transfer enhancement characteristics of Al_2O_3 nanofluid flow in a micro-channel heat sink. Peyghambarzadeh et al. [195] showed experimentally that, when using water as base fluid, CuO nanoparticles provide better heat transfer than Al_2O_3, but are more prone to deposit upon the channel walls. They also measured deterioration in performance at both higher flow rates and higher nanoparticle concentrations because of deposition effects, and reported that high nanoparticle concentrations increase the heat transfer coefficient but decrease Nu. As shown in Fig. 7, Nu enhancement with Al_2O_3 and CuO nanofluids improves with increasing Re in the low Re range, reaching maximum value before decreasing with further

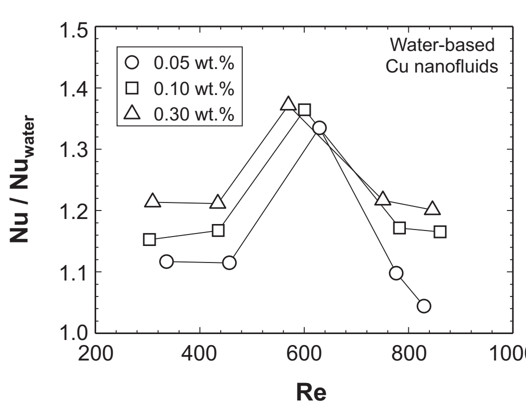

Fig. 6. Nusselt number ratio for Cu nanofluid compared to that for water (base fluid) versus Reynolds number in a micro-channel heat sink with 560-μm hydraulic diameter for different nanoparticle concentrations. Adapted from Azizi et al. [178].

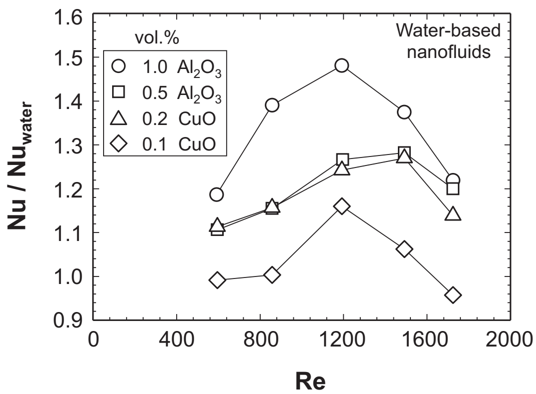

Fig. 7. Nusselt number ratio for Al_2O_3 and CuO nanofluids to that for water (base fluid) versus Reynolds number in a heat sink containing 400 μm × 560 μm micro-channels. Adapted from Peyghambarzadeh et al. [195].

increases in *Re*. Sivakumar et al. [196] also showed that CuO nanofluid provides better heat transfer coefficient enhancement than Al_2O_3 nanofluid. Salman et al. [197,198] showed numerically that dispersing SiO_2 nanoparticles in ethylene glycol (base liquid) provides the highest *Nu*, followed by ZnO, CuO, and Al_2O_3, and *Nu* increases with decreasing nanoparticle size. Mohammed et al. [199] found that heat transfer coefficient for water-based Al_2O_3 nanofluid is superior to those for SiO_2, Ag, and TiO_2, and heat transfer rate decreases with increasing nanoparticle concentration in the 2–10 vol% range. Using a micro-channel heat sink with access ports between channels, Tokit et al. [200] showed that Al_2O_3 nanofluid provides the highest enhancement in *Nu*, followed by CuO and SiO_2. Mohammed et al. [201] compared the thermal and hydraulic performances of Al_2O_3, Ag, CuO, diamond, SiO_2, and TiO_2 nanofluids using a micro-channel heat sink featuring triangular channels, and showed that diamond provides the highest heat transfer coefficient and Ag lowest pressure drop. These findings are proof that it is difficult to identify an optimum nanoparticle material, given the simultaneous advantageous and disadvantageous trends for individual materials.

Nimmagadda and Venkatasubbaiah [202] showed numerically that thermal performance of hybrid nanofluids containing both Al_2O_3 and Ag nanoparticles is superior to that using the individual nanoparticle materials for the same volumetric concentration. The superiority in heat transfer enhancement using hybrid nanofluids was confirmed numerically by Labib et al. [203] for Al_2O_3-CNT nanofluids. On the other hand, Suresh et al. [204] showed experimentally that 0.1 vol% Al_2O_3-Cu nanofluid yields slightly higher friction factor than Al_2O_3 nanofluid.

Zhang et al. [205] reported that *Nu* enhancement using Al_2O_3 nanofluids in laminar flow increases with increasing *Re*, as well as with increasing nanoparticle concentration in the range of 0.25–0.77 vol%. Jung et al. [206] found experimentally that pressure loss for Al_2O_3 nanofluids is similar to that for water (base fluid). Nitiapiruk et al. [207] studied experimentally effects of uncertainties in thermophysical properties on *Nu* and friction factor. They showed that using different models to calculate thermal conductivity has no considerable effect on *Nu* prediction, but different friction factor models have profound influences on pressure drop. Escher et al. [208] compared *Nu* in a micro-channel heat sink for SiO_2 nanofluids in concentrations up to 31 vol% to theoretical predictions accounting for changes in thermal properties. They reported deviations of less than 10%, and concluded that (1) the influence of nanoparticle addition on heat transfer is quite minor, and (2) standard correlations are quite effective at predicting convective heat transfer for nanofluids, provided the thermophysical properties of the nanofluid were used.

Koo and Kleinstreuer [209] investigated the thermal performance of CuO nanofluids flowing through a micro-channel sink, and recommended several strategies for enhancing heat transfer performance: high Prandtl number base fluid, nanoparticles in high volume concentration with elevated thermal conductivity and dielectric constant very close to that of the base fluid, micro-channels with high aspect ratio, and treated channel walls that resist nanoparticle accumulation. Given the trade-off between increased thermal conductivity and increased viscosity, the latter was deemed more significant for very narrow channels, raising pressure drop penalty and pumping power for the micro-channel heat sink.

Raisi et al. [210] showed that the slip boundary condition is important to analysis of thermal performance of nanofluid flow in a micro-channel heat sink, pointing out that, while its effect on heat transfer rate is negligible at low *Re*, increasing the slip velocity coefficient increases heat transfer rate at high *Re*. Nikkhah et al. [211] found that, for *Re* = 1–100, *Nu* for nanofluids increases with increasing slip coefficient. On the other hand, Karimipour et al. [212], using the lattice Boltzmann method (LBM), showed for very low *Re* (down to 0.01), that heat transfer coefficients for Cu, Ag, and Al_2O_3 nanofluids decrease with increasing slip coefficient.

For micro-channel heat sinks with internal fins, Bhattacharya et al. [213] found that use of nanofluids can enhance heat sink thermal performance by reducing fin thermal resistance. Hung et al. [214] showed numerically that thermal resistance for a micro-channel heat sink first decreases and then increases with increasing nanoparticle volume concentrations and, for moderate nanoparticle sizes, thermal resistance decreases with decreasing particle size, and heat transfer improvement is dictated far more by nanoparticle concentration than by nanoparticle size. Experiments by Byrne et al. [215] showed the importance of using surfactant to achieve a well-dispersed, stable suspension of nanofluid, with little heat transfer improvement realized without the use of surfactant.

2.2.3. Predictive models

Ghazvini and Shokouhmand [216] compared thermal performance for CuO nanofluid flow in a micro-channel heat sink based on two different approaches: fin model and porous media model. The fin model was based on the assumption of uniform fluid temperature normal to the flow direction, while the porous media model employed a modified Darcy equation for the fluid, and two-equation model for heat transfer between solid and fluid. Using the porous media model, Hatami and Ganji [217] concluded that Brownian motion of Cu nanoparticles, which carries heat and distributes it to the surroundings, intensifies with increasing particle concentration, decreasing temperature difference between wall and liquid. Tsai and Chein [218] described nanofluid flow and heat transfer in a micro-channel heat sink using a two-equation model, while the heat sink was treated as porous medium. They showed that the nanofluid could enhance heat transfer performance of the heat sink only where porosity and channel aspect ratio are below specific threshold values. A similar porous media model was adopted by Abbassi and Aghanajafi [219] to investigate Cu nanofluid flow in a micro-channel heat sink. Chen and Ding [220] also used a porous media model and concluded that temperature distribution of the channel wall is not sensitive to the inertial effects, but fluid temperature distribution and total thermal resistance change appreciably.

Xuan et al. [221] developed a mesoscopic model employing LBM to simulate ferrofluid flow through a micro-channel. They showed that heat transfer could be enhanced when magnetic field gradient is orientated parallel to the incoming stream, while an opposite gradient compromises heat transfer. They also showed that when the gradient is perpendicular to the flow direction, heat transfer is either enhanced or suppressed, depending on orientation synergy of magnetic field gradient and temperature gradient. Also using the LBM method, Yang and Lai [222,223] showed that temperature distribution is more uniform in nanofluid than pure water because of higher heat conduction rate in solid particles. Mital [224,225] developed a semi-empirical numerical model to investigate flow and heat transfer characteristics of nanofluid in a micro-channel heat sink, in which heat transfer performance was measured by 'heat transfer enhancement ratio' (HTR), defined as ratio of average heat transfer coefficient for nanofluid to that for water corresponding to equal pumping power. They showed that HTR is affected mostly by nanoparticle volume fraction, followed by nanoparticle diameter, while effects of other parameters, including *Re*, are rather weak. In their analysis, maximum HTR was achieved with the smallest nanoparticle diameter because of tendency of very small particles to improve heat transfer without affecting pumping power. Additionally, maximum HTR for a fixed *Re* was achieved at an optimal value of volume fraction. Wang et al. [226,227] developed a 'combined optimization' model, based on a simplified conjugate-gradient method and three-dimensional nanofluid-cooled micro-channel heat sink model, to investigate optimal geometric structure for a silicon heat sink.

2.3. Numerical approaches

2.3.1. Single-phase models

Two numerical simulation methods have been employed to model nanofluid heat transfer: *single-phase method*, in which the nanofluid is modeled as homogeneous mixture of nanoparticles and base liquid, and *two-phase method*, where nanoparticles and base liquid are treated as separate phases with separate models used to solve for momentum and heat transfer for each phase. The two-phase method can be classified further into two modeling approaches. For low particle volume fractions, the Eulerian-Lagrangian method is commonly used, in which base fluid is described using an Eulerian model and particles a Lagrangian model. While, for high particle volume fractions, the Eulerian-Eulerian method is preferred, which includes *volume of fluid*, *mixture*, and *Eulerian* treatments [228]. But, for micro-channels in particular, Singh et al. [229] suggested that the Eulerian-Lagrangian method is better suited for high *Re* conditions and the single-phase method for low *Re*.

It should be noted that most earlier numerical models of nanofluid flow employed the single-phase method. They include works by Maïga et al. [99,117], Akbarinia and Behzadmehr [230,231], Akbari and co-workers [232,233], He et al. [234], Namburu et al. [235], Mansour et al. [236], Izadi et al. [237], Ahmed et al. [238], Demir et al. [239], Bayat and Nikseresht [240,241], Moraveji et al. [242,243], Seyf and Mohammadian [244], and Manca et al. [245]. He et al. employed both Newtonian and non-Newtonian depictions to prove that non-Newtonian character of nanofluids has a measurable influence on overall enhancement. Corcione et al. [246] proved the existence of an optimal particle concentration for either maximum heat transfer at constant driving power, or minimum cost of operation at constant heat transfer rate; the optimum concentration was found to increase with increasing nanofluid bulk temperature, increasing *Re*, or decreasing length-to-diameter ratio, but was fairly independent of nanoparticle diameter. Kamali and Binesh [247] showed that CNT nanofluids exhibit non-Newtonian behavior with shear-thinning feature, and presented analysis based on the non-Newtonian power law model.

Using the LBM method, Ahmed and Eslamian [248] examined effects of Brownian force and thermophoresis on nanofluid heat transfer in micro-channels. While thermophoresis effects were negligible, those of Brownian force were quite significant, especially for $Re = 1–10$, rendering the nanofluid nonhomogeneous. On the other hand, for $Re > 100$, they found nanofluids to behave homogeneously. But for $Re > 725$, Mokmeli and Saffar-Avval [249] employed a different single-phase method, the *dispersion model*, which addresses irregular movement of nanoparticles, to simulate nanofluid heat transfer. Fig. 8 shows that the dispersion model provides better predictive accuracy than the homogenous model. Mojarrad et al. [250] showed that the homogenous single-phase model underestimates, while the two-phase mixture model overestimates, heat transfer results. It is important to point out that, while the Eulerian-Lagrangian two-phase model provides reasonable predictions of thermal behavior for nanofluids, it is very time demanding and requires appreciable computer capacity. Instead, the single-phase dispersion model, which has also shown high predictive accuracy, is much simpler to implement. Özerinç et al. [251] showed that the single-phase depiction, with the assumptions of temperature-dependent thermal conductivity and thermal dispersion, is a fairly accurate approach for analysis of nanofluid heat transfer.

It should be noted, however, that a key problem with the single-phase method is lack of accurate models or relations for thermal conductivity and viscosity of nanofluids. This notion is evident from a study by Mansour et al. [252], who emphasized the need for accurate property predictions by pointing out that important parameters, such as required tube length for fixed mass flow rate and bulk temperature change, or pumping power for fixed heat transfer rate, vary significantly with the nanofluid's thermophysical properties. On the other hand, as commented by Magyari [253], the homogeneous model, which does not account for Brownian diffusion or thermophoresis, is essentially equivalent to standard models for the base fluid, *i.e.*, it does not exhibit pronounced particularities when used to model nanofluids.

2.3.2. Eulerian-Eulerian two-phase models

Using the two-phase mixture method, Mirmasoumi and Behzadmehr [254,255] found the heat transfer coefficient to increase appreciably with decreasing nanoparticle mean diameter. This finding was confirmed by Kalteh et al. [256] using an Eulerian two-phase model, and Akbarinia and Laur [257] using a two-phase mixture model. Allahyari et al. [258] used the two-phase mixture model to investigate laminar convective heat transfer of a nanofluid through an inclined tube with circumferentially non-uniform heating, and follow-up study by Allahyari et al. [259] addressed nanofluid flow in a horizontal tube. Esmaeilnejad et al. [260] used the same model to investigate heat transfer behavior of non-Newtonian nanofluids, and concluded that heat transfer

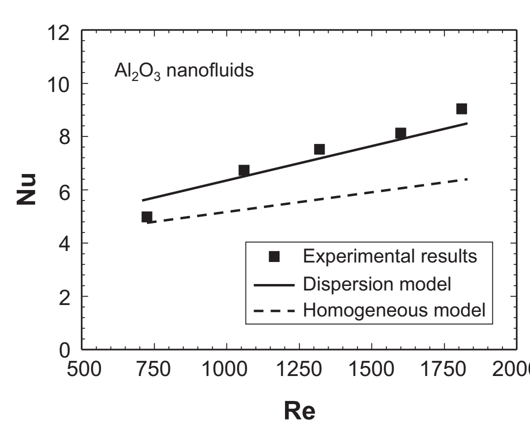

Fig. 8. Comparison of predictions of dispersion model and homogenous model with experimental results for Al_2O_3 nanofluid. Adapted from Mokmeli and Saffar-Avval [249].

enhancement using Al_2O_3 nanoparticles is superior to that using CuO, but the latter provide lower pressure drop. Using the two-phase mixture model and assuming constant fluid properties (except for density), Moghari et al. [261] investigated Al_2O_3 nanofluid flow in an annulus, and Shariat et al. [262] in an elliptical channel. Heris et al. [263] and Aghanajafi et al. [264] examined laminar heat transfer of Al_2O_3 and CuO nanofluids, respectively, in triangular channels. Besides thermal conductivity enhancement, Heris et al. showed that addition of nanoparticles into base fluid also affects flow structure, and ensuing random movement and dispersion of nanoparticles contribute to the heat transfer enhancement. They also showed that *Nu* increases with decreasing diameter or increasing concentration of nanoparticles.

Kalteh et al. [256] found that relative velocity and temperature between the phases are quite small, and distribution of nanoparticle concentration is uniform, which justifies treating nanofluid as a homogeneous solution. They also attributed the underestimation of heat transfer enhancement by homogeneous models to insufficient accuracy of nanofluid thermophysical property models. However, Kalteh et al. [265] showed in follow-up work that the two-phase method provides better accuracy than the homogeneous method in predicting nanofluid heat transfer in a micro-channel heat sink, and works by Akbaridoust et al. [266], Fard et al. [267], and Behzadmehr et al. [268] confirmed this finding. In regards to entrance region effects, Göktepe et al. [269] showed that the two-phase method predicts the heat transfer coefficient and friction factor more accurately than the single-phase method. Behzadmehr et al. reported that accuracy of the two-phase method could be improved by using accurate thermophysical properties for the nanofluid instead of those based on volume weighted averaging of nanoparticle and base fluid. Lotfi et al. [270], and Ghale et al. [271] also confirmed superior predictive accuracy of the two-phase mixture model compared to the single-phase model, indicating that the latter generally underestimates *Nu*. Moraveji and Ardehali [272] assessed the effectiveness of the single-phase model along with three types of two-phase models: volume of fluid, mixture, and Eulerian. They showed that hydrodynamic and thermal characteristics predicted by the different two-phase models are very close to one another [273], whereas those predicted by the single-phase model are far less accurate. They concluded that the two-phase mixture model is a better overall choice in terms of good predictive accuracy and reduced running time and CPU usage.

On the other hand, Akbari et al. [228] found that single-phase and two-phase models predict almost identical flow fields. However, thermal predictions of the two-phase model were very sensitive to nanoparticle volume fraction, which led to overprediction of experimental data with increasing volume fraction. They also showed that predictions of the three Eulerian-Eulerian two-phase methods (volume of fluid, mixture, and Eulerian) are essentially the same [274]. Shown in Fig. 9(a)–(c) are comparisons of heat transfer coefficients calculated using the single-phase model and three different two-phase models with experimental data for Al_2O_3 nanofluids at *Re* = 1050 and different volumetric fractions. In contrast, the single-phase model provided good predictions for turbulent flow [228].

It is important to note that most numerical models of nanofluid heat transfer ignore thermophysical property variations with temperature. As indicated by Kamyar et al. [275], better predictive accuracy could be realized with the same models by incorporating temperature-dependent property variations, especially those of thermal conductivity and viscosity.

2.3.3. Eulerian- Lagrangian two-phase models

He et al. [66] published a pioneering investigation of nanofluid entrance region effects using the Eulerian-Lagrangian two-phase model. Bianco et al. [276,277] reported that predictions of the

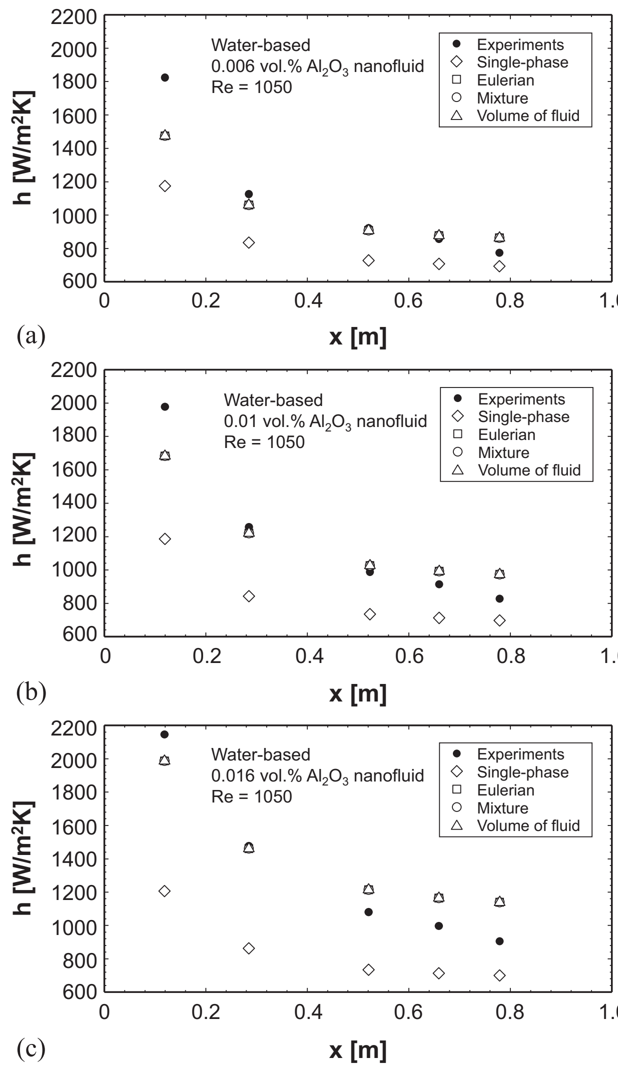

Fig. 9. Comparison of convective heat transfer coefficient calculated using single-phase model and three different two-phase models with experimental data for water-based Al_2O_3 nanofluid at *Re* = 1050 and volume fractions of (a) 0.006 vol%, (b) 0.01 vol%, and (c) 0.016 vol%. Adapted from Akbari et al. [274].

single-phase and Eulerian-Lagrangian two-phase model are fairly similar, with maximum difference in average heat transfer coefficient of 11%. Using the Eulerian-Lagrangian two-phase model, Tahir and Mital [278] investigated effects of three independent variables: nanoparticle diameter, volume concentration, and *Re*; they reported that the heat transfer coefficient increases linearly with increases in *Re* and/or particle concentration, but exhibits a non-linear parabolic decrease with increasing nanoparticle size. Mahdavi et al. [279] used the Discrete Phase Model (DPM), a Eulerian-Lagrangian-based method, which treats base fluid as continuous phase and nanoparticles as discrete phase, to simulate motion of nanoparticles using an equation for force balance on individual nanoparticles; this method did not require use of empirical correlations for thermophysical properties. This model was effective at capturing volume fraction distribution for ZrO_2 nanofluid flow in a tube, and showed that slip velocity between nanoparticles and base fluid is not negligible. As shown in Fig. 10, nanoparticles exhibit more uniform distribution in base fluid at low volume concentrations than at high concentrations, which points to increased likelihood of nanoparticle clustering with increasing volume fraction.

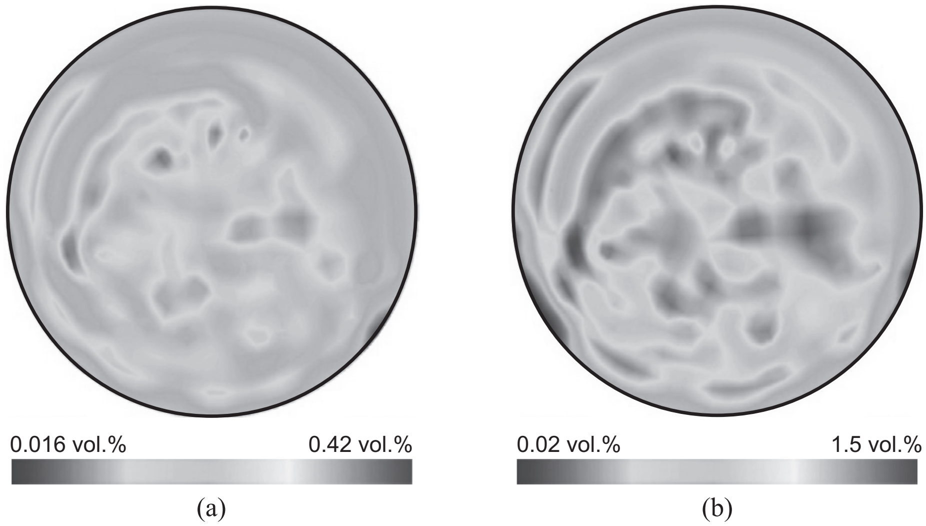

Fig. 10. Nanoparticle concentration distribution for water-based ZrO_2 nanofluid in a 4.5-mm diameter tube with initial particle concentrations of (a) 0.32 vol% at *Re* = 356, and (b) 1.32 vol% at *Re* = 293. Adapted from Mahdavi et al. [279].

Overall, using different numerical methods to investigate nanofluid heat transfer in channels has received increased emphasis from the scientific community in recent years. Despite the numerous works presented, there remain several limitations for most methods used. For example, because of inherent nature of many of these methods, distribution of particle concentration is often poorly predicted. This leads to great difficulty in predicting particle clustering in base fluid at high nanoparticle concentrations, which is known to have appreciable adverse heat transfer effects. Absent ability to address this clustering problem causes a majority of numerical studies to predict monotonic heat transfer enhancement with increasing nanoparticle concentration because of increased thermal conductivity, which is not true for very high concentrations. It should also be pointed out that non-Newtonian features of nanofluids are ignored in most numerical efforts. Therefore, additional work is needed to address both the clustering phenomenon and non-Newtonian aspects of nanofluid flows.

2.4. Entropy analysis

2.4.1. Macro-channel flow

Entropy analysis of nanofluids has attracted significant attention in recent years as investigators sought means to minimize total entropy generation as important basis for design and selection of channel structure as well as working fluid. Moghaddami et al. [280] reported that adding nanoparticles into base fluid increases entropy generation when pressure drop irreversibility is dominant. Bianco et al. [281] proposed an analytical method to determine optimal *Re* for minimal entropy generation, whose magnitude decreased with increasing nanoparticle concentration. Leong et al. [282] studied entropy generation for nanofluid flow through a circular tube with constant wall temperature, and showed that TiO_2 nanofluid contributes lower total dimensionless entropy generation than Al_2O_3 nanofluid. Singh et al. [283] addressed impact of tube dimensions on entropy generation. They concluded that Al_2O_3 nanofluid with high viscosity is not suitable for the use in either macro-channels (10 mm) under turbulent flow conditions or micro-channels (0.1 mm) under laminar. Sohel et al. [284] reported that entropy generation rate could be decreased by decreasing channel diameter and/or increasing nanoparticle volumetric concentration. They also showed that copper nanoparticles exhibit lower entropy generation than alumina, and water provides better performance than ethylene glycol as base fluid because of higher thermal conductivity of the former. These trends are reflected in Fig. 11, which shows variation of entropy generation ratio, defined as the ratio of entropy generation of nanofluid to that of base fluid, with volume concentration for both base fluids as well as Cu and Al_2O_3 nanoparticles. Bahiraei and co-workers [285,286] found that entropy generation rate is also strongly influenced by particle migration, especially for large particles and high concentrations.

2.4.2. Micro-channel flow

As to micro-channels, Li and Kleinstreuer [287] demonstrated existence of an optimal *Re* range for minimal entropy generation, which was lower for micro-channels with high aspect ratio. At low *Re*, very low volume fraction nanofluids with metal nanoparticles provided excellent cooling performance as well as helped minimize entropy generation because of superior thermal properties. Shalchi-Tabrizi and Seyf [288] showed that overall entropy generation rate for Al_2O_3 nanofluid flow in tangential micro-channel heat sink decreases with increasing nanoparticle volume fraction and/or increasing *Re*, and decreasing nanoparticle size.

Hung [289] showed analytically that neglecting viscous dissipation leads to overestimation of heat transfer enhancement for nanofluid flow in micro-channels. However, their analysis was based on constant nanofluid properties, and ignored any temperature dependence. Mah et al. [290] used entropy analysis to show that both thermal performance and exergetic effectiveness of

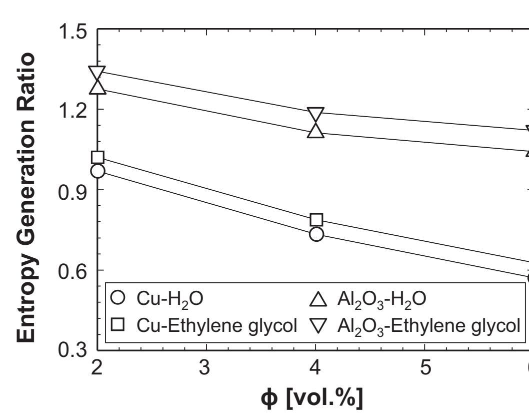

Fig. 11. Variation of entropy generation ratio for different nanofluids with volume concentration at *Re* = 10,000. Adapted from Sohel et al. [284].

nanofluid flow in micro-channels decrease with increasing nanoparticle volume fraction. Ting et al. [291] pointed to important contribution of streamwise conduction resulting from increased conductivity, especially for low Peclet numbers and high nanoparticle concentrations. Follow-up study by Ting et al. [292] accounted for effects of streamwise conduction and found, where heat transfer irreversibility was dominant, that increasing micro-channel's aspect ratio enhances exergetic efficiency. In contrast, when fluid friction irreversibility was dominant, choice of working fluid was more important than the micro-channel's aspect ratio. Ting et al. [293] also addressed optimization of nanofluid flow and heat transfer in a micro-channel heat sink using the theory of field synergy. They found that, under heating conditions, degree of synergy between velocity and temperature deteriorates as a result of viscous dissipation, which compromises overall heat transfer performance. On the other hand, degree of synergy increased with decreasing nanoparticle size and/or increasing micro-channel size. But under cooling conditions, they found that viscous dissipation improves field synergy. Ting et al. [294,295] also examined nanofluid flow in porous media embedded in a micro-channel. They showed that ignoring viscous effects leads to significant overestimation (as much as 60%) of the nanofluid's thermal performance. They also found that low channel aspect ratio causes nanoparticles to greatly increase entropy generation, thereby compromising thermodynamic efficiency. On the other hand, for high channel aspect ratios, entropy generation decreased with increasing nanoparticle concentration at low *Re*, but this trend reversed above a critical value of *Re* = 100.

2.5. Hybrid enhancement techniques

2.5.1. Use of inserts

Aside from heat transfer in straight and smooth channels, investigators have also explored combining heat transfer merits of nanofluids with those of commonly used enhancement techniques, such as channel inserts and use of helical, corrugated, and ribbed channels, as well as with application of active, externally induced flow enhancement methods, such as use of ultrasonic vibration.

Suresh et al. [296] investigated flow of Al_2O_3 nanofluid in a circular tube fitted internally with spiraled rod inserts and showed 48% increase in mean *Nu* under turbulent conditions and 0.5 vol% concentration; they also indicated that pressure drop penalty with this scheme is comparable to that for pure water. Suresh et al. also assessed performance of 0.1 vol% Al_2O_3 and CuO nanofluids in a circular duct fitted with helical screw tape inserts under transition flow conditions [297] and laminar [298]. They concluded that, for equal pumping power, CuO nanofluid provides better heat transfer performance than Al_2O_3 nanofluid in both flow regimes. Sharma et al. [134,135] reported benefits of Al_2O_3 nanofluid along a tube fitted with twisted tape inserts. Azmi et al. [299] reported that, without use of inserts, TiO_2 nanofluid with 1.0 vol% concentration yields up to 23.2% heat transfer enhancement. However, with twisted tape inserts, despite 48.1% heat transfer enhancement at 1.0 vol% concentration, friction factor was almost twice that for pure water. Wongcharee and Eiamsa-ard [300] showed that simultaneous use of CuO nanofluid and modified twisted tape with alternate axes improves *Nu* appreciably compared to standard twisted tape, and by up to 13.8 times that for plain tube. Using Fluent, Pathipakka and Sivashanmugam [301] provided insight into motion of Al_2O_3 nanofluid in a tube fitted with helical twist inserts.

Chandrasekar et al. [302] achieved increased heat transfer enhancement for laminar flow of 0.1 vol% Al_2O_3 nanofluid in a circular tube that was fitted with wire coil inserts, attributing much of this enhancement to thermal dispersion and back-mixing flattening temperature distribution and increasing temperature gradient between wall and nanofluid. Follow-up work by Chandrasekar et al. [303] extended these findings to the transition regime corresponding to *Re* = 2500–5000.

Tullius and Bayazitoglu [304] showed that coating the channel walls with CNT arrays (in full or circular staggered fin patterns) provides little or no increase in heat transfer enhancement for 0.01 vol% Al_2O_3 nanofluid. Khoshvaght-Aliabadi et al. [305] provided both *Nu* and friction factor correlations for Cu nanofluid flow through seven different types of plate-fin channels, including plain, perforated, offset-strip, louvered, wavy, vortex-generator, and pin. Follow-up study by Khoshvaght-Aliabadi and Alizadeh [306] investigated heat transfer characteristics for Cu nanofluid flow in straight tubes modified with different types of inserts, including perforated-tape, jagged-tape, twisted-tape, helical-screw, vortex-generator, and offset-strip, and showed that best heat transfer performance is achieved with the vortex-generator insert.

Servati et al. [307] used the LBM method to investigate effects of vertical and uniform magnetic field on flow and heat transfer characteristics of Al_2O_3 nanofluid in a horizontal channel partially filled with porous medium. Use of porous media was also investigated by Hajipour and Dehkordi [308,309] for nanofluid flow in a vertical channel, and by Siavashi et al. [310] an annular pipe (partially or completely filled with porous medium). Nazari et al. [311] reported 57% heat transfer enhancement for 1.5 vol% Al_2O_3 nanofluid at *Re* = 3704, which was realized at the expense of 39% pressure drop penalty. Follow-up study by Nazari and Toghraie [312] addressed nanofluid heat transfer in porous-medium-filled sinusoidal channel. Ashtiani et al. [313] reported heat transfer enhancement for CNT nanofluid flow through flattened tubes under uniform temperature conditions. Saeedinia et al. [314] reported 45% increase in heat transfer coefficient but 63% pressure drop penalty for oil-based CuO nanofluid flow in a tube fitted with wire coil inserts. Sun and Yang [315] examined heat transfer characteristics of R141b-based nanofluids in an internally threaded tube using different nanoparticle materials (Cu, CuO, Al, and Al_2O_3), and showed that higher conductivity nanoparticles provide more superior heat transfer performance [316].

Mohammed et al. [317] opted for use of louvered strip inserts to enhance heat transfer for Al_2O_3, CuO, SiO_2, and ZnO nanofluids with 1–4 vol% concentrations and nanoparticle sizes of 20–50 nm. They showed 367–411% increases in *Nu* for the insert with highest slant angle of 30° and lowest pitch of 30 mm, but with a corresponding friction coefficient 10 times that of a smooth tube. Overall, *Nu* increased with decreasing nanoparticle size and, to a lesser extent, increasing nanoparticle volume concentration, with SiO_2 providing the most superior performance.

2.5.2. Helical channels

Akhavan-Behabadi et al. [318] and Pakdaman et al. [319,320] studied heat transfer enhancement for CNT nanofluid flow in the thermal entrance region of vertical helically coiled tubes; *Nu* was increased by a factor of 10 compared to flow of base fluid through a straight tube [318]. Darzi et al. [321] experimentally investigated heat transfer performance of SiO_2 nanofluid flow through a helically corrugated tube. In follow-up study, Darzi et al. [322] provided numerical heat transfer predictions for turbulent Al_2O_3 nanofluid flow inside similar tubes. Kannadasan et al. [323] investigated turbulent CuO nanofluid flow in a helically coiled channel, and showed only minor differences in heat transfer enhancement for horizontal and vertical flow orientations when compared to that of the base fluid (water). Jamal-Abad et al. [324] observed fluctuations in *Nu* for laminar flow of Al and Cu nanofluids in a spiral coil, which they attributed to secondary flow effects. Using oil-based CuO nanofluids, Hashemi and Akhavan-Behabadi [325] showed that using a helical tube instead of a straight tube provides better enhancement in heat transfer coefficient than achieved by replacing the base fluid with nanofluid in a straight tube.

Huminic and Huminic [326], Mohammed and Narrein [327,328], and Sasmito et al. [329] presented numerical treatments of laminar heat transfer characteristics of various nanofluids in circular or square helical channels. Khairul et al. [330] analytically addressed heat transfer coefficient and entropy generation for helically coiled tube flows of water-based CuO, Al_2O_3 and ZnO nanofluids, of which CuO nanofluids provided best overall performance. Kahani et al. [331] found that Al_2O_3 nanofluid flow in a helical coiled tube provides better heat transfer enhancement than TiO_2 nanofluid, possibly because of better thermal conductivity and smaller nanoparticle size for the former. Jamshidi et al. [332] reported that use of constant versus temperature-dependent thermophysical properties of nanofluids has strong influence on predicted thermal performance for flow in a coiled tube. Akbari et al. [333] and Alikhani et al. [334] used a modified two-phase mixture model to investigate nanofluid heat transfer in a curved tube.

2.5.3. Corrugated channels

Yang et al. [335] reported heat transfer enhancement results for R141b-based CNT nanofluids inside a corrugated tube. Khoshvaght-Aliabadi and Sahamiyan [336,337], Yang et al. [338], Ahmed et al. [238,339,340], and Akbarzadeh et al. [341] addressed heat transfer characteristics of nanofluids in corrugated or wavy mini-channel heat sinks. Wongcharee and Eiamsa-ard [342] investigated heat transfer characteristics of 0.3–0.7 vol% CuO nanofluids, and found that heat transfer is improved most with use of corrugated tubes fitted with twisted tape, especially as nanoparticle concentration is increased. They also showed that counter arrangement of corrugated tubes (with fitted with twisted tape) provides better heat transfer performance than parallel arrangement.

2.5.4. Ribbed channels

Using a single-phase model, Manca et al. [343] and Parsazadeh et al. [344] simulated turbulent forced convection of nanofluids in rectangular-ribbed channels, while Gravndyan et al. [345] and Akbari et al. [346] addressed laminar convection. Alipour et al. [347] studied heat transfer of nanofluids in T-semi-ribbed micro-channels, while Andreozzi et al. [348] and Mohammed et al. [349] compared thermal performances of triangular, rectangular, and trapezoidal ribs. Vanaki and Mohammed [350] also investigated effects of rib shape (rectangular, triangular, upstream-pointing wedge, and downstream-pointing wedge) in both in-line and staggered arrangements. Yang et al. [351] compared single-phase and two-phase model predictions for nanofluid flow in ribbed channels, and reported that the single-phase model provides considerably lower *Nu* than the two-phase model.

2.5.5. Other techniques

Zhang et al. [352] investigated a hybrid enhancement technique involving use of SiO_2 nanofluid and transverse vibration of heating surface, which was quite effective at enhancing heat transfer performance. Ahmed et al. [353,354] devised a hybrid technique combing use of nanofluid and vortex generator in triangular duct. Kuppusamy et al. [355] numerically investigated nanofluid heat transfer in trapezoidally-grooved micro-channel heat sink, and found that increasing lower line and decreasing upper line of the trapezoidal groove improves cooling performance, implying that a heat sink with triangular grooves is preferred to one with rectangular grooves. Rayatzadeh et al. [356] proposed applying continuous ultrasonic field in the nanofluid's reservoir to prevent nanoparticle sedimentation or agglomeration, which they showed to enhance *Nu* dramatically for laminar flow. Li et al. [357] numerically addressed thermal and hydraulic performances of Al_2O_3 nanofluid in micro-channels with dimple and protrusion structures. Madhesh et al. [358] explored heat transfer enhancement characteristics of Cu-TiO_2 hybrid nanocomposite in base fluid (water), which was different from hybrid nanofluids with two or more types of particles suspended in base fluid simultaneously. Yarmand et al. [359] examined thermal performance of hybrid nanocomposite of Ag and functionalized graphene nanoplatelets in water, TEM images of which are shown in Fig. 12. They achieved maximum enhancement in Nusselt number of 32.7% at 0.1 wt% concentration and Re = 17,500 compared to base fluid.

Overall, the majority of afore-mentioned studies provided ample evidence of superior thermal performance with use of hybrid techniques. However, a key drawback in most, especially for nanofluid through internally modified channels, was severe pressure drop penalty, which must be weighed very carefully against any heat transfer benefits.

2.6. Important anomalies and concerns

2.6.1. Nanofluid destabilization

Despite the many merits pointed out by investigators, nanofluids have also been scrutinized in terms of viability as effective coolants. One important concern is long-term stability. For example, Ferrouillat et al. [133] performed tests to address nanofluid stability at high temperatures. They showed that 34 wt% SiO_2 nanofluid destabilizes when channel inlet temperature is increased above 80 °C. This phenomenon is reflected in Fig. 13, which compares friction factor versus *Re* before and after the destabilization. Shown are 1.5 and 3.0 fold increases in friction factor in the laminar and turbulent regimes, respectively, as a result of the destabilization. Bianco et al. [360] adopted two separate measures for overall effec-

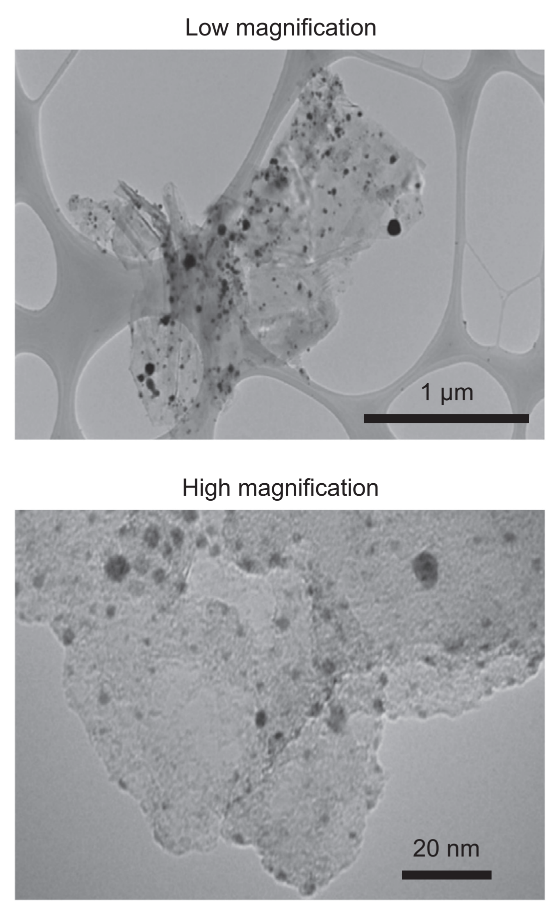

Fig. 12. TEM images of nanocomposite of graphene nanoplatelets and Ag in water; black spots indicate Ag nanoparticles. Adapted from Yarmand et al. [359].

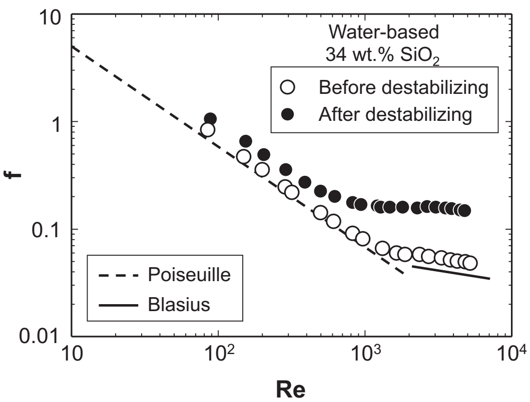

Fig. 13. Darcy coefficient for water-based 34 wt% SiO_2 nanofluid in 4-mm diameter tube before and after destabilization. Adapted from Ferrouillat et al. [133].

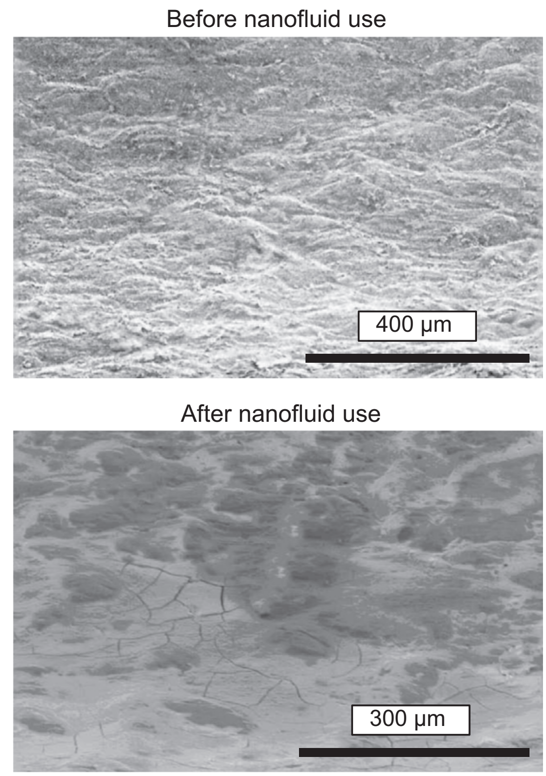

Fig. 14. Surface morphology before and after single-phase convective heating of water-based 3.7 vol% SiC nanofluid along a stainless steel tube. Adapted from Yu et al. [136].

tiveness of nanofluids: performance evaluation criterion (PEC) and entropy generation. They concluded that, because of increases in liquid viscosity and pumping power, nanofluids do not represent a viable choice where the objective is to maximize energy efficiency, as better performance is realized with the base fluid (water) alone.

Nguyen et al. [361] showed experimentally existence of a critical temperature, which was influenced by both nanoparticle concentration and size, above which viscosity of water-based Al_2O_3 nanofluid increased dramatically, precipitating hysteresis in cooling performance and raising serious concerns regarding cooling reliability of nanofluids. Sommers and Yerkes [362] also showed that viscosity of propanol-based Al_2O_3 nanofluid increases nonlinearly and sharply with increasing concentration, while density, specific heat, and thermal conductivity increase in a linear fashion. They reported visible discoloration of the nanofluid after prolonged circulation in the cooling loop at high flow rates and temperatures; attributing the degradation to nano-abrasion effects. Bergman [363] reported that nanofluid single-phase heat transfer enhancement or deterioration is operating conditions and channel dimensions specific. Yu et al. [136] observed clear deposition of nanoparticles into 100-particle thick wall coating, as shown in Fig. 14. While the coating did not influence heat transfer, they suggested that accumulation of nanoparticles would lead to constriction and eventual clogging of flow passages.

Zangeneh et al. [364] showed experimentally that different nanoparticle synthesis methods have significant influence on heat transfer performance of ZnO nanofluids. For example, nanoparticles with cylindrical morphology, functionalized by amine and oxidized by UV irradiation, yielded best thermal performance, and those functionalized by fatty acid worst. Additionally, nanoparticles having nanotube shape provided better performance than those spherical.

Overall, as indicated by Liang and Mudawar [58], nanofluids pose a host of practical problems, such as clustering, sedimentation and precipitation of particles, clogging of flow passages, erosion to heating surface, nanoparticle deposition, transient heat transfer performance, high cost, nanofluids production difficulties, and lack of strict quality assurance.

2.6.2. Inconsistent criteria in performance evaluation

Wu et al. [365] showed that nanofluids could be treated as homogeneous fluids, and enhancement effects of Brownian motion, thermophoresis, and diffusiophoresis on heat transfer characteristics are insignificant compared to those resulting from improved thermophysical properties. Further, their experiments with 0.78–7.04 wt% water-based Al_2O_3 nanofluid flow through a double-pipe helically coiled heat exchanger, yielded 0.37–3.43% enhancement in heat transfer coefficient compared to the base fluid for equal flow velocity. Moreover, they examined two different criteria for evaluating the merits of nanofluids, one based on equal *Re* and the other equal mass flow rate. They suggested that the criterion of equal *Re* is misleading because, for equal *Re*, increased viscosity with the nanofluid would correspond to higher flow velocity, and therefore provide seemingly better performance for nanofluid compared to that of base fluid. This conclusion is clearly reflected by comparing Fig. 15(a) and (b). In Fig. 15(a), which compares heat transfer coefficients for nanofluids to that for water based on the criterion of equal *Re*, which has been adopted by several investigators to demonstrate the benefits of nanofluids. Notice that, while this figure seems to point to appreciable enhancement with the nanofluids, Fig. 15(b) shows that the enhancement is in fact insignificant when comparing performances based on equal mass flow rate, which proves that the heat transfer enhancement depicted in Fig. 15(a) is an analysis artifact. Similar findings concerning use of *Re* as basis for performance assessment have been reported by Aly et al. [366] and Utomo et al. [367]. Utomo et al. found that *Nu* enhancement with water-based Al_2O_3, TiO_2, and CNT nanofluids is no greater than 10%, well within error bars for classical heat transfer correlations developed for pure liquids, which suggests that nanofluids may be treated as homogenous fluids. They also concluded that nanoparticle presence and their movement due to Brownian diffusion and thermophoresis have insignificant influence on the heat transfer coefficient. Since addition of nanoparticles changes thermophysical properties of the base fluid, reported enhancements in heat transfer coefficient are often inconsistent because of reliance on different performance criteria, such as equal values for flow velocity, *Re*, mass flow rate, or pumping power. Akbarinia et al. [368]

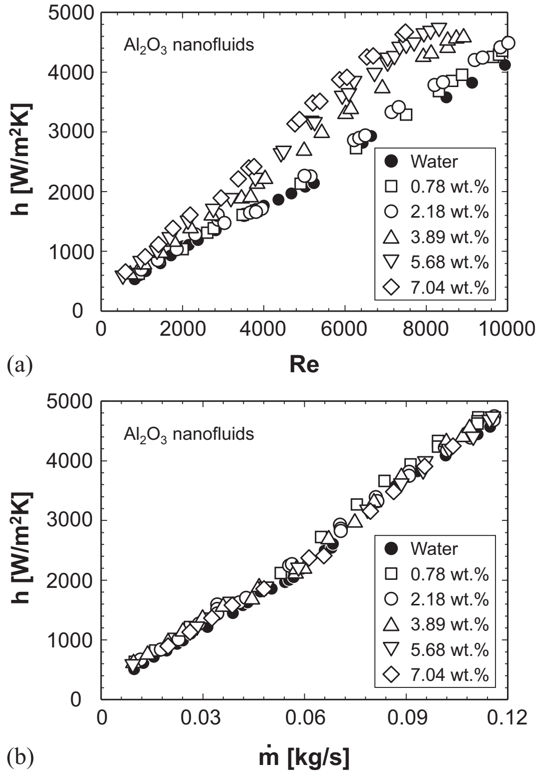

Fig. 15. Comparison of heat transfer coefficients for Al_2O_3 nanofluids and pure water based on criteria of (a) equal *Re* and (b) equal mass flow rate. Adapted from Wu et al. [365].

also pointed out that the apparent heat transfer enhancement when maintaining equal *Re* is the result of increased inlet velocity and not due to increases in nanoparticle concentration.

Using ethylene glycol/water mixture and pure water as base fluids, Timofeeva et al. [369] showed that, compared to base fluid, SiC nanofluids with 16–90 nm nanoparticles yield only limited heat transfer enhancement (below 14.2%) for equal flow velocity, with larger particles providing better performance in both the laminar and turbulent regimes [370]. Yu et al. [371] assessed three different heat transfer enhancement criteria for nanofluids: equal *Re*, equal flow velocity, and equal pumping power. They concluded that the latter is the most unambiguous from a practical point of view, and equal flow velocity could be justifiable under certain operating conditions. However, they stressed that the criterion of equal *Re*, which is the one most commonly used in nanofluid literature, provides a distorted assessment of nanofluid advantages, and must therefore be avoided.

Haghighi et al. [372] assessed heat transfer performances of water-based Al_2O_3, TiO_2, and CeO_2 nanofluids with a concentration of 9.0 wt% in a 0.5-mm diameter stainless steel tube. They reported that use of equal *Re* always points to heat transfer coefficient enhancement with the nanofluids compared to base fluid. However, comparisons based on equal mass flow rate, equal inlet velocity, or equal pumping power showed no such enhancement, and even deterioration for certain conditions. Lelea and Laza [373,374] and Haghighi et al. [375] questioned validity of performance assessments based on equal *Re*, suggesting that use of equal pumping power is more suitable from an application standpoint.

Overall, the articles reviewed in this section point to better assessment of heat transfer performance of nanofluids when using criteria of equal pumping power, equal flow velocity, or equal flow rate, but they all point to any enhancement realized when comparing performances based on equal *Re* as erroneous and violating underlying flow physics.

3. Flow boiling heat transfer

3.1. Flow boiling in macro-channels

3.1.1. Bubble dynamics

As discussed earlier, phase change permits utilization of a coolant's latent heat content in addition to sensible heat. This allows flow boiling to greatly enhance heat transfer coefficient, reduce coolant flow rate for a given heat load, and provide better temperature uniformity than single-phase liquid convection. But, as stated in Section 1.6, channel diameter can have profound influence on heat transfer performance. In particular, while micro-channels can greatly enhance heat transfer coefficient (even for pure fluids), they pose several operational challenges not encountered in macro-channels [13,376–379]. And, adding nanoparticles into base fluid exasperates these challenges. For this reason, flow boiling heat transfer characteristics of nanofluids are segregated below into those for macro-channels and for micro-channels; this section will address findings concerning macro-channels.

Flow boiling visualization experiments in a 21.8-mm channel by Rana et al. [380] showed that adding ZnO nanoparticles into base fluid (water) increased maximum bubble diameter but decreased bubble density; they also noted that heat transfer coefficient increased with increasing nanoparticle concentration below 0.01 vol%. Follow-up study by Rana et al. [381] involved optical void fraction measurements of ZnO nanofluids with concentrations of 0.001–0.01 vol%, which showed that nanoparticles served as suppressing agent, decreasing void fraction with increasing concentration (by up to 86% at 0.01 vol%). They also noted important practical concerns stemming from the nanoparticles tending to alter surface structure and deactivate nucleation from cavities. However, using water-based TiO_2 and Al_2O_3 nanofluids in concentrations of 0.001 and 0.01 vol%, Patra et al. [382] found bubble size to decrease but bubble density increase compared to those for pure water, which enhanced flow boiling heat transfer and delayed departure from nucleate boiling (DNB). They also reported abatement in heat transfer coefficient enhancement with increasing nanoparticle concentration because of an increase in thermal resistance caused by excessive nanoparticle deposition on the heating surface.

Using a modified moving-particle semi-implicit method, Wang and Wu [383] showed numerically that adding Al_2O_3 nanoparticles in water increased bubble departure diameter and frequency. They also predicted flow boiling heat transfer enhancement with nanoparticle diameters in the 20–38 nm range. However, their study was limited to single bubbles and did not address interaction between multiple bubbles. Yu et al. [384] found experimentally that adding Al_2O_3 nanoparticles in water delayed ONB and suppressed onset of flow instabilities. They attributed these trends to decreased size range and number density of nucleating sites, decreased surface wettability, and thinning of thermal boundary layer near the wall.

3.1.2. Heat transfer coefficient

Different trends have been reported in regards to nanofluid flow boiling heat transfer coefficient in macro-channels, with most studies pointing to heat transfer enhancement. Wang and Su [385] showed that average flow boiling *Nu* for water-based Al_2O_3 nanofluid in a vertical 6-mm diameter tube was enhanced by 23% and 45% for 0.1 vol% and 0.5 vol% concentrations, respectively. However, only minor enhancement was achieved at relatively high mass velocities in the range of 350–1100 kg/m^2 s. Follow-up work by Wang et al. [386] culminated in a correlation for saturated flow boiling *Nu* in vertical tubes. Sarafraz and Hormozi [387] found that flow boiling of water-based CNT nanofluids along a 5-mm hydraulic diameter annulus presented better heat transfer enhancement and reduced thermal fouling resistance than both Al_2O_3 and CuO nanofluids. They also reported that heat transfer performance of

CNT nanofluids improved with increasing mass velocity (over 100–1200 kg/m^2s range) and increasing concentration (0.1–0.3 wt% range). Zhang et al. [388] reported that contribution of suspended nanoparticles to heat transfer enhancement gradually abated with increasing mass velocity over the 300–500 kg/m^2 s range. And maximum enhancement in heat transfer coefficient for R123-based CNT nanofluids was achieved at medium vapor qualities for low and medium mass velocities, but low vapor qualities for high mass velocities. Yang and Liu [389] reported that operating pressure had a positive effect on heat transfer coefficient enhancement for water-based CuO nanofluids, suggesting that this was the result of increased deposition in addition to improved thermophysical properties. But they also indicated that CHF enhancement was pressure-independent. Setoodeh et al. [390] reported that heat transfer performance of water-based Al_2O_3 nanofluids improved because of increased surface roughness resulting from intensified vapor nucleation, which also enhanced fluid mixing. Chehade et al. [391] showed experimentally for flow boiling of water-based Ag nanofluids along a channel with rectangular cross-section, that heat transfer coefficient was highest in the entrance region, where vapor quality was lowest, and decreased downstream, and nanoparticles had negligible influence in the high quality region. Using very low concentrations, they achieved maximum enhancement in average heat transfer coefficient of 132% and 162% for 0.000237 and 0.000475 vol%, respectively.

For refrigerant-based nanofluids, Peng et al. [392] showed that R113-based 0–0.5 wt% CuO nanofluids improved heat transfer coefficient by up to 29.7%, and the enhancement was derived from reduction of boundary layer thickness due to both nanoparticle disturbances to the flow and formation of molecular adsorption layer on the surfaces of nanoparticles. Follow-up study by Peng et al. [393] showed that heat transfer enhancement for R113-based CuO nanofluids was accompanied by 20.8% increase in pressure drop. Large increases in pressure drop were also reported by Alawi et al. [394] for R123-based TiO_2 nanofluid flow in tubes with diameters ranging from 6 to 10 mm. Akhavan-Behabadi et al. [395] showed, for flow boiling of R600a/polyester (99/1) mixture-based CuO nanofluid in a horizontal tube, 63% heat transfer coefficient enhancement corresponding to 1.5 wt% concentration. Follow-up study by co-workers Baqeri et al. [396] found that flow boiling heat transfer coefficient could be increased further by increasing concentration to 2 wt%, but further increases to 5 wt% actually reduced the heat transfer coefficient because of both aggregation and settling of nanoparticles. Henderson et al. [397] reported that direct dispersion of SiO_2 nanoparticles in R134a decreased heat transfer coefficient for flow boiling in a 7.9-mm diameter tube because of unstable dispersion of nanoparticles. However, CuO nanoparticles showed good suspension and dispersion in a mixture of R134a and polyolester oil (POE), increasing the boiling heat transfer coefficient by over 100%. Tazarv et al. [398] explored flow boiling performance of R141b-based TiO_2 nanofluids along an 8.825-mm diameter tube and showed that 0.03 vol% concentration presented better heat transfer enhancement than 0.01 vol%. Additionally, the enhancement increased with increasing vapor quality in the 0–0.4 range, but decreased with increasing mass velocity (over 192.5–481.4 kg/m^2s range) because of decreased particle deposition. Mahbubul et al. [399] studied flow boiling heat transfer of R141b containing Al_2O_3 nanoparticles in a 6-mm diameter tube, and proposed existence of an optimal concentration to minimize pressure drop and pumping power for a given level of heat transfer enhancement.

On the other hand, many researchers reported that flow boiling of nanofluid provided no enhancement or even yielded deterioration in heat transfer performance. Kim et al. [400] found no appreciable change in the heat transfer coefficient for flow boiling in a 5.53-mm diameter tube among water-based Al_2O_3, ZnO, and diamond nanofluids. Using water-based TiO_2 nanofluids, Abedini et al. [401] and Afrand et al. [402] measured deterioration in subcooled flow boiling heat transfer coefficient in both horizontal and vertical 10-mm diameter tubes, which they attributed to increased near-wall viscosity caused by nanoparticle deposition; the deterioration was further aggravated with increasing nanoparticle concentration. However, the concentration effect became insignificant for high flow rates [403]. Recent experiments by Abedini et al. [404] showed that, while water-based nanofluids did enhance the single-phase heat transfer coefficient, they had adverse effects on subcooled flow boiling, trends that are clearly captured in Fig. 16. The indicated deterioration was dependent on particle concentration and size, but nanoparticle material (TiO_2, Al_2O_3 and CuO) had relatively minor influence. Follow-up study by Abedini et al. [405] provided a two-phase mixture model for water-based Al_2O_3 nanofluid in a 5.53-mm diameter tube, employing k-epsilon turbulence model, which was capable of predicting both void fraction and temperature distribution. Karimzadehkhouei et al. [406] investigated flow boiling of water-based Al_2O_3 nanofluid for mass velocities of 1200–3400 kg/m^2s and both low concentrations (0.05 and 0.2 wt%) and high (0.5, 1.0 and 1.5 wt %). They showed that low concentrations provided no considerable enhancement in heat transfer coefficient (up to only 7%), but because of deposition of agglomerated nanoparticles on the wall, high concentrations actually decreased the heat transfer coefficient by up to 12%. Sarafraz and Hormozi [407] showed that flow boiling heat transfer coefficient for water-based 0.5–1.5 vol% CuO nanofluid in a 4-mm hydraulic diameter annulus was inferior to that of base fluid, and surface fouling rate increased significantly with increasing concentration.

Zhou et al. [408] constructed a theoretical model for saturated nanofluid flow boiling heat transfer in channels with 0.3×2 mm^2, 0.6×2 mm^2 and 2×2 mm^2 cross-sections. In this model, which accounted for Brownian motion as well as contributions of both nucleate boiling and convective boiling, heat absorbed by nanoparticles from the fluid was deduced using fractal distribution theory, while probability density of random growth of bubbles in nucleate boiling was based on the Markov process. Sarafraz et al. [409] investigated water/ethylene glycol-based CuO nanofluid flow in an annular duct having a hydraulic diameter of 30 mm, and showed deterioration of heat transfer coefficient in the nucleate boiling dominant region, contrasted with significant augmentation in the forced convection dominant region.

Overall, there is general consensus among investigators that both nucleate boiling and convective boiling contribute to the heat transfer process. But, even for pure liquids, determining spatial

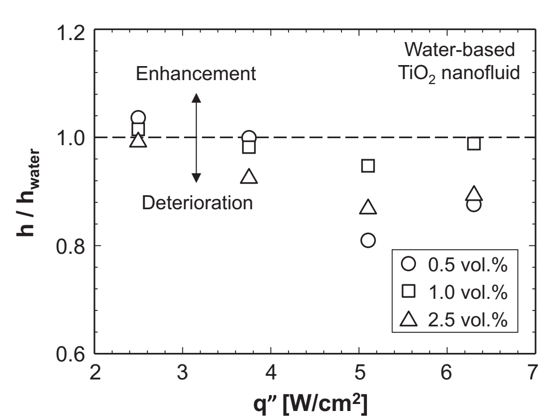

Fig. 16. Variation of ratio of average heat transfer coefficient for TiO_2 nanofluid to that for base fluid (water) versus heat flux for 137 kg/m^2s mass velocity in a 10-mm diameter tube. Adapted from Abedini et al. [404].

extent and contribution of each to overall heat transfer coefficient is a complex endeavor because of dependence on many parameters, including channel shape and dimensions, mass velocity, subcooling, and vapor quality. For nanofluids, there are added complexities brought about by variations in nanoparticle material, size, shape or aspect ratio, and concentration, let alone effects of deposition on the heating wall.

3.1.3. Critical heat flux

Kim et al. [410,411] found experimentally that adding Al_2O_3, ZnO, and diamond nanoparticles into water in concentrations below 0.1 vol% could enhance CHF for subcooled flow boiling in a 5.53-mm diameter stainless steel tube by 40–50%, which they attributed to increased surface wettability caused by nanoparticle deposition. However, the enhancement was absent at relatively low mass velocity of 1500 kg/m^2 s. By excluding electrophoretic effects in electrolytes under electrical heating conditions, Ahn et al. [412] concluded that CHF enhancement for water-based Al_2O_3 nanofluid in a channel with 5×10 mm^2 cross-section was the result of increased wettability, and showed that the enhancement improved with increasing flow velocity. They also tested flow boiling of pure water with the flow channel walls coated with Al_2O_3 nanoparticles, and CHF for pure water was higher with the coated than bare channel, but lower than with the nanofluid and bare channel. Fig. 17(a) compares CHF values for the three cases, while Fig. 17(b) depicts the detachment of nanoparticles from the surface coating during flow boiling.

Kim et al. [413] measured virtually identical values for flow boiling CHF of water-based Al_2O_3 nanofluids along a 10.98-mm diameter tube as concentration was increased from 0.001 to 0.1 vol%, as shown in Fig. 18(a) and (b) for 50 °C and 25 °C inlet subcoolings, respectively. They speculated that lack of concentration effect might be the result of nanoparticle deposition having already reached threshold level even at 0.001 vol%. But, as shown in Fig. 18(a) and (b), they did achieve CHF enhancement at much lower concentrations, which they attributed to increased wettability resulting from nanoparticle deposition on the channel's inner walls, a conclusion also shared by Hashemi and Noie [414]. Follow-up study by Kim et al. [415] involved flow boiling of water-based Al_2O_3 nanofluid in a plain 7.745-mm diameter tube and pure water in an Al_2O_3 nanoparticle-coated tube. The two cases yielded about equal CHF values that were about 80% better than for pure water flowing in a plain tube, which led to the conclusion that CHF enhancement with nanofluids was the result of nanoparticle deposition along the tube's inner surface.

By applying external magnetic field, Lee et al. [416] showed that flow boiling CHF for water-based Fe_3O_4 nanofluid along a 10.92-mm diameter tube can be ameliorated because of improved wettability and re-wetting brought about by nanoparticle deposition on the heating surface. Follow-up study by Lee et al. [417] identified two types of flow boiling CHF in the annular flow regime: departure from nucleate boiling (DNB)-like, corresponding to low exit vapor qualities, and liquid film dryout (LFD), corresponding to high qualities. At low exit qualities, Fe_3O_4 nanofluid enhanced CHF compared to pure water by delaying DNB, however, no CHF (LFD-type) enhancement was observed at high exit qualities. And, when exit quality was increased from 0.07 to 0.74, CHF enhancement reduced and gradually approached near-zero value. Aminfar et al. [418] also examined effects of magnetic field on flow boiling for water-based Fe_3O_4 nanofluid in a vertical annulus with a 12-mm diameter inside heating rod. They measured reduction in CHF with application of magnetic field at very low mass velocities, but significant enhancement at high mass velocities, as shown in Fig. 19(a). They speculated that, since CHF enhancement with nanofluids was caused mainly by increased wettability brought about by the nanoparticle deposition, lack of CHF enhancement at low mass velocities in the presence of magnetic field was the outcome of

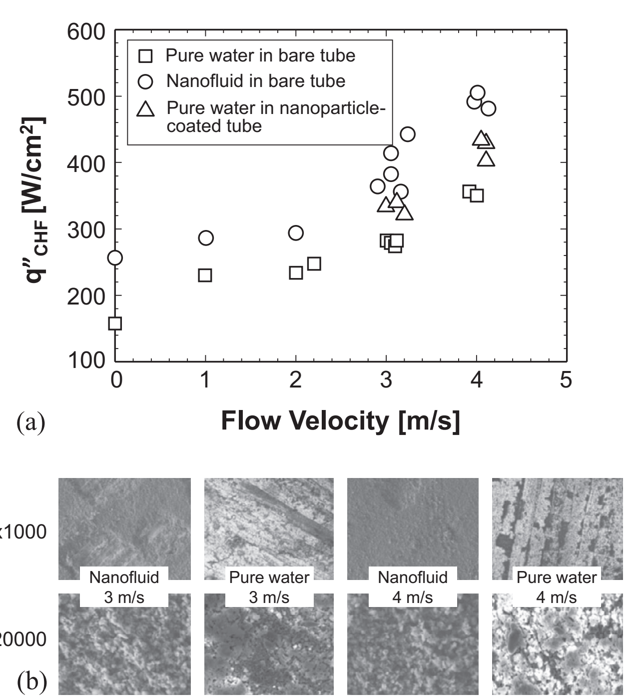

Fig. 17. (a) Comparison of flow boiling CHF for pure water on bare surface, Al_2O_3 nanofluid on bare surface, and pure water on nanoparticle-coated surface for a channel with 5×10-mm^2 cross-section. (b) SEM images of nanoparticle-coated surfaces at different flow velocities. Adapted from Ahn et al. [412].

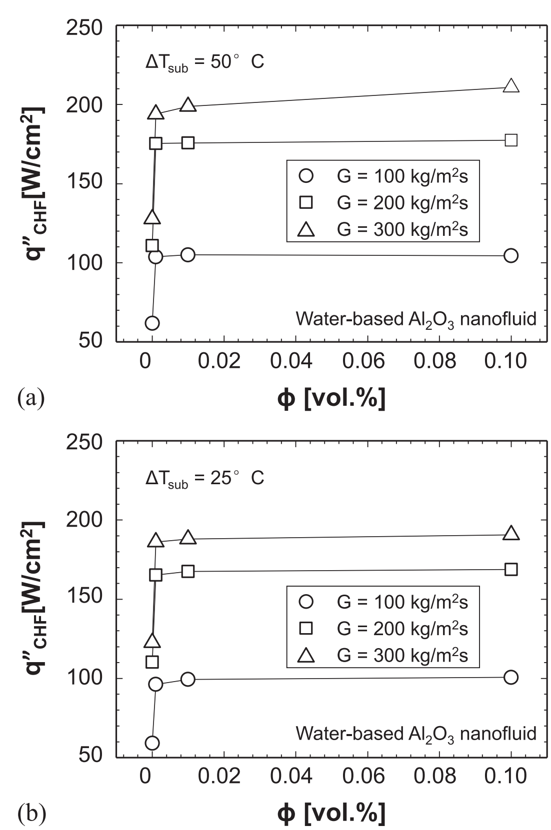

Fig. 18. Variations of flow boiling CHF for water-based Al_2O_3 nanofluid along a 10.98-mm diameter tube with nanoparticle concentration at three mass velocities and inlet subcooling of (a) 50 °C and (b) 25 °C. Adapted from Kim et al. [413].

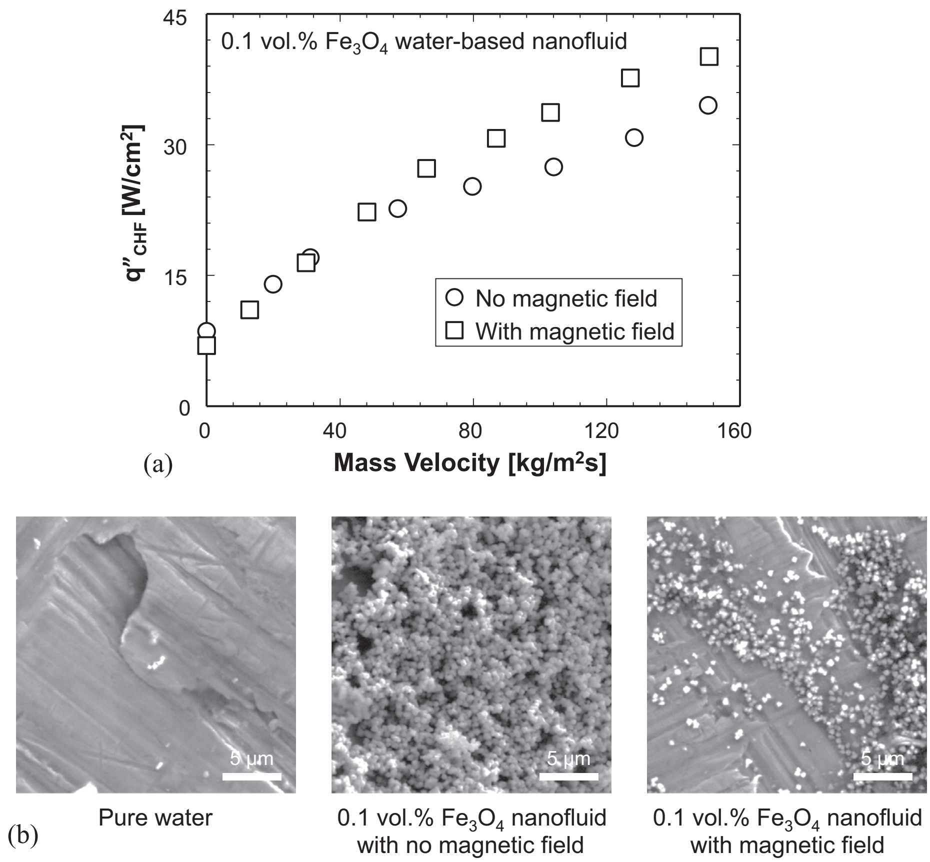

Fig. 19. (a) Flow boiling CHF versus mass velocity for 0.1% Fe_3O_4 water-based nanofluid along a vertical annulus with and without application of magnetic field. (b) SEM images of heating surface after flow boiling at low mass velocity. Adapted from Aminfar et al. [418].

reduced particle deposition on the surface, as shown in Fig. 19(b). Aminfar et al. [419] also investigated effects of non-uniform magnetic field on subcooled nanofluid flow boiling numerically, and found that negative magnetic field gradient can improve CHF enhancement, which they attributed to decreased evaporation rate on the heating surface.

Park and Bang [420] measured flow boiling CHF for water-based graphene oxide nanofluid at a very low concentration of 0.0001 vol % along a curved channel with non-uniform cross-section. They achieved ~20% CHF enhancement at mass velocities of 50 and 100 kg/m^{2}s and 10 °C inlet subcooling, which they attributed to nanoparticle deposition. They also preformed sessile drop experiments on the surface following the boiling tests, which showed that wettability of the surface with the deposition layer did not improve, therefore contradicting most prior studies regarding CHF enhancement mechanisms for nanofluids. Instead, using IR thermography, they observed appreciable changes to thermal activity on the surface, as heat transfer was accelerated with the surface coated with graphene oxide. They suggested that the improved thermal activity delayed ability of bubbles to form hot spots, thereby enhancing CHF. Lee et al. [421] achieved ~100% CHF enhancement for water-based 0.01 vol% graphene oxide nanofluid for flow boiling in a 12.7-mm diameter tube with inlet temperatures of 25 °C and 50 °C, and mass velocities of 100–250 kg/m^2 s. Like many earlier investigators, they attributed this enhancement to improved wettability caused by nanoparticle deposition.

Mohammadpourfard et al. [422] studied numerically flow boiling of water-based Fe_3O_4 nanofluid in an annulus having a 4-mm hydraulic diameter with a twisted fin inserted along the inner wall. Their predictions showed that CHF enhancement was closely associated with improved surface wettability resulting from nanoparticle deposition, which also reduced void fraction. Additionally, they showed that CHF could be augmented by application of transverse magnetic field. This was explained by increased centrifugal force on the liquid intensifying flow turbulence, as well as both decreased bubble departure diameter and increased bubble frequency.

3.2. Flow boiling heat transfer in micro-channels (D < 1 mm)

3.2.1. Heat transfer coefficient

As discussed earlier in Section 1.6, micro-channel cooling has recently emerged as one of the top choices for thermal management of high-flux devices. Aside from the benefits of reduced hydraulic diameter for both single-phase and two-phase micro-channel flows, phase change in the latter allows utilization of the coolant's latent heat content in addition to sensible heat. This enables micro-channel flow boiling to achieve several simultaneous advantages, including greatly enhanced heat transfer coefficient, reduced coolant flow rate and coolant inventory requirements, and better temperature uniformity.

But, also as stated in Section 1.6, very small channel diameter poses multiple challenges, including high pressure drop, increased compressibility and flashing, and greater likelihood of two-phase choking. Adding nanoparticle into base fluid exasperates these challenges in addition to posing additional challenges in terms of both predicting and maintaining cooling performance.

Boudouh et al. [423] studied experimentally flow boiling of water-based Cu nanofluid along a copper heat sink containing 50 parallel rectangular micro-channels having a hydraulic diameter of 800 μm. Using the inverse heat conduction method, they showed that, compared to the base fluid at the same mass velocity, the nanofluid increased local heat flux and local heat transfer coefficient and decreased surface temperature, but also increased pressure drop. They also noted that vapor quality was nanoparticle concentration dependent. Duursma et al. [424] showed that single-phase pressure drop for ethanol-based Al_2O_3 nanofluid flow along a 0.8-mm diameter channel did not change significantly with nanoparticle concentration in the range of 0.01–0.1 vol%. However, two-phase pressure drop was unstable and fluctuating, the frequency and amplitude of which were concentration dependent. Additionally, the nanofluid greatly enhanced flow boiling heat transfer coefficient compared to that for pure ethanol.

Moreira et al. [425] investigated systematically effects of nanoparticle material, size and concentration on heat transfer coefficient for flow boiling in a small diameter tube at heat fluxes up to 35 W/cm^2. They showed that water-based nanofluids with 0.1 vol% concentration decreased the heat transfer coefficient compared to pure water. On the other hand, heat transfer performance for lower concentrations (0.001 and 0.01 vol%) depended on particle size; smaller particles (20–30 nm Al_2O_3, 25 nm Cu, and 15 nm SiO_2) decreased the heat transfer coefficient, while larger particles (40–80 nm Al_2O_3 and 80 nm SiO_2) presented variations between heat transfer coefficients for water and nanofluids that were within measurement uncertainty. Using an optical profiler, images of the heating surfaces following the boiling tests showed deposition morphology that was particle size dependent: deposition of larger nanoparticles was uniform and acquired texture similar to that of the original surface, but smaller nanoparticles produced a deposition layer with pronounced peaks and valleys.

Diao et al. [426] studied flow boiling of R141b-based Al_2O_3 nanofluids with 13 nm nanoparticles along a micro-channel with 0.25×0.5 mm^2 cross-section. They showed that 0.1 vol% nanofluid decreased the heat transfer coefficient, but 0.001 and 0.01 vol% improved performance. Additionally, for 0.01% and 0.1 vol%, heat transfer coefficients for Al_2O_3 nanofluid with bare micro-channel surface and pure R141b with nanoparticle-covered surface were close to one another, implying that any changes to heat transfer performance were dominated by nanoparticle deposition. They also pointed to existence of an optimal nanoparticle concentration below which heat transfer was improved because of increased nucleation density on the porous coating, but over which heat transfer was compromised because of increased thermal resistance.

Zhang et al. [427] found experimentally that heat transfer coefficient for water-based graphene oxide nanofluids in a micro-channel heat sink with 2.5×0.5 mm^2 channels was lower than that for pure water because of formation of non-porous film-like deposition layer, which blocked nucleation sites, and performance degradation worsened with increasing nanoparticle concentration in the range of 0–0.05 wt%. Conversely, increased surface wettability by the deposition layer improved CHF. They proposed that interaction and physical absorption between nanoparticles were key mechanisms governing formation of the deposition layer.

Edel and Mukherjee [428,429] investigated flow boiling of 0.001 vol% Al_2O_3 water-based nanofluid along a single 0.229-mm diameter tube. They showed that nanoparticle addition tended to stabilize bubble growth as well as transition between flow regimes (liquid, two-phase, and vapor). With the nanofluid, an increase in nucleation site density caused flow regime cycle duration to increase firstly and then decrease. Unlike previous investigators, Xu and Xu [430] showed that flow boiling of 0.2 wt% Al_2O_3 water-based nanofluid along a single 0.1×0.25 mm^2 channel did not produce any nanoparticle deposition. They also found that the nanoparticles contributed stability to the boiling process, reduced pressure drop, and enhanced heat transfer, the latter of which was attributed to inhibition of dry patch development and enlargement of percentage of liquid film evaporation region.

Wu et al. [431] studied single-phase and two-phase heat transfer of water-based Al_2O_3 nanofluid in trapezoidal silicon micro-channels having a hydraulic diameter of 194.5 μm. Under single-phase conditions, there were no obvious signs of deposition or adhesion of Al_2O_3 nanoparticles to the channel walls post experiment. However, nanoparticle deposition was observed with increasing wall temperature even at low concentration (0.15 vol %), especially at channel corners where fluid velocity was relatively low and wall temperature high. Once boiling commenced, deposition and adhesion to the channel walls became severe, rendering overall applicability of nanofluid boiling heat transfer in micro-channels very questionable.

Lee and Mudawar [432] investigated heat transfer performance of water-based Al_2O_3 nanofluids in a heat sink containing 341-μm hydraulic diameter micro-channels. They observed some enhancement in single-phase heat transfer coefficient in the laminar range, which they attributed to increased thermal conductivity. But the single-phase heat transfer enhancement was confined to the entrance region and became less apparent in the fully developed region, proving that nanofluids impacted mostly thermal boundary layer development. Despite this enhancement, overall cooling effectiveness of nanofluids was deemed quite miniscule, based on observed large axial temperature rise (associated with decreased specific heat of nanofluid compared to that of base fluid) as well as increased pressure drop. And two-phase cooling was different altogether, as nanoparticles caused catastrophic failure by quickly depositing relatively large clusters along the channel walls, causing serious flow obstruction, and preventing further operation beyond ONB. Lee and Mudawar pointed out that evaporation along the walls, which was a primary mechanism for flow boiling, was the main corporate for the deposit buildup. The extent of this problem is clearly manifest in Fig. 20(a), which compares flow boiling curves for pure water and 1 vol% Al_2O_3 nanofluid, and Fig. 20(b), depicting an image of post boiling nanoparticle clusters after being removed from the micro-channels.

3.2.2. Critical heat flux

Vafaei and Wen [433] investigated flow boiling CHF of water-based Al_2O_3 nanofluids along a single 510-μm diameter circular channel, with average nanoparticle size of 25 nm, low concentrations (below 0.1 vol%), and mass velocities of 600–1650 kg/m^{2}s. Because morphology of the boiling surface was altered following each boiling test, which might yield inconsistent boiling data, they performed each test with a fresh micro-channel. They achieved ~51% CHF enhancement for 0.1 vol% concentration, Fig. 21, which they explained as the result of increased vapor bubble number but shorter bubble lifetime. They also added that, even for very stable nanofluids, surface modification by nanoparticle deposition was always observed, and attributed this phenomenon to several factors, including nanoparticle material, size and concentration, initial surface roughness, nanofluid stability, surface properties, interaction dynamics of nanoparticles with heating surface, and duration of boiling test. Nonetheless, they pointed out that deposition layer thickness was small (few hundred nanometers) compared to hydraulic diameter, implying that the deposition layer might not cause appreciable obstruction to the flow. However, this might not be true with repeated boiling tests using the same channel or prolonged boiling duration.

Follow-up study by Vafaei and Wen [434] identified major roles of nanoparticles in base fluid, including modification of heating surface by deposition, and modification to bubble dynamics by suspended nanoparticles. Vafaei and Wen [435] also modified a CHF correlation for pure liquids by Lee and Mudawar [11] to predict subcooled flow boiling CHF for water-based Al_2O_3 nanofluids.

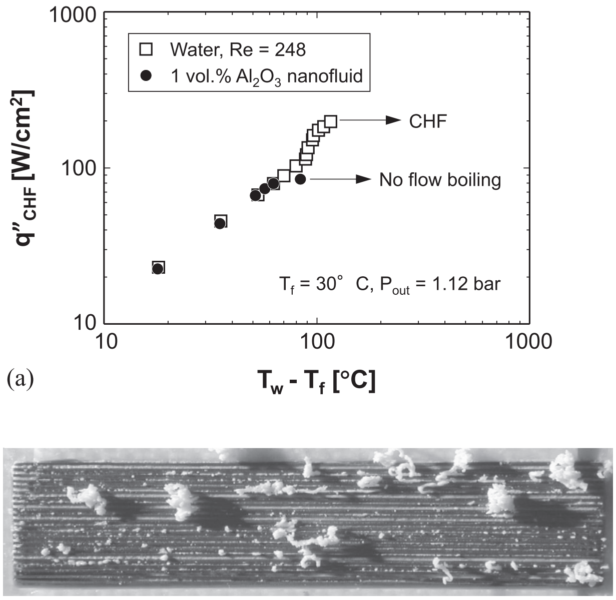

(a)

(b)

Fig. 20. (a) Boiling curves for pure water and 1 vol% Al_2O_3 nanofluid flow in a micro-channel heat sink containing 341-μm hydraulic diameter micro-channels. (b) Image of nanoparticle clusters after being removed from the micro-channels. Adapted from Lee and Mudawar [432].

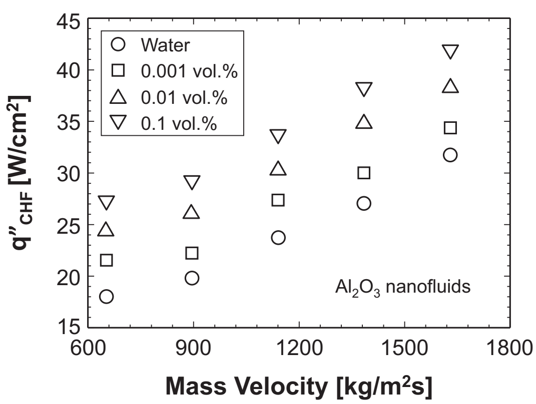

Fig. 21. Variation of subcooled flow boiling CHF versus mass velocity for pure water and water-based Al_2O_3 nanofluids along a 510-μm circular channel. Adapted from Vafaei and Wen [433].

For prediction of CHF for base fluid and nanofluid flow in micro-channels, the reader should consult predictive methods developed by Revellin and Thome [436] and Revellin et al. [437].

Overall, published studies seem to provide contradictory evidence concerning impact of nanofluids on flow boiling heat transfer coefficient in micro-channels. And, while some do point to ability of nanofluids to increase CHF, they also emphasize that this increase is limited to short duration boiling tests. Given the deposition layer buildup after prolonged boiling and/or repeated boiling tests, it is fair to assume that this would ultimately lead to clogging of micro-channels and catastrophic failure of the entire cooling system. This might explain why, for micro-channels, there have been far fewer studies on flow boiling than on single-phase cooling.

4. Concluding remarks

This study reviewed published literature addressing use of nanofluid to enhance flow boiling heat transfer compared to base fluid. The review was segregated into two main sections, one specific to single-phase flow and the other two-phase flow. And each section was further divided to address macro-channel and micro-channel ($D < 1$ mm) findings separately. Included in the review were both experimental and numerical findings concerning several crucial performance parameters, including single-phase and two-phase heat transfer coefficient, pressure drop, and critical heat flux (CHF), each being evaluated based on postulated mechanism responsible for any performance enhancement or deterioration. Other topics addressed were entropy minimization, hybrid enhancement techniques, and nanofluid stability, as well as important practical findings concerning overall viability of nanofluids as effective cooling media. Key observations from this review can be summarized as follows.

(1) Despite differences among investigations, there is general consensus that nanofluids are effective at enhancing single-phase heat transfer coefficient in the entrance region because of reduction of thermal boundary layer thickness, but the enhancement subsides downstream. Some noteworthy parameters that influence single-phase heat transfer include nanoparticle size, shape (spherical, rod-like, and disk-like), and concentration. It is commonly accepted that smaller nanoparticles ameliorate single-phase heat transfer corresponding to only minor increases in pressure drop. Regarding nanoparticle concentration, many studies point to an optimum concentration yielding highest heat transfer enhancement, below which heat transfer benefits from increased concentration, while above which clustering of nanoparticles begins to have adverse effects on heat transfer.
(2) Two mechanisms that have been postulated in many investigations as major contributors to single-phase heat transfer, and adopted in numerical models are Brownian diffusion and thermophoresis.
(3) There is lack of consensus concerning ability of popular friction factor and heat transfer correlations for pure liquids to tackle nanofluids as well.
(4) Two general categories of numerical methods have been used to simulate single-phase nanofluid heat transfer in macro/micro-channels: *single-phase methods* and *two-phase methods*. The former include both homogeneous and dispersion models, while the latter include Eulerian-Eulerian (volume of fluid, mixture, and Eulerian) and Eulerian-Lagrangian models, and Discrete Phase Model (DPM). A major problem with single-phase methods is lack of accurate models or relations for nanofluid viscosity and thermal conductivity. Overall, the two-phase methods, which address interactions between base fluid and nanoparticles, show better predictive accuracy, with few differences realized between different two-phase models. In general, future numerical studies must consider temperature-dependent properties, especially thermal conductivity and viscosity, as well as dependence of heat transfer coefficient on nanoparticle concentration.
(5) Entropy analysis has attracted significant attention in nanofluid studies in recent years because of its importance to practical design of cooling systems. Overall, studies show that entropy generation decreases with decreasing nanoparticle size or increasing concentration.
(6) Several studies addressed use of hybrid enhancement techniques in pursuit of superior single-phase cooling performance of nanofluids. Examples include flow inserts as well as helical, corrugated, and ribbed channels. However, studies reveal that improved heat transfer performance is often accompanied by escalation in pressure drop.
(7) There is significant confusion concerning criteria used to evaluate nanofluid heat transfer performance compared to that of base fluid. Overall, criteria based on equal pumping

power, equal flow velocity, and equal flow rate, provide more sound and realistic assessments, while equal Reynolds number is an inaccurate basis for such evaluation.

(8) Studies point to many important practical problems in the use of nanofluids in single-phase cooling situations, including clustering, sedimentation, and precipitation of nanoparticles, clogging of flow passages, erosion to heating surface, transient heat transfer behavior, high cost and production difficulties, lack of quality assurance, and loss of nanofluid stability above a threshold temperature. Collectively, these issues continue to pose serious obstacles to nanofluid implementation in practical cooling situations.

(9) Two competing mechanisms, nucleate boiling and convective boiling, dominate two-phase heat transfer for nanofluids in micro-channels, like that for pure liquids. And the axial span and extent of contribution of each mechanism are dictated by several channel parameters (shape, diameter, and length), flow parameters (mass velocity, inlet subcooling, and thermophysical properties of base fluid), as well as parameters specific to the nanofluid used (nanoparticle material, shape, size, and concentration). And, while some studies point to the ability of nanofluids to increase CHF, they also emphasize that this increase is limited to short duration boiling tests. Given the deposition layer buildup after prolonged boiling and/or repeated boiling tests, it is fair to assume that this would ultimately lead to clogging of micro-channels and catastrophic failure of the entire cooling system.

(10) Despite the improved understanding of nanofluid flow and heat transfer in both macro-channels and micro-channels, especially over the past two decades, the heat transfer literature is a long way from enabling deployment of nanofluids in engineering applications. One major research topic that requires extensive further study is mitigating the potentially severe problems associated with long-term use of nanofluids. These include sedimentation of nanoparticles and nanofluid transient heat transfer behavior, phenomena that are also observed in nanofluid pool boiling.

Conflicts of interest

The authors declared that there is no conflict of interest.

Acknowledgement

Support of the National Natural Science Foundation of China under Grant No. 51876025 is gratefully acknowledged.

Appendix A. Supplementary material

Supplementary data to this article can be found online at https://doi.org/10.1016/j.ijheatmasstransfer.2019.02.086.

References

[1] I. Mudawar, T.M. Anderson, Parametric investigation into the effects of pressure, subcooling, surface augmentation and choice of coolant on pool boiling in the design of cooling systems for high-power-density electronic chips, J. Electron. Packag. 112 (1990) 375–382.
[2] J. Lee, I. Mudawar, Low-temperature two-phase microchannel cooling for high-heat-flux thermal management of defense electronics, IEEE Trans. Compon. Packag. Technol. 32 (2009) 453–465.
[3] I. Mudawar, Recent advances in high-flux, two-phase thermal management, J. Therm. Sci. Eng. Appl. 5 (2013) 021012.
[4] I. Mudawar, Assessment of high-heat-flux thermal management schemes, IEEE Trans. Compon. Packag. Technol. 24 (2001) 122–141.
[5] T.J. LaClair, I. Mudawar, Thermal transients in a capillary evaporator prior to the initiation of boiling, Int. J. Heat Mass Transfer 43 (2000) 3937–3952.
[6] I. Mudawar, T.M. Anderson, Optimization of enhanced surfaces for high flux chip cooling by pool boiling, J. Electron. Packag. 115 (1993) 89–100.
[7] J.A. Shmerler, I. Mudawar, Local heat transfer coefficient in wavy free-falling turbulent liquid films undergoing uniform sensible heating, Int. J. Heat Mass Transfer 31 (1988) 67–77.
[8] C.O. Gersey, I. Mudawar, Effects of heater length and orientation on the trigger mechanism for near-saturated flow boiling critical heat flux—I. Photographic study and statistical characterization of the near-wall interfacial features, Int. J. Heat Mass Transfer 38 (1995) 629–641.
[9] T.C. Willingham, I. Mudawar, Forced-convection boiling and critical heat flux from a linear array of discrete heat sources, Int. J. Heat Mass Transfer 35 (1992) 2879–2890.
[10] D.E. Maddox, I. Mudawar, Single-and two-phase convective heat transfer from smooth and enhanced microelectronic heat sources in a rectangular channel, J. Heat Transfer 101 (1989) 1045–1052.
[11] J. Lee, I. Mudawar, Critical heat flux for subcooled flow boiling in micro-channel heat sinks, Int. J. Heat Mass Transfer 52 (2009) 3341–3352.
[12] W. Qu, I. Mudawar, S.-Y. Lee, S.T. Wereley, Experimental and computational investigation of flow development and pressure drop in a rectangular micro-channel, J. Electron. Packag. 128 (2006) 1–9.
[13] D.D. Hall, I. Mudawar, Ultra-high critical heat flux (CHF) for subcooled water flow boiling—II: High-CHF database and design equations, Int. J. Heat Mass Transfer 42 (1999) 1429–1456.
[14] S. Mukherjee, I. Mudawar, Pumpless loop for narrow channel and micro-channel boiling, J. Electron. Packag. 125 (2003) 431–441.
[15] D.C. Wadsworth, I. Mudawar, Enhancement of single-phase heat transfer and critical heat flux from an ultra-high-flux simulated microelectronic heat source to a rectangular impinging jet of dielectric liquid, J. Heat Transfer 114 (1992) 764–768.
[16] J.D. Bernardin, I. Mudawar, A Leidenfrost point model for impinging droplets and sprays, J. Heat Transfer 126 (2004) 272–278.
[17] M. Visaria, I. Mudawar, Effects of high subcooling on two-phase spray cooling and critical heat flux, Int. J. Heat Mass Transfer 51 (2008) 5269–5278.
[18] M.K. Sung, I. Mudawar, Single-phase hybrid micro-channel/micro-jet impingement cooling, Int. J. Heat Mass Transfer 51 (2008) 4342–4352.
[19] A.E. Bergles, R.L. Webb, G.H. Junkhan, M.K. Jensen, Bibliography on augmentation of convective heat and mass transfer, Heat Transfer Laboratory Report HTL-19, Iowa State University, 1979.
[20] H. Zhang, I. Mudawar, M.M. Hasan, Experimental assessment of the effects of body force, surface tension force, and inertia on flow boiling CHF, Int. J. Heat Mass Transfer 45 (2002) 4079–4095.
[21] H. Zhang, I. Mudawar, M.M. Hasan, Experimental and theoretical study of orientation effects on flow boiling CHF, Int. J. Heat Mass Transfer 45 (2002) 4463–4477.
[22] H. Zhang, I. Mudawar, M.M. Hasan, Flow boiling CHF in microgravity, Int. J. Heat Mass Transfer 48 (2005) 3107–3118.
[23] C. Konishi, I. Mudawar, Review of flow boiling and critical heat flux in microgravity, Int. J. Heat Mass Transfer 80 (2015) 469–493.
[24] I. Mudawar, Flow boiling and flow condensation in reduced gravity, Adv. Heat Transfer 49 (2017) 225–306.
[25] S.U.S. Choi, Nanofluids: from vision to reality through research, J. Heat Transfer 131 (2009) 033106.
[26] S.J. Kim, I.C. Bang, J. Buongiorno, L.W. Hu, Surface wettability change during pool boiling of nanofluids and its effect on critical heat flux, Int. J. Heat Mass Transfer 50 (2007) 4105–4116.
[27] H. Masuda, A. Ebata, K. Teramae, N. Hishinuma, Alteration of thermal conductivity and viscosity of liquid by dispersing ultrafine particles (dispersion of γ-Al2O3, SiO2, and TiO2 ultra-fine particles), Netsu Bussei 4 (1993) 227–233.
[28] S.U.S. Choi, J.A. Eastman, Enhancing thermal conductivity of fluids with nanoparticles, in: Proceedings of the 1995 ASME International Mechanical Engineering Congress and Exhibition, ASME, San Francisco, USA, 1995.
[29] D. Kim, Y. Kwon, Y. Cho, C. Li, S. Cheong, Y. Hwang, J. Lee, D. Hong, S. Moon, Convective heat transfer characteristics of nanofluids under laminar and turbulent flow conditions, Curr. Appl Phys. 9 (2009) e119–e123.
[30] X.-Q. Wang, A.S. Mujumdar, Heat transfer characteristics of nanofluids: a review, Int. J. Therm. Sci. 46 (2007) 1–19.
[31] D. Wen, G. Lin, S. Vafaei, K. Zhang, Review of nanofluids for heat transfer applications, Particuology 7 (2009) 141–150.
[32] L. Godson, B. Raja, D.M. Lal, S. Wongwises, Enhancement of heat transfer using nanofluids—an overview, Renewable Sustainable Energy Rev. 14 (2010) 629–641.
[33] S.M.S. Murshed, C.A.N. De Castro, M.J.V. Lourenço, M.L.M. Lopes, F.J.V. Santos, A review of boiling and convective heat transfer with nanofluids, Renewable Sustainable Energy Rev. 15 (2011) 2342–2354.
[34] J. Barber, D. Brutin, L. Tadrist, A review on boiling heat transfer enhancement with nanofluids, Nanoscale Res. Lett. 6 (2011) 280.
[35] J.M. Wu, J. Zhao, A review of nanofluid heat transfer and critical heat flux enhancement—research gap to engineering application, Prog. Nucl. Energy 66 (2013) 13–24.
[36] L. Cheng, L. Liu, Boiling and two-phase flow phenomena of refrigerant-based nanofluids: fundamentals, applications and challenges, Int. J. Refrig. 36 (2013) 421–446.
[37] A. Celen, A. Çebi, M. Aktas, O. Mahian, A.S. Dalkilic, S. Wongwises, A review of nanorefrigerants: flow characteristics and applications, Int. J. Refrig. 44 (2014) 125–140.

[38] M. Bahiraei, M. Hangi, Flow and heat transfer characteristics of magnetic nanofluids: a review, J. Magn. Magn. Mater. 374 (2015) 125–138.
[39] X. Fang, Y. Chen, H. Zhang, W. Chen, A. Dong, R. Wang, Heat transfer and critical heat flux of nanofluid boiling: a comprehensive review, Renewable Sustainable Energy Rev. 62 (2016) 924–940.
[40] B.H. Salman, H.A. Mohammed, K.M. Munisamy, A.S. Kherbeet, Characteristics of heat transfer and fluid flow in microtube and microchannel using conventional fluids and nanofluids: a review, Renewable Sustainable Energy Rev. 28 (2013) 848–880.
[41] W. Daungthongsuk, S. Wongwises, A critical review of convective heat transfer of nanofluids, Renewable Sustainable Energy Rev. 11 (2007) 797–817.
[42] O. Mahian, A. Kianifar, C. Kleinstreuer, M.d.A. Al-Nimr, I. Pop, A.Z. Sahin, S. Wongwises, A review of entropy generation in nanofluid flow, Int. J. Heat Mass Transfer 65 (2013) 514–532.
[43] A.M. Hussein, K.V. Sharma, R.A. Bakar, K. Kadirgama, A review of forced convection heat transfer enhancement and hydrodynamic characteristics of a nanofluid, Renewable Sustainable Energy Rev. 29 (2014) 734–743.
[44] A.A. Hussien, M.Z. Abdullah, M.d.A. Al-Nimr, Single-phase heat transfer enhancement in micro/minichannels using nanofluids: theory and applications, Appl. Energy 164 (2016) 733–755.
[45] S. Kakaç, A. Pramuanjaroenkij, Review of convective heat transfer enhancement with nanofluids, Int. J. Heat Mass Transfer 52 (2009) 3187–3196.
[46] W. Yu, D.M. France, E.V. Timofeeva, D. Singh, J.L. Routbort, Comparative review of turbulent heat transfer of nanofluids, Int. J. Heat Mass Transfer 55 (2012) 5380–5396.
[47] L.S. Sundar, M.K. Singh, Convective heat transfer and friction factor correlations of nanofluid in a tube and with inserts: a review, Renewable Sustainable Energy Rev. 20 (2013) 23–35.
[48] H.A. Mohammed, G. Bhaskaran, N.H. Shuaib, R. Saidur, Heat transfer and fluid flow characteristics in microchannels heat exchanger using nanofluids: a review, Renewable Sustainable Energy Rev. 15 (2011) 1502–1512.
[49] S.M. Vanaki, P. Ganesan, H.A. Mohammed, Numerical study of convective heat transfer of nanofluids: a review, Renewable Sustainable Energy Rev. 54 (2016) 1212–1239.
[50] X. Fang, R. Wang, W. Chen, H. Zhang, C. Ma, A review of flow boiling heat transfer of nanofluids, Appl. Therm. Eng. 91 (2015) 1003–1017.
[51] J. Lee, I. Mudawar, Fluid flow and heat transfer characteristics of low temperature two-phase micro-channel heat sinks–Part 1: Experimental methods and flow visualization results, Int. J. Heat Mass Transfer 51 (2008) 4315–4326.
[52] G. Liang, I. Mudawar, Review of mass and momentum interactions during drop impact on a liquid film, Int. J. Heat Mass Transfer 101 (2016) 577–599.
[53] G. Liang, I. Mudawar, Review of drop impact on heated walls, Int. J. Heat Mass Transfer 106 (2017) 103–126.
[54] G. Liang, I. Mudawar, Review of spray cooling–Part 1: Single-phase and nucleate boiling regimes, and critical heat flux, Int. J. Heat Mass Transfer 115 (2017) 1174–1205.
[55] G. Liang, I. Mudawar, Review of spray cooling–Part 2: High temperature boiling regimes and quenching applications, Int. J. Heat Mass Transfer 115 (2017) 1206–1222.
[56] G. Liang, I. Mudawar, Pool boiling critical heat flux (CHF)–Part 1: Review of mechanisms, models, and correlations, Int. J. Heat Mass Transfer 117 (2018) 1352–1367.
[57] G. Liang, I. Mudawar, Pool boiling critical heat flux (CHF)–Part 2: Assessment of models and correlations, Int. J. Heat Mass Transfer 117 (2018) 1368–1383.
[58] G. Liang, I. Mudawar, Review of pool boiling enhancement with additives and nanofluids, Int. J. Heat Mass Transfer 124 (2018) 423–453.
[59] G. Liang, I. Mudawar, Review of pool boiling enhancement by surface modification, Int. J. Heat Mass Transfer 128 (2019) 892–933.
[60] D. Wen, Y. Ding, Experimental investigation into convective heat transfer of nanofluids at the entrance region under laminar flow conditions, Int. J. Heat Mass Transfer 47 (2004) 5181–5188.
[61] C.J. Ho, J.B. Huang, P.S. Tsai, Y.M. Yang, Water-based suspensions of Al_2O_3 nanoparticles and MEPCM particles on convection effectiveness in a circular tube, Int. J. Therm. Sci. 50 (2011) 736–748.
[62] W.Y. Lai, S. Vinod, P.E. Phelan, R. Prasher, Convective heat transfer for water-based alumina nanofluids in a single 1.02-mm tube, J. Heat Transfer 131 (2009) 112401.
[63] M. Hojjat, S.G. Etemad, R. Bagheri, J. Thibault, Convective heat transfer of non-Newtonian nanofluids through a uniformly heated circular tube, Int. J. Therm. Sci. 50 (2011) 525–531.
[64] A.A. Minea, Effect of microtube length on heat transfer enhancement of an water/Al_2O_3 nanofluid at high Reynolds numbers, Int. J. Heat Mass Transfer 62 (2013) 22–30.
[65] D. Wen, Y. Ding, Effect of particle migration on heat transfer in suspensions of nanoparticles flowing through minichannels, Microfluid. Nanofluid. 1 (2005) 183–189.
[66] Y. He, Y. Men, Y. Zhao, H. Lu, Y. Ding, Numerical investigation into the convective heat transfer of TiO_2 nanofluids flowing through a straight tube under the laminar flow conditions, Appl. Therm. Eng. 29 (2009) 1965–1972.
[67] Y. Ding, H. Alias, D. Wen, R.A. Williams, Heat transfer of aqueous suspensions of carbon nanotubes (CNT nanofluids), Int. J. Heat Mass Transfer 49 (2006) 240–250.
[68] Y. Ding, H. Chen, Y. He, A. Lapkin, M. Yeganeh, L. Šiller, Y.V. Butenko, Forced convective heat transfer of nanofluids, Adv. Powder Technol. 18 (2007) 813–824.
[69] P. Garg, J.L. Alvarado, C. Marsh, T.A. Carlson, D.A. Kessler, K. Annamalai, An experimental study on the effect of ultrasonication on viscosity and heat transfer performance of multi-wall carbon nanotube-based aqueous nanofluids, Int. J. Heat Mass Transfer 52 (2009) 5090–5101.
[70] D. Liu, L. Yu, Single-phase thermal transport of nanofluids in a minichannel, J. Heat Transfer 133 (2010) 031009.
[71] M. Karimzadehkhouei, S.E. Yalcin, K. Şendur, M.P. Mengüç, A. Koşar, Pressure drop and heat transfer characteristics of nanofluids in horizontal microtubes under thermally developing flow conditions, Exp. Therm. Fluid Sci. 67 (2015) 37–47.
[72] K.S. Hwang, S.P. Jang, S.U.S. Choi, Flow and convective heat transfer characteristics of water-based Al_2O_3 nanofluids in fully developed laminar flow regime, Int. J. Heat Mass Transfer 52 (2009) 193–199.
[73] R.K. Shah, A.L. London, Laminar Flow Forced Convection in Ducts: A Source Book for Compact Heat Exchanger Analytical Data, Academic Press, New York, 1978.
[74] S.Z. Heris, S.G. Etemad, M.N. Esfahany, Experimental investigation of oxide nanofluids laminar flow convective heat transfer, Int. Commun. Heat Mass Transfer 33 (2006) 529–535.
[75] S.Z. Heris, M.N. Esfahany, S.G. Etemad, Experimental investigation of convective heat transfer of Al_2O_3/water nanofluid in circular tube, Int. J. Heat Fluid Flow 28 (2007) 203–210.
[76] S.Z. Heris, S.G. Etemad, M.N. Esfahany, Convective heat transfer of a Cu/water nanofluid flowing through a circular tube, Exp. Heat Transfer 22 (2009) 217–227.
[77] S.Z. Heris, M.N. Esfahany, G. Etemad, Numerical investigation of nanofluid laminar convective heat transfer through a circular tube, Numer. Heat Transfer Part A 52 (2007) 1043–1058.
[78] D. Lelea, The performance evaluation of Al_2O_3/water nanofluid flow and heat transfer in microchannel heat sink, Int. J. Heat Mass Transfer 54 (2011) 3891–3899.
[79] T.H. Nassan, S.Z. Heris, S.H. Noie, A comparison of experimental heat transfer characteristics for Al_2O_3/water and CuO/water nanofluids in square cross-section duct, Int. Commun. Heat Mass Transfer 37 (2010) 924–928.
[80] M. Rostamani, S.F. Hosseinizadeh, M. Gorji, J.M. Khodadadi, Numerical study of turbulent forced convection flow of nanofluids in a long horizontal duct considering variable properties, Int. Commun. Heat Mass Transfer 37 (2010) 1426–1431.
[81] R.B. Mansour, N. Galanis, C.T. Nguyen, Experimental study of mixed convection with water–Al_2O_3 nanofluid in inclined tube with uniform wall heat flux, Int. J. Therm. Sci. 50 (2011) 403–410.
[82] B.A. Bhanvase, M.R. Sarode, L.A. Putterwar, K.A. Abdullah, M.P. Deosarkar, S.H. Sonawane, Intensification of convective heat transfer in water/ethylene glycol based nanofluids containing TiO_2 nanoparticles, Chem. Eng. Process. Process Intensif. 82 (2014) 123–131.
[83] U. Rea, T. McKrell, L.-W. Hu, J. Buongiorno, Laminar convective heat transfer and viscous pressure loss of alumina–water and zirconia–water nanofluids, Int. J. Heat Mass Transfer 52 (2009) 2042–2048.
[84] K.B. Anoop, T. Sundararajan, S.K. Das, Effect of particle size on the convective heat transfer in nanofluid in the developing region, Int. J. Heat Mass Transfer 52 (2009) 2189–2195.
[85] M.K. Moraveji, M. Darabi, S.M.H. Haddad, R. Davarnejad, Modeling of convective heat transfer of a nanofluid in the developing region of tube flow with computational fluid dynamics, Int. Commun. Heat Mass Transfer 38 (2011) 1291–1295.
[86] M.K. Moraveji, S.M.H. Haddad, M. Darabi, Modeling of forced convective heat transfer of a non-Newtonian nanofluid in the horizontal tube under constant heat flux with computational fluid dynamics, Int. Commun. Heat Mass Transfer 39 (2012) 995–999.
[87] E. Ebrahimnia-Bajestan, H. Niazmand, W. Duangthongsuk, S. Wongwises, Numerical investigation of effective parameters in convective heat transfer of nanofluids flowing under a laminar flow regime, Int. J. Heat Mass Transfer 54 (2011) 4376–4388.
[88] O.A. Akbari, D. Toghraie, A. Karimipour, A. Marzban, G.R. Ahmadi, The effect of velocity and dimension of solid nanoparticles on heat transfer in non-Newtonian nanofluid, Physica E 86 (2017) 68–75.
[89] D.P. Kulkarni, P.K. Namburu, H.E. Bargar, D.K. Das, Convective heat transfer and fluid dynamic characteristics of SiO_2 ethylene glycol/water nanofluid, Heat Transfer Eng. 29 (2008) 1027–1035.
[90] M. Bahiraei, M. Hangi, Investigating the efficacy of magnetic nanofluid as a coolant in double-pipe heat exchanger in the presence of magnetic field, Energy Convers. Manage. 76 (2013) 1125–1133.
[91] Y. He, Y. Jin, H. Chen, Y. Ding, D. Cang, H. Lu, Heat transfer and flow behaviour of aqueous suspensions of TiO_2 nanoparticles (nanofluids) flowing upward through a vertical pipe, Int. J. Heat Mass Transfer 50 (2007) 2272–2281.
[92] S.Z. Heris, T.H. Nassan, S.H. Noie, H. Sardarabadi, M. Sardarabadi, Laminar convective heat transfer of Al_2O_3/water nanofluid through square cross-sectional duct, Int. J. Heat Fluid Flow 44 (2013) 375–382.
[93] B. Mehrjou, S.Z. Heris, K. Mohamadifard, Experimental study of CuO/water nanofluid turbulent convective heat transfer in square cross-section duct, Exp. Heat Transfer 28 (2015) 282–297.

[94] A.K. Santra, S. Sen, N. Chakraborty, Study of heat transfer due to laminar flow of copper–water nanofluid through two isothermally heated parallel plates, Int. J. Therm. Sci. 48 (2009) 391–400.
[95] M.M. Heyhat, F. Kowsary, A.M. Rashidi, M.H. Momenpour, A. Amrollahi, Experimental investigation of laminar convective heat transfer and pressure drop of water-based Al_2O_3 nanofluids in fully developed flow regime, Exp. Therm. Fluid Sci. 44 (2013) 483–489.
[96] C.J. Ho, W.-C. Chen, W.-M. Yan, Experiment on thermal performance of water-based suspensions of Al_2O_3 nanoparticles and MEPCM particles in a minichannel heat sink, Int. J. Heat Mass Transfer 69 (2014) 276–284.
[97] C.J. Ho, W.-C. Chen, W.-M. Yan, Correlations of heat transfer effectiveness in a minichannel heat sink with water-based suspensions of Al_2O_3 nanoparticles and/or MEPCM particles, Int. J. Heat Mass Transfer 69 (2014) 293–299.
[98] L.G. Asirvatham, N. Vishal, S.K. Gangatharan, D.M. Lal, Experimental study on forced convective heat transfer with low volume fraction of CuO/water nanofluid, Energies 2 (2009) 97–119.
[99] S.E.B. Maïga, S.J. Palm, C.T. Nguyen, G. Roy, N. Galanis, Heat transfer enhancement by using nanofluids in forced convection flows, Int. J. Heat Fluid Flow 26 (2005) 530–546.
[100] S.E.B. Maïga, C.T. Nguyen, N. Galanis, G. Roy, Heat transfer behaviours of nanofluids in a uniformly heated tube, Superlattices Microstruct. 35 (2004) 543–557.
[101] L. Yu, D. Liu, F. Botz, Laminar convective heat transfer of alumina-polyalphaolefin nanofluids containing spherical and non-spherical nanoparticles, Exp. Therm. Fluid Sci. 37 (2012) 72–83.
[102] Y. Yang, Z.G. Zhang, E.A. Grulke, W.B. Anderson, G. Wu, Heat transfer properties of nanoparticle-in-fluid dispersions (nanofluids) in laminar flow, Int. J. Heat Mass Transfer 48 (2005) 1107–1116.
[103] H. Chen, W. Yang, Y. He, Y. Ding, L. Zhang, C. Tan, A.A. Lapkin, D.V. Bavykin, Heat transfer and flow behaviour of aqueous suspensions of titanate nanotubes (nanofluids), Powder Technol. 183 (2008) 63–72.
[104] S. Ebrahimi, J. Sabbaghzadeh, M. Lajevardi, I. Hadi, Cooling performance of a microchannel heat sink with nanofluids containing cylindrical nanoparticles (carbon nanotubes), Heat Mass Transfer 46 (2010) 549–553.
[105] H. Aminfar, M. Mohammadpourfard, Y.N. Kahnamouei, A 3D numerical simulation of mixed convection of a magnetic nanofluid in the presence of non-uniform magnetic field in a vertical tube using two phase mixture model, J. Magn. Magn. Mater. 323 (2011) 1963–1972.
[106] R. Azizian, E. Doroodchi, T. McKrell, J. Buongiorno, L.W. Hu, B. Moghtaderi, Effect of magnetic field on laminar convective heat transfer of magnetite nanofluids, Int. J. Heat Mass Transfer 68 (2014) 94–109.
[107] M. Lajvardi, J. Moghimi-Rad, I. Hadi, A. Gavili, T.D. Isfahani, F. Zabihi, J. Sabbaghzadeh, Experimental investigation for enhanced ferrofluid heat transfer under magnetic field effect, J. Magn. Magn. Mater. 322 (2010) 3508–3513.
[108] M. Asfer, B. Mehta, A. Kumar, S. Khandekar, P.K. Panigrahi, Effect of magnetic field on laminar convective heat transfer characteristics of ferrofluid flowing through a circular stainless steel tube, Int. J. Heat Fluid Flow 59 (2016) 74–86.
[109] M. Goharkhah, M. Ashjaee, J. Jamali, Experimental investigation on heat transfer and hydrodynamic behavior of magnetite nanofluid flow in a channel with recognition of the best models for transport properties, Exp. Therm. Fluid Sci. 68 (2015) 582–592.
[110] M. Goharkhah, A. Salarian, M. Ashjaee, M. Shahabadi, Convective heat transfer characteristics of magnetite nanofluid under the influence of constant and alternating magnetic field, Powder Technol. 274 (2015) 258–267.
[111] M. Goharkhah, M. Ashjaee, M. Shahabadi, Experimental investigation on convective heat transfer and hydrodynamic characteristics of magnetite nanofluid under the influence of an alternating magnetic field, Int. J. Therm. Sci. 99 (2016) 113–124.
[112] Y. Xuan, Q. Li, Investigation on convective heat transfer and flow features of nanofluids, J. Heat Transfer 125 (2003) 151–155.
[113] Y. Xuan, W. Roetzel, Conceptions for heat transfer correlation of nanofluids, Int. J. Heat Mass Transfer 43 (2000) 3701–3707.
[114] F.P. Incropera, D.P. DeWitt, Introduction to Heat Transfer, John Wiley & Sons, New York, USA, 1996.
[115] B.C. Pak, Y.I. Cho, Hydrodynamic and heat transfer study of dispersed fluids with submicron metallic oxide particles, Exp. Heat Transfer 11 (1998) 151–170.
[116] W. Duangthongsuk, S. Wongwises, An experimental study on the heat transfer performance and pressure drop of TiO_2-water nanofluids flowing under a turbulent flow regime, Int. J. Heat Mass Transfer 53 (2010) 334–344.
[117] S.E.B. Maïga, C.T. Nguyen, N. Galanis, G. Roy, T. Maré, M. Coqueux, Heat transfer enhancement in turbulent tube flow using Al_2O_3 nanoparticle suspension, Int. J. Numer. Methods Heat Fluid Flow 16 (2006) 275–292.
[118] A.R. Sajadi, M.H. Kazemi, Investigation of turbulent convective heat transfer and pressure drop of TiO_2/water nanofluid in circular tube, Int. Commun. Heat Mass Transfer 38 (2011) 1474–1478.
[119] T.-P. Teng, Y.-H. Hung, C.-S. Jwo, C.-C. Chen, L.-Y. Jeng, Pressure drop of TiO_2 nanofluid in circular pipes, Particuology 9 (2011) 486–491.
[120] L. Godson, B. Raja, D. Mohan Lal, S. Wongwises, Convective heat transfer characteristics of silver-water nanofluid under laminar and turbulent flow conditions, J. Therm. Sci. Eng. Appl. 4 (2012) 031001.
[121] L.G. Asirvatham, B. Raja, D.M. Lal, S. Wongwises, Convective heat transfer of nanofluids with correlations, Particuology 9 (2011) 626–631.
[122] S. Torii, W.-J. Yang, Heat transfer augmentation of aqueous suspensions of nanodiamonds in turbulent pipe flow, J. Heat Transfer 131 (2009) 043203.
[123] E. Sadeghinezhad, M. Mehrali, S.T. Latibari, M. Mehrali, S.N. Kazi, C.S. Oon, H. S.C. Metselaar, Experimental investigation of convective heat transfer using graphene nanoplatelet based nanofluids under turbulent flow conditions, Ind. Eng. Chem. Res. 53 (2014) 12455–12465.
[124] M. Mehrali, E. Sadeghinezhad, M.A. Rosen, S.T. Latibari, M. Mehrali, H.S.C. Metselaar, S.N. Kazi, Effect of specific surface area on convective heat transfer of graphene nanoplatelet aqueous nanofluids, Exp. Therm. Fluid Sci. 68 (2015) 100–108.
[125] E. Sadeghinezhad, H. Togun, M. Mehrali, P.S. Nejad, S.T. Latibari, T. Abdulrazzaq, S.N. Kazi, H.S.C. Metselaar, An experimental and numerical investigation of heat transfer enhancement for graphene nanoplatelets nanofluids in turbulent flow conditions, Int. J. Heat Mass Transfer 81 (2015) 41–51.
[126] H. Akhavan-Zanjani, M. Saffar-Avval, M. Mansourkiaei, M. Ahadi, F. Sharif, Turbulent convective heat transfer and pressure drop of graphene–water nanofluid flowing inside a horizontal circular tube, J. Dispersion Sci. Technol. 35 (2014) 1230–1240.
[127] H. Akhavan-Zanjani, M. Saffar-Avval, M. Mansourkiaei, F. Sharif, M. Ahadi, Experimental investigation of laminar forced convective heat transfer of Graphene–water nanofluid inside a circular tube, Int. J. Therm. Sci. 100 (2016) 316–323.
[128] M.H. Esfe, S. Saedodin, O. Mahian, S. Wongwises, Heat transfer characteristics and pressure drop of COOH-functionalized DWCNTs/water nanofluid in turbulent flow at low concentrations, Int. J. Heat Mass Transfer 73 (2014) 186–194.
[129] M.H. Esfe, S. Saedodin, M. Mahmoodi, Experimental studies on the convective heat transfer performance and thermophysical properties of MgO–water nanofluid under turbulent flow, Exp. Therm. Fluid Sci. 52 (2014) 68–78.
[130] V. Gnielinski, New equations for heat and mass transfer in turbulent pipe and channel flow, Int. Chem. Eng. 16 (1976) 359–368.
[131] W. Williams, J. Buongiorno, L.-W. Hu, Experimental investigation of turbulent convective heat transfer and pressure loss of alumina/water and zirconia/water nanoparticle colloids (nanofluids) in horizontal tubes, J. Heat Transfer 130 (2008) 042412.
[132] M.H. Kayhani, H. Soltanzadeh, M.M. Heyhat, M. Nazari, F. Kowsary, Experimental study of convective heat transfer and pressure drop of TiO_2/water nanofluid, Int. Commun. Heat Mass Transfer 39 (2012) 456–462.
[133] S. Ferrouillat, A. Bontemps, J.-P. Ribeiro, J.-A. Gruss, O. Soriano, Hydraulic and heat transfer study of SiO_2/water nanofluids in horizontal tubes with imposed wall temperature boundary conditions, Int. J. Heat Fluid Flow 32 (2011) 424–439.
[134] K.V. Sharma, L.S. Sundar, P.K. Sarma, Estimation of heat transfer coefficient and friction factor in the transition flow with low volume concentration of Al_2O_3 nanofluid flowing in a circular tube and with twisted tape insert, Int. Commun. Heat Mass Transfer 36 (2009) 503–507.
[135] L.S. Sundar, K.V. Sharma, Turbulent heat transfer and friction factor of Al_2O_3 nanofluid in circular tube with twisted tape inserts, Int. J. Heat Mass Transfer 53 (2010) 1409–1416.
[136] W. Yu, D.M. France, D.S. Smith, D. Singh, E.V. Timofeeva, J.L. Routbort, Heat transfer to a silicon carbide/water nanofluid, Int. J. Heat Mass Transfer 52 (2009) 3606–3612.
[137] L.S. Sundar, M.K. Singh, I. Bidkin, A.C.M. Sousa, Experimental investigations in heat transfer and friction factor of magnetic Ni nanofluid flowing in a tube, Int. J. Heat Mass Transfer 70 (2014) 224–234.
[138] M. Hojjat, S.G. Etemad, R. Bagheri, J. Thibault, Turbulent forced convection heat transfer of non-Newtonian nanofluids, Exp. Therm. Fluid Sci. 35 (2011) 1351–1356.
[139] A. Zamzamian, S.N. Oskouie, A. Doosthoseini, A. Joneidi, M. Pazouki, Experimental investigation of forced convective heat transfer coefficient in nanofluids of Al_2O_3/EG and CuO/EG in a double pipe and plate heat exchangers under turbulent flow, Exp. Therm. Fluid Sci. 35 (2011) 495–502.
[140] J. Buongiorno, Convective transport in nanofluids, J. Heat Transfer 128 (2005) 240–250.
[141] P.K. Singh, P.V. Harikrishna, T. Sundararajan, S.K. Das, Experimental and numerical investigation into the heat transfer study of nanofluids in microchannel, J. Heat Transfer 133 (2011) 121701.
[142] C. Yang, W. Li, A. Nakayama, Convective heat transfer of nanofluids in a concentric annulus, Int. J. Therm. Sci. 71 (2013) 249–257.
[143] C. Yang, W. Li, Y. Sano, M. Mochizuki, A. Nakayama, On the anomalous convective heat transfer enhancement in nanofluids: a theoretical answer to the nanofluids controversy, J. Heat Transfer 135 (2013) 054504.
[144] A. Malvandi, S.A. Moshizi, E.G. Soltani, D.D. Ganji, Modified Buongiorno's model for fully developed mixed convection flow of nanofluids in a vertical annular pipe, Comput. Fluids 89 (2014) 124–132.
[145] A. Malvandi, D.D. Ganji, Brownian motion and thermophoresis effects on slip flow of alumina/water nanofluid inside a circular microchannel in the presence of a magnetic field, Int. J. Therm. Sci. 84 (2014) 196–206.
[146] A. Malvandi, D.D. Ganji, Magnetic field effect on nanoparticles migration and heat transfer of water/alumina nanofluid in a channel, J. Magn. Magn. Mater. 362 (2014) 172–179.
[147] A. Malvandi, D.D. Ganji, Effects of nanoparticle migration on hydromagnetic mixed convection of alumina/water nanofluid in vertical channels with asymmetric heating, Physica E 66 (2015) 181–196.

[148] A. Malvandi, S.A. Moshizi, D.D. Ganji, Effect of magnetic fields on heat convection inside a concentric annulus filled with Al_2O_3–water nanofluid, Adv. Powder Technol. 25 (2014) 1817–1824.
[149] S.A. Moshizi, A. Malvandi, D.D. Ganji, I. Pop, A two-phase theoretical study of Al_2O_3–water nanofluid flow inside a concentric pipe with heat generation/absorption, Int. J. Therm. Sci. 84 (2014) 347–357.
[150] A. Malvandi, D.D. Ganji, Mixed convective heat transfer of water/alumina nanofluid inside a vertical microchannel, Powder Technol. 263 (2014) 37–44.
[151] A. Malvandi, S.A. Moshizi, D.D. Ganji, Two-component heterogeneous mixed convection of alumina/water nanofluid in microchannels with heat source/sink, Adv. Powder Technol. 27 (2016) 245–254.
[152] A. Malvandi, S.A. Moshizi, D.D. Ganji, Effects of temperature-dependent thermophysical properties on nanoparticle migration at mixed convection of nanofluids in vertical microchannels, Powder Technol. 303 (2016) 7–19.
[153] F. Hedayati, G. Domairry, Effects of nanoparticle migration and asymmetric heating on mixed convection of TiO_2–H_2O nanofluid inside a vertical microchannel, Powder Technol. 272 (2015) 250–259.
[154] F. Hedayati, G. Domairry, Nanoparticle migration effects on fully developed forced convection of TiO_2–water nanofluid in a parallel plate microchannel, Particuology 24 (2016) 96–107.
[155] F. Hedayati, A. Malvandi, M.H. Kaffash, D.D. Ganji, Fully developed forced convection of alumina/water nanofluid inside microchannels with asymmetric heating, Powder Technol. 269 (2015) 520–531.
[156] F. Garoosi, L. Jahanshaloo, S. Garoosi, Numerical simulation of mixed convection of the nanofluid in heat exchangers using a Buongiorno model, Powder Technol. 269 (2015) 296–311.
[157] D.A. Nield, A.V. Kuznetsov, Forced convection in a parallel-plate channel occupied by a nanofluid or a porous medium saturated by a nanofluid, Int. J. Heat Mass Transfer 70 (2014) 430–433.
[158] M.J. Maghrebi, M. Nazari, T. Armaghani, Forced convection heat transfer of nanofluids in a porous channel, Transp. Porous Media 93 (2012) 401–413.
[159] H. Xu, T. Fan, I. Pop, Analysis of mixed convection flow of a nanofluid in a vertical channel with the Buongiorno mathematical model, Int. Commun. Heat Mass Transfer 44 (2013) 15–22.
[160] E.R.d. Schio, M. Celli, A. Barletta, Effects of Brownian diffusion and thermophoresis on the laminar forced convection of a nanofluid in a channel, J. Heat Transfer 136 (2013).
[161] P.F. Alvariño, J.M.S. Jabardo, A. Arce, M.I.L. Galdo, A numerical investigation of laminar flow of a water/alumina nanofluid, Int. J. Heat Mass Transfer 59 (2013) 423–432.
[162] M.M. Heyhat, F. Kowsary, Effect of particle migration on flow and convective heat transfer of nanofluids flowing through a circular pipe, J. Heat Transfer 132 (2010) 062401.
[163] U. Khan, N. Ahmed, S.T. Mohyud-Din, Heat transfer effects on carbon nanotubes suspended nanofluid flow in a channel with non-parallel walls under the effect of velocity slip boundary condition: a numerical study, Neural Comput. Appl. 28 (2017) 37–46.
[164] A. Malvandi, D.D. Ganji, Magnetohydrodynamic mixed convective flow of Al_2O_3–water nanofluid inside a vertical microtube, J. Magn. Magn. Mater. 369 (2014) 132–141.
[165] W.H. Azmi, K.V. Sharma, P.K. Sarma, R. Mamat, S. Anuar, V. Dharma Rao, Experimental determination of turbulent forced convection heat transfer and friction factor with SiO_2 nanofluid, Exp. Therm. Fluid Sci. 51 (2013) 103–111.
[166] L.S. Sundar, M.T. Naik, K.V. Sharma, M.K. Singh, T.C.S. Reddy, Experimental investigation of forced convection heat transfer and friction factor in a tube with Fe_3O_4 magnetic nanofluid, Exp. Therm. Fluid Sci. 37 (2012) 65–71.
[167] G.H. Ko, K. Heo, K. Lee, D.S. Kim, C. Kim, Y. Sohn, M. Choi, An experimental study on the pressure drop of nanofluids containing carbon nanotubes in a horizontal tube, Int. J. Heat Mass Transfer 50 (2007) 4749–4753.
[168] M. Zarringhalam, A. Karimipour, D. Toghraie, Experimental study of the effect of solid volume fraction and Reynolds number on heat transfer coefficient and pressure drop of CuO–Water nanofluid, Exp. Therm. Fluid Sci. 76 (2016) 342–351.
[169] A.A.A. Arani, J. Amani, Experimental study on the effect of TiO_2–water nanofluid on heat transfer and pressure drop, Exp. Therm. Fluid Sci. 42 (2012) 107–115.
[170] A.A.A. Arani, J. Amani, Experimental investigation of diameter effect on heat transfer performance and pressure drop of TiO_2–water nanofluid, Exp. Therm. Fluid Sci. 44 (2013) 520–533.
[171] M. Nasiri, S.G. Etemad, R. Bagheri, Experimental heat transfer of nanofluid through an annular duct, Int. Commun. Heat Mass Transfer 38 (2011) 958–963.
[172] S.M. Fotukian, M.N. Esfahany, Experimental investigation of turbulent convective heat transfer of dilute γ-Al_2O_3/water nanofluid inside a circular tube, Int. J. Heat Fluid Flow 31 (2010) 606–612.
[173] S.M. Fotukian, M.N. Esfahany, Experimental study of turbulent convective heat transfer and pressure drop of dilute CuO/water nanofluid inside a circular tube, Int. Commun. Heat Mass Transfer 37 (2010) 214–219.
[174] M. Vakili, A. Mohebbi, H. Hashemipour, Experimental study on convective heat transfer of TiO_2 nanofluids, Heat Mass Transfer 49 (2013) 1159–1165.
[175] M.S. Mojarrad, A. Keshavarz, M. Ziabasharhagh, M.M. Raznahan, Experimental investigation on heat transfer enhancement of alumina/water and alumina/water–ethylene glycol nanofluids in thermally developing laminar flow, Exp. Therm. Fluid Sci. 53 (2014) 111–118.
[176] D. Lelea, C. Nisulescu, The micro-tube heat transfer and fluid flow of water based Al_2O_3 nanofluid with viscous dissipation, Int. Commun. Heat Mass Transfer 38 (2011) 704–710.
[177] A.R. Chabi, S. Zarrinabadi, S.M. Peyghambarzadeh, S.H. Hashemabadi, M. Salimi, Local convective heat transfer coefficient and friction factor of CuO/water nanofluid in a microchannel heat sink, Heat Mass Transfer 53 (2017) 661–671.
[178] Z. Azizi, A. Alamdari, M.R. Malayeri, Convective heat transfer of Cu–water nanofluid in a cylindrical microchannel heat sink, Energy Convers. Manage. 101 (2015) 515–524.
[179] Z. Azizi, A. Alamdari, M.R. Malayeri, Thermal performance and friction factor of a cylindrical microchannel heat sink cooled by Cu-water nanofluid, Appl. Therm. Eng. 99 (2016) 970–978.
[180] S.P. Jang, S.U.S. Choi, Cooling performance of a microchannel heat sink with nanofluids, Appl. Therm. Eng. 26 (2006) 2457–2463.
[181] E. Farsad, S.P. Abbasi, M.S. Zabihi, J. Sabbaghzadeh, Numerical simulation of heat transfer in a micro channel heat sinks using nanofluids, Heat Mass Transfer 47 (2011) 479–490.
[182] R. Chein, G. Huang, Analysis of microchannel heat sink performance using nanofluids, Appl. Therm. Eng. 25 (2005) 3104–3114.
[183] C.J. Ho, L.C. Wei, Z.W. Li, An experimental investigation of forced convective cooling performance of a microchannel heat sink with Al_2O_3/water nanofluid, Appl. Therm. Eng. 30 (2010) 96–103.
[184] C.J. Ho, W.C. Chen, An experimental study on thermal performance of Al_2O_3/water nanofluid in a minichannel heat sink, Appl. Therm. Eng. 50 (2013) 516–522.
[185] J. Wang, J. Zhu, X. Zhang, Y. Chen, Heat transfer and pressure drop of nanofluids containing carbon nanotubes in laminar flows, Exp. Therm. Fluid Sci. 44 (2013) 716–721.
[186] J. Lee, P.E. Gharagozloo, B. Kolade, J.K. Eaton, K.E. Goodson, Nanofluid convection in microtubes, J. Heat Transfer 132 (2010) 092401.
[187] R. Chein, J. Chuang, Experimental microchannel heat sink performance studies using nanofluids, Int. J. Therm. Sci. 46 (2007) 57–66.
[188] J. Li, C. Kleinstreuer, Thermal performance of nanofluid flow in microchannels, Int. J. Heat Fluid Flow 29 (2008) 1221–1232.
[189] H.A. Mohammed, P. Gunnasegaran, N.H. Shuaib, Heat transfer in rectangular microchannels heat sink using nanofluids, Int. Commun. Heat Mass Transfer 37 (2010) 1496–1503.
[190] H.A. Mohammed, P. Gunnasegaran, N.H. Shuaib, Influence of various base nanofluids and substrate materials on heat transfer in trapezoidal microchannel heat sinks, Int. Commun. Heat Mass Transfer 38 (2011) 194–201.
[191] H.A. Mohammed, G. Bhaskaran, N.H. Shuaib, R. Saidur, Numerical study of heat transfer enhancement of counter nanofluids flow in rectangular microchannel heat exchanger, Superlattices Microstruct. 50 (2011) 215–233.
[192] B. Rimbault, C.T. Nguyen, N. Galanis, Experimental investigation of CuO–water nanofluid flow and heat transfer inside a microchannel heat sink, Int. J. Therm. Sci. 84 (2014) 275–292.
[193] M.R. Sohel, R. Saidur, M.F.M. Sabri, M. Kamalisarvestani, M.M. Elias, A. Ijam, Investigating the heat transfer performance and thermophysical properties of nanofluids in a circular micro-channel, Int. Commun. Heat Mass Transfer 42 (2013) 75–81.
[194] M.R. Sohel, S.S. Khaleduzzaman, R. Saidur, A. Hepbasli, M.F.M. Sabri, I.M. Mahbubul, An experimental investigation of heat transfer enhancement of a minichannel heat sink using Al_2O_3–H_2O nanofluid, Int. J. Heat Mass Transfer 74 (2014) 164–172.
[195] S.M. Peyghambarzadeh, S.H. Hashemabadi, A.R. Chabi, M. Salimi, Performance of water based CuO and Al_2O_3 nanofluids in a Cu–Be alloy heat sink with rectangular microchannels, Energy Convers. Manage. 86 (2014) 28–38.
[196] A. Sivakumar, N. Alagumurthi, T. Senthilvelan, Experimental investigation of forced convective heat transfer performance in nanofluids of Al_2O_3/water and CuO/water in a serpentine shaped micro channel heat sink, Heat Mass Transfer 52 (2016) 1265–1274.
[197] B.H. Salman, H.A. Mohammed, A.S. Kherbeet, Heat transfer enhancement of nanofluids flow in microtube with constant heat flux, Int. Commun. Heat Mass Transfer 39 (2012) 1195–1204.
[198] B.H. Salman, H.A. Mohammed, K.M. Munisamy, A.S. Kherbeet, Three-dimensional numerical investigation of nanofluids flow in microtube with different values of heat flux, Heat Transfer Asian Res. 44 (2015) 599–619.
[199] H.A. Mohammed, G. Bhaskaran, N.H. Shuaib, H.I. Abu-Mulaweh, Influence of nanofluids on parallel flow square microchannel heat exchanger performance, Int. Commun. Heat Mass Transfer 38 (2011) 1–9.
[200] E.M. Tokit, H.A. Mohammed, M.Z. Yusoff, Thermal performance of optimized interrupted microchannel heat sink (IMCHS) using nanofluids, Int. Commun. Heat Mass Transfer 39 (2012) 1595–1604.
[201] H.A. Mohammed, P. Gunnasegaran, N.H. Shuaib, The impact of various nanofluid types on triangular microchannels heat sink cooling performance, Int. Commun. Heat Mass Transfer 38 (2011) 767–773.
[202] R. Nimmagadda, K. Venkatasubbaiah, Conjugate heat transfer analysis of micro-channel using novel hybrid nanofluids (Al_2O_3+Ag/Water), Eur. J. Mech. B 52 (2015) 19–27.
[203] M.N. Labib, M.J. Nine, H. Afrianto, H. Chung, H. Jeong, Numerical investigation on effect of base fluids and hybrid nanofluid in forced convective heat transfer, Int. J. Therm. Sci. 71 (2013) 163–171.

[204] S. Suresh, K.P. Venkitaraj, P. Selvakumar, M. Chandrasekar, Effect of Al_2O_3–Cu/water hybrid nanofluid in heat transfer, Exp. Therm. Fluid Sci. 38 (2012) 54–60.
[205] H. Zhang, S. Shao, H. Xu, C. Tian, Heat transfer and flow features of Al_2O_3–water nanofluids flowing through a circular microchannel – Experimental results and correlations, Appl. Therm. Eng. 61 (2013) 86–92.
[206] J.-Y. Jung, H.-S. Oh, H.-Y. Kwak, Forced convective heat transfer of nanofluids in microchannels, Int. J. Heat Mass Transfer 52 (2009) 466–472.
[207] P. Nitiapiruk, O. Mahian, A.S. Dalkilic, S. Wongwises, Performance characteristics of a microchannel heat sink using TiO_2/water nanofluid and different thermophysical models, Int. Commun. Heat Mass Transfer 47 (2013) 98–104.
[208] W. Escher, T. Brunschwiler, N. Shalkevich, A. Shalkevich, T. Burgi, B. Michel, D. Poulikakos, On the cooling of electronics with nanofluids, J. Heat Transfer 133 (2011) 051401.
[209] J. Koo, C. Kleinstreuer, Laminar nanofluid flow in microheat-sinks, Int. J. Heat Mass Transfer 48 (2005) 2652–2661.
[210] A. Raisi, B. Ghasemi, S.M. Aminossadati, A numerical study on the forced convection of laminar nanofluid in a microchannel with both slip and no-slip conditions, Numer. Heat Transfer, Part A 59 (2011) 114–129.
[211] Z. Nikkhah, A. Karimipour, M.R. Safaei, P. Forghani-Tehrani, M. Goodarzi, M. Dahari, S. Wongwises, Forced convective heat transfer of water/functionalized multi-walled carbon nanotube nanofluids in a microchannel with oscillating heat flux and slip boundary condition, Int. Commun. Heat Mass Transfer 68 (2015) 69–77.
[212] A. Karimipour, A.H. Nezhad, A. D'Orazio, M.H. Esfe, M.R. Safaei, E. Shirani, Simulation of copper–water nanofluid in a microchannel in slip flow regime using the lattice Boltzmann method, Eur. J. Mech. B 49 (2015) 89–99.
[213] P. Bhattacharya, A.N. Samanta, S. Chakraborty, Numerical study of conjugate heat transfer in rectangular microchannel heat sink with Al_2O_3/H_2O nanofluid, Heat Mass Transfer 45 (2009) 1323–1333.
[214] T.-C. Hung, W.-M. Yan, X.-D. Wang, C.-Y. Chang, Heat transfer enhancement in microchannel heat sinks using nanofluids, Int. J. Heat Mass Transfer 55 (2012) 2559–2570.
[215] M.D. Byrne, R.A. Hart, A.K. da Silva, Experimental thermal–hydraulic evaluation of CuO nanofluids in microchannels at various concentrations with and without suspension enhancers, Int. J. Heat Mass Transfer 55 (2012) 2684–2691.
[216] M. Ghazvini, H. Shokouhmand, Investigation of a nanofluid-cooled microchannel heat sink using fin and porous media approaches, Energy Convers. Manage. 50 (2009) 2373–2380.
[217] M. Hatami, D.D. Ganji, Thermal and flow analysis of microchannel heat sink (MCHS) cooled by Cu–water nanofluid using porous media approach and least square method, Energy Convers. Manage. 78 (2014) 347–358.
[218] T.-H. Tsai, R. Chein, Performance analysis of nanofluid-cooled microchannel heat sinks, Int. J. Heat Fluid Flow 28 (2007) 1013–1026.
[219] H. Abbassi, C. Aghanajafi, Evaluation of heat transfer augmentation in a nanofluid-cooled microchannel heat sink, J. Fusion Energy 25 (2006) 187–196.
[220] C.-H. Chen, C.-Y. Ding, Study on the thermal behavior and cooling performance of a nanofluid-cooled microchannel heat sink, Int. J. Therm. Sci. 50 (2011) 378–384.
[221] Y. Xuan, Q. Li, M. Ye, Investigations of convective heat transfer in ferrofluid microflows using lattice-Boltzmann approach, Int. J. Therm. Sci. 46 (2007) 105–111.
[222] Y.-T. Yang, F.-H. Lai, Lattice Boltzmann simulation of heat transfer and fluid flow in a microchannel with nanofluids, Heat Mass Transfer 47 (2011) 1229–1240.
[223] Y.-T. Yang, F.-H. Lai, Numerical study of flow and heat transfer characteristics of alumina-water nanofluids in a microchannel using the lattice Boltzmann method, Int. Commun. Heat Mass Transfer 38 (2011) 607–614.
[224] M. Mital, Analytical analysis of heat transfer and pumping power of laminar nanofluid developing flow in microchannels, Appl. Therm. Eng. 50 (2013) 429–436.
[225] M. Mital, Semi-analytical investigation of electronics cooling using developing nanofluid flow in rectangular microchannels, Appl. Therm. Eng. 52 (2013) 321–327.
[226] X.-D. Wang, A. Bin, J.-L. Xu, Optimal geometric structure for nanofluid-cooled microchannel heat sink under various constraint conditions, Energy Convers. Manage. 65 (2013) 528–538.
[227] X.-D. Wang, B. An, L. Lin, D.-J. Lee, Inverse geometric optimization for geometry of nanofluid-cooled microchannel heat sink, Appl. Therm. Eng. 55 (2013) 87–94.
[228] M. Akbari, N. Galanis, A. Behzadmehr, Comparative assessment of single and two-phase models for numerical studies of nanofluid turbulent forced convection, Int. J. Heat Fluid Flow 37 (2012) 136–146.
[229] P.K. Singh, P.V. Harikrishna, T. Sundararajan, S.K. Das, Experimental and numerical investigation into the hydrodynamics of nanofluids in microchannels, Exp. Therm. Fluid Sci. 42 (2012) 174–186.
[230] A. Akbarinia, A. Behzadmehr, Numerical study of laminar mixed convection of a nanofluid in horizontal curved tubes, Appl. Therm. Eng. 27 (2007) 1327–1337.
[231] A. Akbarinia, Impacts of nanofluid flow on skin friction factor and Nusselt number in curved tubes with constant mass flow, Int. J. Heat Fluid Flow 29 (2008) 229–241.
[232] M. Akbari, A. Behzadmehr, Developing mixed convection of a nanofluid in a horizontal tube with uniform heat flux, Int. J. Numer. Methods Heat Fluid Flow 17 (2007) 566–586.
[233] M. Akbari, A. Behzadmehr, F. Shahraki, Fully developed mixed convection in horizontal and inclined tubes with uniform heat flux using nanofluid, Int. J. Heat Fluid Flow 29 (2008) 545–556.
[234] Y. He, Y. Men, X. Liu, H. Lu, H. Chen, Y. Ding, Study on forced convective heat transfer of non-newtonian nanofluids, J. Therm. Sci. 18 (2009) 20–26.
[235] P.K. Namburu, D.K. Das, K.M. Tanguturi, R.S. Vajjha, Numerical study of turbulent flow and heat transfer characteristics of nanofluids considering variable properties, Int. J. Therm. Sci. 48 (2009) 290–302.
[236] R.B. Mansour, N. Galanis, C.T. Nguyen, Developing laminar mixed convection of nanofluids in an inclined tube with uniform wall heat flux, Int. J. Numer. Methods Heat Fluid Flow 19 (2009) 146–164.
[237] M. Izadi, A. Behzadmehr, D. Jalali-Vahida, Numerical study of developing laminar forced convection of a nanofluid in an annulus, Int. J. Therm. Sci. 48 (2009) 2119–2129.
[238] M.A. Ahmed, N.H. Shuaib, M.Z. Yusoff, A.H. Al-Falahi, Numerical investigations of flow and heat transfer enhancement in a corrugated channel using nanofluid, Int. Commun. Heat Mass Transfer 38 (2011) 1368–1375.
[239] H. Demir, A.S. Dalkilic, N.A. Kürekci, W. Duangthongsuk, S. Wongwises, Numerical investigation on the single phase forced convection heat transfer characteristics of TiO_2 nanofluids in a double-tube counter flow heat exchanger, Int. Commun. Heat Mass Transfer 38 (2011) 218–228.
[240] J. Bayat, A.H. Nikseresht, Thermal performance and pressure drop analysis of nanofluids in turbulent forced convective flows, Int. J. Therm. Sci. 60 (2012) 236–243.
[241] J. Bayat, A.H. Nikseresht, Investigation of the different base fluid effects on the nanofluids heat transfer and pressure drop, Heat Mass Transfer 47 (2011) 1089–1099.
[242] M.K. Moraveji, R.M. Ardehali, A. Ijam, CFD investigation of nanofluid effects (cooling performance and pressure drop) in mini-channel heat sink, Int. Commun. Heat Mass Transfer 40 (2013) 58–66.
[243] M.K. Moraveji, M. Hejazian, Modeling of turbulent forced convective heat transfer and friction factor in a tube for Fe_3O_4 magnetic nanofluid with computational fluid dynamics, Int. Commun. Heat Mass Transfer 39 (2012) 1293–1296.
[244] H.R. Seyf, S.K. Mohammadian, Thermal and hydraulic performance of counterflow microchannel heat exchangers with and without nanofluids, J. Heat Transfer 133 (2011) 081801.
[245] O. Manca, S. Nardini, D. Ricci, S. Tamburrino, Numerical investigation on mixed convection in triangular cross-section ducts with nanofluids, Adv. Mech. Eng. 4 (2012) 139370.
[246] M. Corcione, M. Cianfrini, A. Quintino, Heat transfer of nanofluids in turbulent pipe flow, Int. J. Therm. Sci. 56 (2012) 58–69.
[247] R. Kamali, A.R. Binesh, Numerical investigation of heat transfer enhancement using carbon nanotube-based non-Newtonian nanofluids, Int. Commun. Heat Mass Transfer 37 (2010) 1153–1157.
[248] M. Ahmed, M. Eslamian, Laminar forced convection of a nanofluid in a microchannel: effect of flow inertia and external forces on heat transfer and fluid flow characteristics, Appl. Therm. Eng. 78 (2015) 326–338.
[249] A. Mokmeli, M. Saffar-Avval, Prediction of nanofluid convective heat transfer using the dispersion model, Int. J. Therm. Sci. 49 (2010) 471–478.
[250] M.S. Mojarrad, A. Keshavarz, A. Shokouhi, Nanofluids thermal behavior analysis using a new dispersion model along with single-phase, Heat Mass Transfer 49 (2013) 1333–1343.
[251] S. Özerinç, A.G. Yazıcıoğlu, S. Kakaç, Numerical analysis of laminar forced convection with temperature-dependent thermal conductivity of nanofluids and thermal dispersion, Int. J. Therm. Sci. 62 (2012) 138–148.
[252] R.B. Mansour, N. Galanis, C.T. Nguyen, Effect of uncertainties in physical properties on forced convection heat transfer with nanofluids, Appl. Therm. Eng. 27 (2007) 240–249.
[253] E. Magyari, Comment on the homogeneous nanofluid models applied to convective heat transfer problems, Acta Mech. 222 (2011) 381–385.
[254] S. Mirmasoumi, A. Behzadmehr, Effect of nanoparticles mean diameter on mixed convection heat transfer of a nanofluid in a horizontal tube, Int. J. Heat Fluid Flow 29 (2008) 557–566.
[255] S. Mirmasoumi, A. Behzadmehr, Numerical study of laminar mixed convection of a nanofluid in a horizontal tube using two-phase mixture model, Appl. Therm. Eng. 28 (2008) 717–727.
[256] M. Kalteh, A. Abbassi, M. Saffar-Avval, J. Harting, Eulerian-Eulerian two-phase numerical simulation of nanofluid laminar forced convection in a microchannel, Int. J. Heat Fluid Flow 32 (2011) 107–116.
[257] A. Akbarinia, R. Laur, Investigating the diameter of solid particles effects on a laminar nanofluid flow in a curved tube using a two phase approach, Int. J. Heat Fluid Flow 30 (2009) 706–714.
[258] S. Allahyari, A. Behzadmehr, S.M.H. Sarvari, Conjugate heat transfer of laminar mixed convection of a nanofluid through an inclined tube with circumferentially non-uniform heating, Nanoscale Res. Lett. 6 (2011) 360.
[259] S. Allahyari, A. Behzadmehr, S.M.H. Sarvari, Conjugate heat transfer of laminar mixed convection of a nanofluid through a horizontal tube with circumferentially non-uniform heating, Int. J. Therm. Sci. 50 (2011) 1963–1972.

[260] A. Esmaeilnejad, H. Aminfar, M.S. Neistanak, Numerical investigation of forced convection heat transfer through microchannels with non-Newtonian nanofluids, Int. J. Therm. Sci. 75 (2014) 76–86.
[261] R.M. Moghari, A. Akbarinia, M. Shariat, F. Talebi, R. Laur, Two phase mixed convection Al_2O_3–water nanofluid flow in an annulus, Int. J. Multiphase Flow 37 (2011) 585–595.
[262] M. Shariat, A. Akbarinia, A.H. Nezhad, A. Behzadmehr, R. Laur, Numerical study of two phase laminar mixed convection nanofluid in elliptic ducts, Appl. Therm. Eng. 31 (2011) 2348–2359.
[263] S.Z. Heris, S.H. Noie, E. Talaii, J. Sargolzaei, Numerical investigation of Al_2O_3/water nanofluid laminar convective heat transfer through triangular ducts, Nanoscale Res. Lett. 6 (2011) 179.
[264] A. Aghanajafi, D. Toghraie, B. Mehmandoust, Numerical simulation of laminar forced convection of water-CuO nanofluid inside a triangular duct, Physica E 85 (2017) 103–108.
[265] M. Kalteh, A. Abbassi, M. Saffar-Avval, A. Frijns, A. Darhuber, J. Harting, Experimental and numerical investigation of nanofluid forced convection inside a wide microchannel heat sink, Appl. Therm. Eng. 36 (2012) 260–268.
[266] F. Akbaridoust, M. Rakhsha, A. Abbassi, M. Saffar-Avval, Experimental and numerical investigation of nanofluid heat transfer in helically coiled tubes at constant wall temperature using dispersion model, Int. J. Heat Mass Transfer 58 (2013) 480–491.
[267] M.H. Fard, M.N. Esfahany, M.R. Talaie, Numerical study of convective heat transfer of nanofluids in a circular tube two-phase model versus single-phase model, Int. Commun. Heat Mass Transfer 37 (2010) 91–97.
[268] A. Behzadmehr, M. Saffar-Avval, N. Galanis, Prediction of turbulent forced convection of a nanofluid in a tube with uniform heat flux using a two phase approach, Int. J. Heat Fluid Flow 28 (2007) 211–219.
[269] S. Göktepe, K. Atalık, H. Ertürk, Comparison of single and two-phase models for nanofluid convection at the entrance of a uniformly heated tube, Int. J. Therm. Sci. 80 (2014) 83–92.
[270] R. Lotfi, Y. Saboohi, A.M. Rashidi, Numerical study of forced convective heat transfer of nanofluids: comparison of different approaches, Int. Commun. Heat Mass Transfer 37 (2010) 74–78.
[271] Z.Y. Ghale, M. Haghshenasfard, M.N. Esfahany, Investigation of nanofluids heat transfer in a ribbed microchannel heat sink using single-phase and multiphase CFD models, Int. Commun. Heat Mass Transfer 68 (2015) 122–129.
[272] M.K. Moraveji, R.M. Ardehali, CFD modeling (comparing single and two-phase approaches) on thermal performance of Al_2O_3/water nanofluid in mini-channel heat sink, Int. Commun. Heat Mass Transfer 44 (2013) 157–164.
[273] M. Hejazian, M.K. Moraveji, A. Beheshti, Comparative study of Euler and mixture models for turbulent flow of Al_2O_3 nanofluid inside a horizontal tube, Int. Commun. Heat Mass Transfer 52 (2014) 152–158.
[274] M. Akbari, N. Galanis, A. Behzadmehr, Comparative analysis of single and two-phase models for CFD studies of nanofluid heat transfer, Int. J. Therm. Sci. 50 (2011) 1343–1354.
[275] A. Kamyar, R. Saidur, M. Hasanuzzaman, Application of computational fluid dynamics (CFD) for nanofluids, Int. J. Heat Mass Transfer 55 (2012) 4104–4115.
[276] V. Bianco, F. Chiacchio, O. Manca, S. Nardini, Numerical investigation of nanofluids forced convection in circular tubes, Appl. Therm. Eng. 29 (2009) 3632–3642.
[277] V. Bianco, O. Manca, S. Nardini, Numerical investigation on nanofluids turbulent convection heat transfer inside a circular tube, Int. J. Therm. Sci. 50 (2011) 341–349.
[278] S. Tahir, M. Mital, Numerical investigation of laminar nanofluid developing flow and heat transfer in a circular channel, Appl. Therm. Eng. 39 (2012) 8–14.
[279] M. Mahdavi, M. Sharifpur, J.P. Meyer, CFD modelling of heat transfer and pressure drops for nanofluids through vertical tubes in laminar flow by Lagrangian and Eulerian approaches, Int. J. Heat Mass Transfer 88 (2015) 803–813.
[280] M. Moghaddami, A. Mohammadzade, S.A.V. Esfehani, Second law analysis of nanofluid flow, Energy Convers. Manage. 52 (2011) 1397–1405.
[281] V. Bianco, S. Nardini, O. Manca, Enhancement of heat transfer and entropy generation analysis of nanofluids turbulent convection flow in square section tubes, Nanoscale Res. Lett. 6 (2011) 252.
[282] K.Y. Leong, R. Saidur, T.M.I. Mahlia, Y.H. Yau, Entropy generation analysis of nanofluid flow in a circular tube subjected to constant wall temperature, Int. Commun. Heat Mass Transfer 39 (2012) 1169–1175.
[283] P.K. Singh, K.B. Anoop, T. Sundararajan, S.K. Das, Entropy generation due to flow and heat transfer in nanofluids, Int. J. Heat Mass Transfer 53 (2010) 4757–4767.
[284] M.R. Sohel, R. Saidur, N.H. Hassan, M.M. Elias, S.S. Khaleduzzaman, I.M. Mahbubul, Analysis of entropy generation using nanofluid flow through the circular microchannel and minichannel heat sink, Int. Commun. Heat Mass Transfer 46 (2013) 85–91.
[285] M. Bahiraei, F. Abdi, Development of a model for entropy generation of water-TiO_2 nanofluid flow considering nanoparticle migration within a minichannel, Chemom. Intell. Lab. Syst. 157 (2016) 16–28.
[286] M. Bahiraei, S.M. Majd, Prediction of entropy generation for nanofluid flow through a triangular minichannel using neural network, Adv. Powder Technol. 27 (2016) 673–683.
[287] J. Li, C. Kleinstreuer, Entropy generation analysis for nanofluid flow in microchannels, J. Heat Transfer 132 (2010) 122401.
[288] A. Shalchi-Tabrizi, H.R. Seyf, Analysis of entropy generation and convective heat transfer of Al_2O_3 nanofluid flow in a tangential micro heat sink, Int. J. Heat Mass Transfer 55 (2012) 4366–4375.
[289] Y.M. Hung, Analytical study on forced convection of nanofluids with viscous dissipation in microchannels, Heat Transfer Eng. 31 (2010) 1184–1192.
[290] W.H. Mah, Y.M. Hung, N. Guo, Entropy generation of viscous dissipative nanofluid flow in microchannels, Int. J. Heat Mass Transfer 55 (2012) 4169–4182.
[291] T.W. Ting, Y.M. Hung, N. Guo, Effects of streamwise conduction on thermal performance of nanofluid flow in microchannel heat sinks, Energy Convers. Manage. 78 (2014) 14–23.
[292] T.W. Ting, Y.M. Hung, N. Guo, Entropy generation of nanofluid flow with streamwise conduction in microchannels, Energy 64 (2014) 979–990.
[293] T.W. Ting, Y.M. Hung, N. Guo, Field-synergy analysis of viscous dissipative nanofluid flow in microchannels, Int. J. Heat Mass Transfer 73 (2014) 483–491.
[294] T.W. Ting, Y.M. Hung, N. Guo, Entropy generation of viscous dissipative nanofluid flow in thermal non-equilibrium porous media embedded in microchannels, Int. J. Heat Mass Transfer 81 (2015) 862–877.
[295] T.W. Ting, Y.M. Hung, N. Guo, Viscous dissipative forced convection in thermal non-equilibrium nanofluid-saturated porous media embedded in microchannels, Int. Commun. Heat Mass Transfer 57 (2014) 309–318.
[296] S. Suresh, P. Selvakumar, M. Chandrasekar, V.S. Raman, Experimental studies on heat transfer and friction factor characteristics of Al_2O_3/water nanofluid under turbulent flow with spiraled rod inserts, Chem. Eng. Process. Process Intensif. 53 (2012) 24–30.
[297] S. Suresh, K.P. Venkitaraj, P. Selvakumar, M. Chandrasekar, A comparison of thermal characteristics of Al_2O_3/water and CuO/water nanofluids in transition flow through a straight circular duct fitted with helical screw tape inserts, Exp. Therm. Fluid Sci. 39 (2012) 37–44.
[298] S. Suresh, K.P. Venkitaraj, P. Selvakumar, Comparative study on thermal performance of helical screw tape inserts in laminar flow using Al_2O_3/water and CuO/water nanofluids, Superlattices Microstruct. 49 (2011) 608–622.
[299] W.H. Azmi, K.V. Sharma, P.K. Sarma, R. Mamat, S. Anuar, Comparison of convective heat transfer coefficient and friction factor of TiO_2 nanofluid flow in a tube with twisted tape inserts, Int. J. Therm. Sci. 81 (2014) 84–93.
[300] K. Wongcharee, S. Eiamsa-ard, Enhancement of heat transfer using CuO/water nanofluid and twisted tape with alternate axis, Int. Commun. Heat Mass Transfer 38 (2011) 742–748.
[301] G. Pathipakka, P. Sivashanmugam, Heat transfer behaviour of nanofluids in a uniformly heated circular tube fitted with helical inserts in laminar flow, Superlattices Microstruct. 47 (2010) 349–360.
[302] M. Chandrasekar, S. Suresh, A.C. Bose, Experimental studies on heat transfer and friction factor characteristics of Al_2O_3/water nanofluid in a circular pipe under laminar flow with wire coil inserts, Exp. Therm. Fluid Sci. 34 (2010) 122–130.
[303] M. Chandrasekar, S. Suresh, A.C. Bose, Experimental studies on heat transfer and friction factor characteristics of Al_2O_3/water nanofluid in a circular pipe under transition flow with wire coil inserts, Heat Transfer Eng. 32 (2011) 485–496.
[304] J.F. Tullius, Y. Bayazitoglu, Effect of Al_2O_3/H_2O nanofluid on MWNT circular fin structures in a minichannel, Int. J. Heat Mass Transfer 60 (2013) 523–530.
[305] M. Khoshvaght-Aliabadi, F. Hormozi, A. Zamzamian, Experimental analysis of thermal–hydraulic performance of copper–water nanofluid flow in different plate-fin channels, Exp. Therm. Fluid Sci. 52 (2014) 248–258.
[306] M. Khoshvaght-Aliabadi, A. Alizadeh, An experimental study of Cu–water nanofluid flow inside serpentine tubes with variable straight-section lengths, Exp. Therm. Fluid Sci. 61 (2015) 1–11.
[307] A.A. Servati V, K. Javaherdeh, H.R. Ashorynejad, Magnetic field effects on force convection flow of a nanofluid in a channel partially filled with porous media using Lattice Boltzmann Method, Adv. Powder Technol. 25 (2014) 666–675.
[308] M. Hajipour, A.M. Dehkordi, Analysis of nanofluid heat transfer in parallel-plate vertical channels partially filled with porous medium, Int. J. Therm. Sci. 55 (2012) 103–113.
[309] M. Hajipour, A.M. Dehkordi, Mixed-convection flow of Al_2O_3–H_2O nanofluid in a channel partially filled with porous metal foam: experimental and numerical study, Exp. Therm. Fluid Sci. 53 (2014) 49–56.
[310] M. Siavashi, H.R.T. Bahrami, H. Saffari, Numerical investigation of flow characteristics, heat transfer and entropy generation of nanofluid flow inside an annular pipe partially or completely filled with porous media using two-phase mixture model, Energy 93 (2015) 2451–2466.
[311] M. Nazari, M. Ashouri, M.H. Kayhani, A. Tamayol, Experimental study of convective heat transfer of a nanofluid through a pipe filled with metal foam, Int. J. Therm. Sci. 88 (2015) 33–39.
[312] S. Nazari, D. Toghraie, Numerical simulation of heat transfer and fluid flow of water-CuO nanofluid in a sinusoidal channel with a porous medium, Physica E 87 (2017) 134–140.
[313] D. Ashtiani, M.A. Akhavan-Behabadi, M.F. Pakdaman, An experimental investigation on heat transfer characteristics of multi-walled CNT-heat transfer oil nanofluid flow inside flattened tubes under uniform wall temperature condition, Int. Commun. Heat Mass Transfer 39 (2012) 1404–1409.
[314] M. Saeedinia, M.A. Akhavan-Behabadi, M. Nasr, Experimental study on heat transfer and pressure drop of nanofluid flow in a horizontal coiled wire inserted tube under constant heat flux, Exp. Therm. Fluid Sci. 36 (2012) 158–168.

[315] B. Sun, D. Yang, Experimental study on the heat transfer characteristics of nanorefrigerants in an internal thread copper tube, Int. J. Heat Mass Transfer 64 (2013) 559–566.
[316] B. Sun, D. Yang, Flow boiling heat transfer characteristics of nano-refrigerants in a horizontal tube, Int. J. Refrig. 38 (2014) 206–214.
[317] H.A. Mohammed, H.A. Hasan, M.A. Wahid, Heat transfer enhancement of nanofluids in a double pipe heat exchanger with louvered strip inserts, Int. Commun. Heat Mass Transfer 40 (2013) 36–46.
[318] M.A. Akhavan-Behabadi, M.F. Pakdaman, M. Ghazvini, Experimental investigation on the convective heat transfer of nanofluid flow inside vertical helically coiled tubes under uniform wall temperature condition, Int. Commun. Heat Mass Transfer 39 (2012) 556–564.
[319] M.F. Pakdaman, M.A. Akhavan-Behabadi, P. Razi, An experimental investigation on thermo-physical properties and overall performance of MWCNT/heat transfer oil nanofluid flow inside vertical helically coiled tubes, Exp. Therm. Fluid Sci. 40 (2012) 103–111.
[320] M.F. Pakdaman, M.A. Akhavan-Behabadi, P. Razi, An empirical study on the pressure drop characteristics of nanofluid flow inside helically coiled tubes, Int. J. Therm. Sci. 65 (2013) 206–213.
[321] A.A.R. Darzi, M. Farhadi, K. Sedighi, R. Shafaghat, K. Zabihi, Experimental investigation of turbulent heat transfer and flow characteristics of SiO_2/water nanofluid within helically corrugated tubes, Int. Commun. Heat Mass Transfer 39 (2012) 1425–1434.
[322] A.A.R. Darzi, M. Farhadi, K. Sedighi, S. Aallahyari, M.A. Delavar, Turbulent heat transfer of Al_2O_3–water nanofluid inside helically corrugated tubes: Numerical study, Int. Commun. Heat Mass Transfer 41 (2013) 68–75.
[323] N. Kannadasan, K. Ramanathan, S. Suresh, Comparison of heat transfer and pressure drop in horizontal and vertical helically coiled heat exchanger with CuO/water based nano fluids, Exp. Therm. Fluid Sci. 42 (2012) 64–70.
[324] M.T. Jamal-Abad, A. Zamzamian, M. Dehghan, Experimental studies on the heat transfer and pressure drop characteristics of Cu–water and Al–water nanofluids in a spiral coil, Exp. Therm. Fluid Sci. 47 (2013) 206–212.
[325] S.M. Hashemi, M.A. Akhavan-Behabadi, An empirical study on heat transfer and pressure drop characteristics of CuO–base oil nanofluid flow in a horizontal helically coiled tube under constant heat flux, Int. Commun. Heat Mass Transfer 39 (2012) 144–151.
[326] G. Huminic, A. Huminic, Heat transfer characteristics in double tube helical heat exchangers using nanofluids, Int. J. Heat Mass Transfer 54 (2011) 4280–4287.
[327] H.A. Mohammed, K. Narrein, Thermal and hydraulic characteristics of nanofluid flow in a helically coiled tube heat exchanger, Int. Commun. Heat Mass Transfer 39 (2012) 1375–1383.
[328] K. Narrein, H.A. Mohammed, Influence of nanofluids and rotation on helically coiled tube heat exchanger performance, Thermochim. Acta 564 (2013) 13–23.
[329] A.P. Sasmito, J.C. Kurnia, A.S. Mujumdar, Numerical evaluation of laminar heat transfer enhancement in nanofluid flow in coiled square tubes, Nanoscale Res. Lett. 6 (2011) 376.
[330] M.A. Khairul, R. Saidur, M.M. Rahman, M.A. Alim, A. Hossain, Z. Abdin, Heat transfer and thermodynamic analyses of a helically coiled heat exchanger using different types of nanofluids, Int. J. Heat Mass Transfer 67 (2013) 398–403.
[331] M. Kahani, S.Z. Heris, S.M. Mousavi, Comparative study between metal oxide nanopowders on thermal characteristics of nanofluid flow through helical coils, Powder Technol. 246 (2013) 82–92.
[332] N. Jamshidi, M. Farhadi, K. Sedighi, D.D. Ganji, Optimization of design parameters for nanofluids flowing inside helical coils, Int. Commun. Heat Mass Transfer 39 (2012) 311–317.
[333] O.A. Akbari, M.R. Safaei, M. Goodarzi, N.S. Akbar, M. Zarringhalam, G.A.S. Shabani, M. Dahari, A modified two-phase mixture model of nanofluid flow and heat transfer in a 3-D curved microtube, Adv. Powder Technol. 27 (2016) 2175–2185.
[334] S. Alikhani, A. Behzadmehr, M. Saffar-Avval, Numerical study of nanofluid mixed convection in a horizontal curved tube using two-phase approach, Heat Mass Transfer 47 (2011) 107–118.
[335] D. Yang, B. Sun, H. Li, X. Fan, Experimental study on the heat transfer and flow characteristics of nanorefrigerants inside a corrugated tube, Int. J. Refrig. 56 (2015) 213–223.
[336] M. Khoshvaght-Aliabadi, M. Sahamiyan, Performance of nanofluid flow in corrugated minichannels heat sink (CMCHS), Energy Convers. Manage. 108 (2016) 297–308.
[337] M. Khoshvaght-Aliabadi, Influence of different design parameters and Al_2O_3-water nanofluid flow on heat transfer and flow characteristics of sinusoidal-corrugated channels, Energy Convers. Manage. 88 (2014) 96–105.
[338] Y.-T. Yang, Y.-H. Wang, P.-K. Tseng, Numerical optimization of heat transfer enhancement in a wavy channel using nanofluids, Int. Commun. Heat Mass Transfer 51 (2014) 9–17.
[339] M.A. Ahmed, M.Z. Yusoff, N.H. Shuaib, Effects of geometrical parameters on the flow and heat transfer characteristics in trapezoidal-corrugated channel using nanofluid, Int. Commun. Heat Mass Transfer 42 (2013) 69–74.
[340] M.A. Ahmed, N.H. Shuaib, M.Z. Yusoff, Numerical investigations on the heat transfer enhancement in a wavy channel using nanofluid, Int. J. Heat Mass Transfer 55 (2012) 5891–5898.
[341] M. Akbarzadeh, S. Rashidi, M. Bovand, R. Ellahi, A sensitivity analysis on thermal and pumping power for the flow of nanofluid inside a wavy channel, J. Mol. Liq. 220 (2016) 1–13.
[342] K. Wongcharee, S. Eiamsa-ard, Heat transfer enhancement by using CuO/water nanofluid in corrugated tube equipped with twisted tape, Int. Commun. Heat Mass Transfer 39 (2012) 251–257.
[343] O. Manca, S. Nardini, D. Ricci, A numerical study of nanofluid forced convection in ribbed channels, Appl. Therm. Eng. 37 (2012) 280–292.
[344] M. Parsazadeh, H.A. Mohammed, F. Fathinia, Influence of nanofluid on turbulent forced convective flow in a channel with detached rib-arrays, Int. Commun. Heat Mass Transfer 46 (2013) 97–105.
[345] Q. Gravndyan, O.A. Akbari, D. Toghraie, A. Marzban, R. Mashayekhi, R. Karimi, F. Pourfattah, The effect of aspect ratios of rib on the heat transfer and laminar water/TiO_2 nanofluid flow in a two-dimensional rectangular microchannel, J. Mol. Liq. 236 (2017) 254–265.
[346] O.A. Akbari, D. Toghraie, A. Karimipour, M.R. Safaei, M. Goodarzi, H. Alipour, M. Dahari, Investigation of rib's height effect on heat transfer and flow parameters of laminar water–Al_2O_3 nanofluid in a rib-microchannel, Appl. Math. Comput. 290 (2016) 135–153.
[347] H. Alipour, A. Karimipour, M.R. Safaei, D.T. Semiromi, O.A. Akbari, Influence of T-semi attached rib on turbulent flow and heat transfer parameters of a silver-water nanofluid with different volume fractions in a three-dimensional trapezoidal microchannel, Physica E 88 (2017) 60–76.
[348] A. Andreozzi, O. Manca, S. Nardini, D. Ricci, Forced convection enhancement in channels with transversal ribs and nanofluids, Appl. Therm. Eng. 98 (2016) 1044–1053.
[349] H.A. Mohammed, A.N. Al-Shamani, J.M. Sheriff, Thermal and hydraulic characteristics of turbulent nanofluids flow in a rib–groove channel, Int. Commun. Heat Mass Transfer 39 (2012) 1584–1594.
[350] S.M. Vanaki, H.A. Mohammed, Numerical study of nanofluid forced convection flow in channels using different shaped transverse ribs, Int. Commun. Heat Mass Transfer 67 (2015) 176–188.
[351] Y.-T. Yang, H.-W. Tang, B.-Y. Zeng, C.-H. Wu, Numerical simulation and optimization of turbulent nanofluids in a three-dimensional rectangular rib-grooved channel, Int. Commun. Heat Mass Transfer 66 (2015) 71–79.
[352] L. Zhang, J. Lv, M. Bai, D. Guo, Effect of vibration on forced convection heat transfer for SiO_2–water nanofluids, Heat Transfer Eng. 36 (2015) 452–461.
[353] H.E. Ahmed, M.I. Ahmed, M.Z. Yusoff, Heat transfer enhancement in a triangular duct using compound nanofluids and turbulators, Appl. Therm. Eng. 91 (2015) 191–201.
[354] H.E. Ahmed, H.A. Mohammed, M.Z. Yusoff, Heat transfer enhancement of laminar nanofluids flow in a triangular duct using vortex generator, Superlattices Microstruct. 52 (2012) 398–415.
[355] N.R. Kuppusamy, H.A. Mohammed, C.W. Lim, Numerical investigation of trapezoidal grooved microchannel heat sink using nanofluids, Thermochim. Acta 573 (2013) 39–56.
[356] H.R. Rayatzadeh, M. Saffar-Avval, M. Mansourkiaei, A. Abbassi, Effects of continuous sonication on laminar convective heat transfer inside a tube using water–TiO_2 nanofluid, Exp. Therm. Fluid Sci. 48 (2013) 8–14.
[357] P. Li, D. Zhang, Y. Xie, Heat transfer and flow analysis of Al_2O_3–water nanofluids in microchannel with dimple and protrusion, Int. J. Heat Mass Transfer 73 (2014) 456–467.
[358] D. Madhesh, R. Parameshwaran, S. Kalaiselvam, Experimental investigation on convective heat transfer and rheological characteristics of Cu–TiO_2 hybrid nanofluids, Exp. Therm. Fluid Sci. 52 (2014) 104–115.
[359] H. Yarmand, S. Gharehkhani, G. Ahmadi, S.F.S. Shirazi, S. Baradaran, E. Montazer, M.N.M. Zubir, M.S. Alehashem, S.N. Kazi, M. Dahari, Graphene nanoplatelets–silver hybrid nanofluids for enhanced heat transfer, Energy Convers. Manage. 100 (2015) 419–428.
[360] V. Bianco, O. Manca, S. Nardini, Performance analysis of turbulent convection heat transfer of Al_2O_3 water-nanofluid in circular tubes at constant wall temperature, Energy 77 (2014) 403–413.
[361] C.T. Nguyen, F. Desgranges, N. Galanis, G. Roy, T. Maré, S. Boucher, H. Angue Mintsa, Viscosity data for Al_2O_3–water nanofluid—hysteresis: is heat transfer enhancement using nanofluids reliable?, Int J. Therm. Sci. 47 (2008) 103–111.
[362] A.D. Sommers, K.L. Yerkes, Experimental investigation into the convective heat transfer and system-level effects of Al_2O_3-propanol nanofluid, J. Nanopart. Res. 12 (2010) 1003–1014.
[363] T.L. Bergman, Effect of reduced specific heats of nanofluids on single phase, laminar internal forced convection, Int. J. Heat Mass Transfer 52 (2009) 1240–1244.
[364] A. Zangeneh, A. Vatani, Z. Fakhroeian, S.M. Peyghambarzadeh, Experimental study of forced convection and subcooled flow boiling heat transfer in a vertical annulus using different novel functionalized ZnO nanoparticles, Appl. Therm. Eng. 109 (2016) 789–802.
[365] Z. Wu, L. Wang, B. Sundén, Pressure drop and convective heat transfer of water and nanofluids in a double-pipe helical heat exchanger, Appl. Therm. Eng. 60 (2013) 266–274.
[366] W.I.A. Aly, Numerical study on turbulent heat transfer and pressure drop of nanofluid in coiled tube-in-tube heat exchangers, Energy Convers. Manage. 79 (2014) 304–316.
[367] A.T. Utomo, E.B. Haghighi, A.I.T. Zavareh, M. Ghanbarpourgeravi, H. Poth, R. Khodabandeh, B. Palm, A.W. Pacek, The effect of nanoparticles on laminar heat transfer in a horizontal tube, Int. J. Heat Mass Transfer 69 (2014) 77–91.
[368] A. Akbarinia, M. Abdolzadeh, R. Laur, Critical investigation of heat transfer enhancement using nanofluids in microchannels with slip and non-slip flow regimes, Appl. Therm. Eng. 31 (2011) 556–565.

[369] E.V. Timofeeva, W. Yu, D.M. France, D. Singh, J.L. Routbort, Base fluid and temperature effects on the heat transfer characteristics of SiC in ethylene glycol/H_2O and H_2O nanofluids, J. Appl. Phys. 109 (2011) 014914.
[370] E.V. Timofeeva, D.S. Smith, Y. Wenhua, D.M. France, D. Singh, J.L. Routbort, Particle size and interfacial effects on thermo-physical and heat transfer characteristics of water-based α-SiC nanofluids, Nanotechnology 21 (2010) 215703.
[371] W. Yu, D.M. France, E.V. Timofeeva, D. Singh, J.L. Routbort, Thermophysical property-related comparison criteria for nanofluid heat transfer enhancement in turbulent flow, Appl. Phys. Lett. 96 (2010) 213109.
[372] E.B. Haghighi, M. Saleemi, N. Nikkam, Z. Anwar, I. Lumbreras, M. Behi, S.A. Mirmohammadi, H. Poth, R. Khodabandeh, M.S. Toprak, M. Muhammed, B. Palm, Cooling performance of nanofluids in a small diameter tube, Exp. Therm. Fluid Sci. 49 (2013) 114–122.
[373] D. Lelea, I. Laza, The particle thermal conductivity influence of nanofluids on thermal performance of the microtubes, Int. Commun. Heat Mass Transfer 59 (2014) 61–67.
[374] D. Lelea, I. Laza, The water based Al_2O_3 nanofluid flow and heat transfer in tangential microtube heat sink with multiple inlets, Int. J. Heat Mass Transfer 69 (2014) 264–275.
[375] E.B. Haghighi, M. Saleemi, N. Nikkam, R. Khodabandeh, M.S. Toprak, M. Muhammed, B. Palm, Accurate basis of comparison for convective heat transfer in nanofluids, Int. Commun. Heat Mass Transfer 52 (2014) 1–7.
[376] S.-M. Kim, I. Mudawar, Flow condensation in parallel micro-channels–Part 2: Heat transfer results and correlation technique, Int. J. Heat Mass Transfer 55 (2012) 984–994.
[377] S.-M. Kim, I. Mudawar, Universal approach to predicting two-phase frictional pressure drop for adiabatic and condensing mini/micro-channel flows, Int. J. Heat Mass Transfer 55 (2012) 3246–3261.
[378] S.-M. Kim, I. Mudawar, Universal approach to predicting saturated flow boiling heat transfer in mini/micro-channels – Part I. Dryout incipience quality, Int. J. Heat Mass Transfer 64 (2013) 1226–1238.
[379] C.R. Kharangate, I. Mudawar, Review of computational studies on boiling and condensation, Int. J. Heat Mass Transfer 108 (2017) 1164–1196.
[380] K.B. Rana, A.K. Rajvanshi, G.D. Agrawal, A visualization study of flow boiling heat transfer with nanofluids, J. Visualization 16 (2013) 133–143.
[381] K.B. Rana, G.D. Agrawal, J. Mathur, U. Puli, Measurement of void fraction in flow boiling of ZnO–water nanofluids using image processing technique, Nucl. Eng. Des. 270 (2014) 217–226.
[382] N. Patra, V. Gupta, E. Pradyumna, R. Singh, P. Ghosh, R.S. Singh, A. Nayak, Delay in DNB for flow boiling of diluted oxide based nanofluids, Exp. Therm. Fluid Sci. 89 (2017) 211–218.
[383] Y. Wang, J.M. Wu, Numerical simulation on single bubble behavior during Al_2O_3/H_2O nanofluids flow boiling using Moving Particle Simi-implicit method, Prog. Nucl. Energy 85 (2015) 130–139.
[384] L. Yu, A. Sur, D. Liu, Flow boiling heat transfer and two-phase flow instability of nanofluids in a minichannel, J. Heat Transfer 137 (2015) 051502.
[385] Y. Wang, G.H. Su, Experimental investigation on nanofluid flow boiling heat transfer in a vertical tube under different pressure conditions, Exp. Therm. Fluid Sci. 77 (2016) 116–123.
[386] Y. Wang, K.H. Deng, B. Liu, J.M. Wu, G.H. Su, A correlation of nanofluid flow boiling heat transfer based on the experimental results of AlN/H_2O and Al_2O_3/H_2O nanofluid, Exp. Therm. Fluid Sci. 80 (2017) 376–383.
[387] M.M. Sarafraz, F. Hormozi, Comparatively experimental study on the boiling thermal performance of metal oxide and multi-walled carbon nanotube nanofluids, Powder Technol. 287 (2016) 412–430.
[388] S.Y. Zhang, Z. Ge, H.T. Wang, H. Wang, Characteristics of flow boiling heat transfer and pressure drop of MWCNT–R123 nanorefrigerant: experimental investigations and correlations, Nanoscale Microscale Thermophys. Eng. 20 (2016) 97–120.
[389] X.-F. Yang, Z.-H. Liu, Flow boiling heat transfer in the evaporator of a loop thermosyphon operating with CuO based aqueous nanofluid, Int. J. Heat Mass Transfer 55 (2012) 7375–7384.
[390] H. Setoodeh, A. Keshavarz, A. Ghasemian, A. Nasouhi, Subcooled flow boiling of alumina/water nanofluid in a channel with a hot spot: an experimental study, Appl. Therm. Eng. 90 (2015) 384–394.
[391] A.A. Chehade, H.L. Gualous, S.L. Masson, F. Fardoun, A. Besq, Boiling local heat transfer enhancement in minichannels using nanofluids, Nanoscale Res. Lett. 8 (2013) 130.
[392] H. Peng, G. Ding, W. Jiang, H. Hu, Y. Gao, Heat transfer characteristics of refrigerant-based nanofluid flow boiling inside a horizontal smooth tube, Int. J. Refrig. 32 (2009) 1259–1270.
[393] H. Peng, G. Ding, W. Jiang, H. Hu, Y. Gao, Measurement and correlation of frictional pressure drop of refrigerant-based nanofluid flow boiling inside a horizontal smooth tube, Int. J. Refrig. 32 (2009) 1756–1764.
[394] O.A. Alawi, N.A.C. Sidik, A.S. Kherbeet, Measurements and correlations of frictional pressure drop of TiO_2/R123 flow boiling inside a horizontal smooth tube, Int. Commun. Heat Mass Transfer 61 (2015) 42–48.
[395] M.A. Akhavan-Behabadi, M. Nasr, S. Baqeri, Experimental investigation of flow boiling heat transfer of R-600a/oil/CuO in a plain horizontal tube, Exp. Therm. Fluid Sci. 58 (2014) 105–111.
[396] S. Baqeri, M.A. Akhavan-Behabadi, B. Ghadimi, Experimental investigation of the forced convective boiling heat transfer of R-600a/oil/nanoparticle, Int. Commun. Heat Mass Transfer 55 (2014) 71–76.
[397] K. Henderson, Y.-G. Park, L. Liu, A.M. Jacobi, Flow-boiling heat transfer of R-134a-based nanofluids in a horizontal tube, Int. J. Heat Mass Transfer 53 (2010) 944–951.
[398] S. Tazarv, M. Saffar-Avval, F. Khalvati, E. Mirzaee, Z. Mansoori, Experimental investigation of saturated flow boiling heat transfer to TiO_2/R141b nanorefrigerant, Exp. Heat Transfer 29 (2016) 188–204.
[399] I.M. Mahbubul, R. Saidur, M.A. Amalina, Heat transfer and pressure drop characteristics of Al_2O_3-R141b nanorefrigerant in horizontal smooth circular tube, Procedia Eng. 56 (2013) 323–329.
[400] S.J. Kim, T. McKrell, J. Buongiorno, L.-W. Hu, Subcooled flow boiling heat transfer of dilute alumina, zinc oxide, and diamond nanofluids at atmospheric pressure, Nucl. Eng. Des. 240 (2010) 1186–1194.
[401] E. Abedini, A. Behzadmehr, H. Rajabnia, S.M.H. Sarvari, S.H. Mansouri, Experimental investigation and comparison of subcooled flow boiling of TiO_2 nanofluid in a vertical and horizontal tube, J. Mech. Eng. Sci. 227 (2012) 1742–1753.
[402] M. Afrand, E. Abedini, H. Teimouri, Experimental investigation and simulation of flow boiling of nanofluids in different flow directions, Physica E 87 (2017) 248–253.
[403] E. Abedini, A. Behzadmehr, S.M.H. Sarvari, S.H. Mansouri, Numerical investigation of subcooled flow boiling of a nanofluid, Int. J. Therm. Sci. 64 (2013) 232–239.
[404] E. Abedini, T. Zarei, M. Afrand, S. Wongwises, Experimental study of transition flow from single phase to two phase flow boiling in nanofluids, J. Mol. Liq. 231 (2017) 11–19.
[405] E. Abedini, T. Zarei, H. Rajabnia, R. Kalbasi, M. Afrand, Numerical investigation of vapor volume fraction in subcooled flow boiling of a nanofluid, J. Mol. Liq. 238 (2017) 281–289.
[406] M. Karimzadehkhouei, M. Sezen, K. Şendur, M.P. Mengüç, A. Koşar, Subcooled flow boiling heat transfer of γ-Al_2O_3/water nanofluids in horizontal microtubes and the effect of surface characteristics and nanoparticle deposition, Appl. Therm. Eng. 127 (2017) 536–546.
[407] M.M. Sarafraz, F. Hormozi, Scale formation and subcooled flow boiling heat transfer of CuO–water nanofluid inside the vertical annulus, Exp. Therm. Fluid Sci. 52 (2014) 205–214.
[408] J. Zhou, X. Luo, Z. Feng, J. Xiao, J. Zhang, F. Guo, H. Li, Saturated flow boiling heat transfer investigation for nanofluid in minichannel, Exp. Therm. Fluid Sci. 85 (2017) 189–200.
[409] M.M. Sarafraz, F. Hormozi, M. Kamalgharibi, Sedimentation and convective boiling heat transfer of CuO-water/ethylene glycol nanofluids, Heat Mass Transfer 50 (2014) 1237–1249.
[410] S.J. Kim, T. McKrell, J. Buongiorno, L.-W. Hu, Experimental study of flow critical heat flux in alumina-water, zinc-oxide-water, and diamond-water nanofluids, J. Heat Transfer 131 (2009) 043204.
[411] S.J. Kim, T. McKrell, J. Buongiorno, L.-W. Hu, Alumina nanoparticles enhance the flow boiling critical heat flux of water at low pressure, J. Heat Transfer 130 (2008) 044501.
[412] H.S. Ahn, H. Kim, H. Jo, S. Kang, W. Chang, M.H. Kim, Experimental study of critical heat flux enhancement during forced convective flow boiling of nanofluid on a short heated surface, Int. J. Multiphase Flow 36 (2010) 375–384.
[413] T.I. Kim, Y.H. Jeong, S.H. Chang, An experimental study on CHF enhancement in flow boiling using Al_2O_3 nano-fluid, Int. J. Heat Mass Transfer 53 (2010) 1015–1022.
[414] M. Hashemi, S.H. Noie, Study of flow boiling heat transfer characteristics of critical heat flux using carbon nanotubes and water nanofluid, J. Therm. Anal. Calorim. 130 (2017) 2199–2209.
[415] T.I. Kim, W.J. Chang, S.H. Chang, Flow boiling CHF enhancement using Al_2O_3 nanofluid and an Al_2O_3 nanoparticle deposited tube, Int. J. Heat Mass Transfer 54 (2011) 2021–2025.
[416] T. Lee, J.H. Lee, Y.H. Jeong, Flow boiling critical heat flux characteristics of magnetic nanofluid at atmospheric pressure and low mass flux conditions, Int. J. Heat Mass Transfer 56 (2013) 101–106.
[417] T. Lee, D.H. Kam, J.H. Lee, Y.H. Jeong, Effects of two-phase flow conditions on flow boiling CHF enhancement of magnetite-water nanofluids, Int. J. Heat Mass Transfer 74 (2014) 278–284.
[418] H. Aminfar, M. Mohammadpourfard, R. Maroofiazar, Experimental study on the effect of magnetic field on critical heat flux of ferrofluid flow boiling in a vertical annulus, Exp. Therm. Fluid Sci. 58 (2014) 156–169.
[419] H. Aminfar, M. Mohammadpourfard, R. Maroofiazar, Numerical study of non-uniform magnetic fields effects on subcooled nanofluid flow boiling, Prog. Nucl. Energy 74 (2014) 232–241.
[420] S.D. Park, I.C. Bang, Flow boiling CHF enhancement in an external reactor vessel cooling (ERVC) channel using graphene oxide nanofluid, Nucl. Eng. Des. 265 (2013) 310–318.
[421] S.W. Lee, K.M. Kim, I.C. Bang, Study on flow boiling critical heat flux enhancement of graphene oxide/water nanofluid, Int. J. Heat Mass Transfer 65 (2013) 348–356.
[422] M. Mohammadpourfard, H. Aminfar, M. Karimi, Numerical investigation of non-uniform transverse magnetic field effects on the swirling flow boiling of magnetic nanofluid in annuli, Int. Commun. Heat Mass Transfer 75 (2016) 240–252.
[423] M. Boudouh, H.L. Gualous, M. De Labachelerie, Local convective boiling heat transfer and pressure drop of nanofluid in narrow rectangular channels, Appl. Therm. Eng. 30 (2010) 2619–2631.

[424] G. Duursma, K. Sefiane, A. Dehaene, S. Harmand, Y. Wang, Flow and heat transfer of single-and two-phase boiling of nanofluids in microchannels, Heat Transfer Eng. 36 (2015) 1252–1265.
[425] T.A. Moreira, F.J.d. Nascimento, G. Ribatski, An investigation of the effect of nanoparticle composition and dimension on the heat transfer coefficient during flow boiling of aqueous nanofluids in small diameter channels (1.1mm), Exp. Therm. Fluid Sci. 89 (2017) 72–89.
[426] Y.H. Diao, Y. Liu, R. Wang, Y.H. Zhao, L. Guo, X. Tang, Effects of nanofluids and nanocoatings on the thermal performance of an evaporator with rectangular microchannels, Int. J. Heat Mass Transfer 67 (2013) 183–193.
[427] C. Zhang, L. Zhang, H. Xu, D. Wang, B. Ye, Investigation of flow boiling performance and the resulting surface deposition of graphene oxide nanofluid in microchannels, Exp. Therm. Fluid Sci. 86 (2017) 1–10.
[428] Z. Edel, A. Mukherjee, Experimental investigation of nanofluid flow boiling in a single microchannel, in: Proceedings of the ASME 2012 Summer Heat Transfer Conference, Rio Grande, Puerto Rico, 2012, pp. 487–494.
[429] Z. Edel, A. Mukherjee, Flow boiling dynamics of water and nanofluids in a single microchannel at different heat fluxes, J. Heat Transfer 137 (2015) 011501.
[430] L. Xu, J. Xu, Nanofluid stabilizes and enhances convective boiling heat transfer in a single microchannel, Int. J. Heat Mass Transfer 55 (2012) 5673–5686.
[431] X. Wu, H. Wu, P. Cheng, Pressure drop and heat transfer of Al_2O_3-H_2O nanofluids through silicon microchannels, J. Micromech. Microeng. 19 (2009) 105020.
[432] J. Lee, I. Mudawar, Assessment of the effectiveness of nanofluids for single-phase and two-phase heat transfer in micro-channels, Int. J. Heat Mass Transfer 50 (2007) 452–463.
[433] S. Vafaei, D. Wen, Critical heat flux (CHF) of subcooled flow boiling of alumina nanofluids in a horizontal microchannel, J. Heat Transfer 132 (2010) 102404.
[434] S. Vafaei, D. Wen, Flow boiling heat transfer of alumina nanofluids in single microchannels and the roles of nanoparticles, J. Nanopart. Res. 13 (2011) 1063–1073.
[435] S. Vafaei, D. Wen, Critical heat flux of nanofluids inside a single microchannel: experiments and correlations, Chem. Eng. Res. Des. 92 (2014) 2339–2351.
[436] R. Revellin, J.R. Thome, A theoretical model for the prediction of the critical heat flux in heated microchannels, Int. J. Heat Mass Transfer 51 (2008) 1216–1225.
[437] R. Revellin, K. Mishima, J.R. Thome, Status of prediction methods for critical heat fluxes in mini and microchannels, Int. J. Heat Fluid Flow 30 (2009) 983–992.